



*Research Project Number TPF-5(193) Supplement #73  
Sponsoring Agency Code RFP-IOWA-1*

# **ATTACHMENT OF A COMBINATION BRIDGE RAIL TO CONCRETE PARAPET UTILIZING EPOXY ADHESIVE ANCHORS**

Submitted by

Robert W. Bielenberg, M.S.M.E., E.I.T.  
Research Associate Engineer

John D. Reid, Ph.D., P.E.  
Professor

Scott K. Rosenbaugh, M.S.C.E., E.I.T.  
Research Associate Engineer

Austin J. Haase  
Undergraduate Research Assistant

Ronald K. Faller, Ph.D., P.E.  
Research Associate Professor  
MwRSF Director

## **MIDWEST ROADSIDE SAFETY FACILITY**

Nebraska Transportation Center  
University of Nebraska-Lincoln  
130 Whittier Research Center  
2200 Vine Street  
Lincoln, Nebraska 68583-0853  
(402) 472-0965

Submitted to

## **IOWA DEPARTMENT OF TRANSPORTATION**

Office of Design  
Iowa Department of Transportation  
800 Lincoln Way  
Ames, IA 50010

MwRSF Research Report No. TRP-03-325-15

November 3, 2015

## TECHNICAL REPORT DOCUMENTATION PAGE

1. Report No. <b>TRP-03-325-15</b>	2.	3. Recipient's Accession No.	
4. Title and Subtitle <b>Attachment of Combination Rails to Concrete Parapets Utilizing Epoxy Adhesive Anchors</b>		5. Report Date <b>November 3, 2015</b>	
		6.	
7. Author(s) <b>Bielenberg, R.W., Reid, J.D., Rosenbaugh, S.K., Haase, A.J., and Faller, R.K.</b>		8. Performing Organization Report No. <b>TRP-03-325-15</b>	
9. Performing Organization Name and Address <b>Midwest Roadside Safety Facility (MwRSF) Nebraska Transportation Center University of Nebraska-Lincoln 130 Whittier Research Center 2200 Vine Street Lincoln, Nebraska 68583-0853</b>		10. Project/Task/Work Unit No.	
		11. Contract © or Grant (G) No. <b>TPF-5(193) Supplement #73</b>	
12. Sponsoring Organization Name and Address <b>Iowa Department Of Transportation Office of Design Iowa Department of Transportation 800 Lincoln Way Ames, IA 50010</b>		13. Type of Report and Period Covered <b>Final Report: TRP-03-325-15</b>	
		14. Sponsoring Agency Code <b>RPFP-IOWA-1</b>	
15. Supplementary Notes <b>Prepared in cooperation with U.S. Department of Transportation, Federal Highway Administration.</b>			
16. Abstract <p>The Iowa Department of Transportation (IaDOT) was interested in investigating the use of epoxy adhesive anchorages for the attachment of posts used in the BR27C combination bridge rail system. Alternative anchorage concepts were developed using a modified version of the ACI 318-11 procedures for embedded anchor design. Four design concepts were developed for review by IaDOT, including: (1) a four-bolt square anchorage, (2) a four-bolt spread anchorage, (3) a two-bolt centered anchorage, and (4) a two-bolt offset anchorage. IaDOT representatives selected the four-bolt spread anchorage and the two-bolt offset anchorage as the preferred designs for evaluation. In addition to these two proposed configurations, IaDOT also requested that the researchers evaluate a third option that had been previously installed on the US-20 bridge near Hardin, IA.</p> <p>The proposed alternative anchorages and the original cast-in-place anchorage for the BR27C combination bridge rail were evaluated through dynamic component testing. The test of the original cast-in-place anchorage was used as a baseline for comparison with the alternative designs. Test no. IBP-1 of the original cast-in-place anchorage developed a peak load of 22.9 kips (101.9 kN) at a deflection of 1.5 in. (38 mm). All three of the tested alternative anchorages provided greater load capacity than the original cast-in-place design and were deemed acceptable surrogates. Of the three alternative designs, the two-bolt offset design was deemed the best option.</p>			
17. Document Analysis/Descriptors <b>Highway Safety, Crash Test, Roadside Appurtenances, Combination Bridge Rail, Dynamic Component Testing, Epoxy Adhesive Anchorage</b>		18. Availability Statement <b>No restrictions. Document available from: National Technical Information Services, Springfield, Virginia 22161</b>	
19. Security Class (this report) <b>Unclassified</b>	20. Security Class (this page) <b>Unclassified</b>	21. No. of Pages <b>118</b>	22. Price

## **DISCLAIMER STATEMENT**

This report was completed with funding from the Federal Highway Administration, U.S. Department of Transportation, and the Iowa Department of Transportation. The contents of this report reflect the views and opinions of the authors who are responsible for the facts and the accuracy of the data presented herein. The contents do not necessarily reflect the official views or policies of the Iowa Department of Transportation, the Federal Highway Administration, nor the U.S. Department of Transportation. This report does not constitute a standard, specification, regulation, product endorsement, or an endorsement of manufacturers.

## **UNCERTAINTY OF MEASUREMENT STATEMENT**

The Midwest Roadside Safety Facility (MwRSF) has determined the uncertainty of measurements for several parameters involved in standard full-scale crash testing and non-standard testing of roadside safety features. Information regarding the uncertainty of measurements for critical parameters is available upon request by the sponsor and the Federal Highway Administration.

## **INDEPENDENT APPROVING AUTHORITY**

The Independent Approving Authority (IAA) for the data contained herein was Dr. Jennifer Schmidt, Research Assistant Professor.

## **ACKNOWLEDGEMENTS**

The authors wish to acknowledge several sources that made a contribution to this project:

(1) the Iowa Department of Transportation; and (2) MwRSF personnel for constructing the barriers and conducting the crash tests.

Acknowledgement is also given to the following individuals who made a contribution to the completion of this research project.

### **Midwest Roadside Safety Facility**

J.C. Holloway, M.S.C.E., E.I.T., Test Site Manager  
K.A. Lechtenberg, M.S.M.E., E.I.T., Research Associate Engineer  
J.D. Schmidt, Ph.D., P.E., Research Assistant Professor  
C.S. Stolle, Ph.D., Research Assistant Professor  
A.T. Russell, B.S.B.A., Shop Manager  
K.L. Krenk, B.S.M.A., former Maintenance Mechanic  
S.M. Tighe, Laboratory Mechanic  
D.S. Charroin, Laboratory Mechanic  
M.A. Rasmussen, Laboratory Mechanic  
E.W. Krier, Laboratory Mechanic  
Undergraduate and Graduate Research Assistants

### **Iowa Department of Transportation**

Chris Poole, P.E., Roadside Safety Engineer  
Brian Smith, P.E., Methods Engineer



## TABLE OF CONTENTS

TECHNICAL REPORT DOCUMENTATION PAGE .....	i
DISCLAIMER STATEMENT .....	ii
UNCERTAINTY OF MEASUREMENT STATEMENT .....	ii
INDEPENDENT APPROVING AUTHORITY.....	ii
ACKNOWLEDGEMENTS .....	iii
TABLE OF CONTENTS.....	iv
LIST OF FIGURES .....	vi
LIST OF TABLES .....	viii
1 INTRODUCTION .....	1
1.1 Background .....	1
1.2 Objective .....	3
1.3 Scope.....	3
2 DESIGN OF ALTERNATIVE EPOXY ADHESIVE ANCHORAGE.....	5
2.1 Design Methodology.....	5
2.2 IaDOT BR27C Combination Bridge Rail.....	6
2.3 Alternative Anchorage Design Calculations.....	10
2.4 Alternative Anchorage Concepts .....	15
2.4.1 Four-Bolt Square Anchorage .....	15
2.4.2 Four-Bolt Spread Anchorage .....	17
2.4.3 Two-Bolt Centered Anchorage .....	17
2.4.4 Two-Bolt Offset Anchorage .....	20
2.5 Selection of Preferred Alternative Anchorage Concepts for Evaluation .....	20
3 POST TESTING CONDITIONS.....	26
3.1 Purpose.....	26
3.2 Scope.....	26
3.3 Equipment and Instrumentation.....	50
3.3.1 Bogie Vehicle.....	50
3.3.2 Accelerometers .....	51
3.3.3 Retroreflective Optic Speed Trap .....	51
3.3.4 Digital Photography .....	52
3.4 End of Test Determination.....	52
3.5 Data Processing.....	52
4 COMPONENT TESTING RESULTS AND DISCUSSION .....	54
4.1 Results.....	54
4.1.1 Test No. IBP-1 .....	55
4.1.2 Test No. IBP-2 .....	60

4.1.3 Test No. IBP-3 ..... 65

4.1.4 Test No. IBP-4 ..... 69

4.2 Discussion ..... 73

5 SUMMARY, CONCLUSIONS, AND RECOMMENDATIONS..... 81

6 REFERENCES ..... 83

7 APPENDICES ..... 84

    Appendix A. Alternative Epoxy Adhesive Anchor Design Calculations ..... 85

    Appendix B. Material Specifications ..... 94

    Appendix C. Bogie Test Results ..... 109

## LIST OF FIGURES

Figure 1. Proposed BR27C Combination Rail Attachment .....	2
Figure 2. BR27C Design on Concrete Bridge Deck and Sidewalk .....	7
Figure 3. IaDOT Revised BR27C Parapet Design.....	9
Figure 4. Concrete Area of Influence for Two Adjacent Anchors on Concrete Parapet .....	12
Figure 5. Comparison of ACI 318-11 Concrete Breakout and Hybrid Failure Assumptions.....	14
Figure 6. Four-Bolt Square Alternative Anchorage Concept .....	16
Figure 7. Four-Bolt Spread Alternative Anchorage Concept .....	18
Figure 8. Two-Bolt Centered Alternative Anchorage Concept .....	19
Figure 9. Two-Bolt Offset Alternative Anchorage Concept.....	21
Figure 10. BR27C Installation on US-20 Bridge Near Hardin, IA.....	22
Figure 11. BR27C Installation on US-20 Bridge Near Hardin, IA.....	23
Figure 12. BR27C Installation on US-20 Bridge Near Hardin, IA.....	24
Figure 13. BR27C Installation on US-20 Bridge Near Hardin, IA.....	25
Figure 14. Bogie Testing Matrix and Setup.....	29
Figure 15. Cast-in-Place Test Setup, Test No. IBP-1 .....	30
Figure 16. Four-Anchor Test Setup, Test No. IBP-2.....	31
Figure 17. Two-Anchor Offset Test Setup, Test No. IBP-3 .....	32
Figure 18. US-20 River Bridge Test Setup, Test No. IBP-4.....	33
Figure 19. System Layout .....	34
Figure 20. Post Layout Details.....	35
Figure 21. Cast-in-Place Component Details, Test No. IBP-1 .....	36
Figure 22. Four-Anchor Spread Component Details, Test No. IBP-2.....	37
Figure 23. Two-Anchor Offset Component Details, Test No. IBP-3 .....	38
Figure 24. US-20 River Bridge Component Details, Test No. IBP-4.....	39
Figure 25. Rebar Assembly Details .....	40
Figure 26. Additional Rebar Assembly Details .....	41
Figure 27. Bill of Bars .....	42
Figure 28. Concrete Details .....	43
Figure 29. Bill of Materials.....	44
Figure 30. Test Installation Photographs .....	45
Figure 31. Pre-Test Installation Photographs, Test No. IBP-1 .....	46
Figure 32. Pre-Test Installation Photographs, Test No. IBP-2 .....	47
Figure 33. Pre-Test Installation Photographs, Test No. IBP-3 .....	48
Figure 34. Pre-Test Installation Photographs, Test No. IBP-4 .....	49
Figure 35. Rigid-Frame Bogie on Guidance Track .....	50
Figure 36. Sequential Photographs, Test No. IBP-1 .....	57
Figure 37. Post-Impact Photographs, Test No. IBP-1 .....	58
Figure 38. SLICE-2 Force vs. Deflection and Energy vs. Deflection, Test No. IBP-1 .....	59
Figure 39. Sequential Photographs, Test No. IBP-2.....	62
Figure 40. Four-Anchor Post-Impact Photographs, Test No. IBP-2.....	63
Figure 41. SLICE-2 Force vs. Deflection and Energy vs. Deflection, Test No. IBP-2 .....	64
Figure 42. Sequential Photographs, Test No. IBP-3 .....	66
Figure 43. Post-Impact Photographs, Test No. IBP-3 .....	67
Figure 44. SLICE-2 Force vs. Deflection and Energy vs. Deflection, Test No. IBP-3 .....	68
Figure 45. Sequential Photographs, Test No. IBP-4.....	70

Figure 46. US-20 River Bridge Post-Impact Photographs, Test No. IBP-4 .....	71
Figure 47. SLICE-2 Force vs. Deflection and Energy vs. Deflection, Test No. IBP-4 .....	72
Figure 48. SLICE-2 Force vs. Deflection Comparison, All Bogie Tests .....	77
Figure 49. SLICE-2 Force vs. Deflection Comparison Zoom, All Bogie Tests .....	78
Figure 50. SLICE-2 Energy vs. Deflection Comparison, All Bogie Tests .....	79
Figure 51 SLICE-2 Energy vs. Deflection Comparison Zoom, All Bogie Tests .....	80
Figure A-1. Tensile Adhesive Anchorage Calculations, Four-Bolt Square Anchorage Concept .....	86
Figure A-2. Shear Adhesive Anchorage Calculations, Four-Bolt Square Anchorage Concept .....	87
Figure A-3. Tensile Adhesive Anchorage Calculations, Four-Bolt Spread Anchorage Concept .....	88
Figure A-4. Shear Adhesive Anchorage Calculations, Four-Bolt Spread Anchorage Concept .....	89
Figure A-5. Tensile Adhesive Anchorage Calculations, Two-Bolt Centered Anchorage Concept .....	90
Figure A-6. Shear Adhesive Anchorage Calculations, Two-Bolt Centered Anchorage Concept .....	91
Figure A-7. Tensile Adhesive Anchorage Calculations, Two-Bolt Offset Anchorage Concept .....	92
Figure A-8. Shear Adhesive Anchorage Calculations, Two-Bolt Offset Anchorage Concept.....	93
Figure B-1. Bill of Materials, Test Nos. IBP-1 through IBP-2.....	95
Figure B-2. Bill of Materials, Test Nos. IBP-3 through IBP-4.....	96
Figure B-3. Rebar Material Specification, Test Nos. IBP-1 through IBP-4.....	97
Figure B-4. Rebar Material Test Report, Test Nos. IBP-1 through IBP-4 .....	98
Figure B-5. Rebar Material Test Report, Test Nos. IBP-1through IBP-4 .....	99
Figure B-6. Concrete Material Test Report for Footing Pour.....	100
Figure B-7. Concrete Material Test Report for Footing Pour.....	101
Figure B-8. Concrete Material Test Report for Parapet Pour .....	102
Figure B-9. Concrete Material Specification, Footing Pour .....	103
Figure B-10. Concrete Material Specification, Parapet Pour .....	104
Figure B-11. Concrete Material Specification, Footing Pour .....	105
Figure B-12. Concrete Material Specification, Parapet Pour .....	106
Figure B-13. Concrete Gradation Specification, Test Nos. IBP-1 through IBP-4.....	107
Figure B-14. Aggregate Quality Analysis, Test Nos. IBP-1 through IBP-4.....	108
Figure C-1. Test No. IBP-1 Results (SLICE-1).....	110
Figure C-2. Test No. IBP-1 Results (SLICE-2).....	111
Figure C-3. Test No. IBP-2 Results (SLICE-1).....	112
Figure C-4. Test No. IBP-2 Results (SLICE-2).....	113
Figure C-5. Test No. IBP-3 Results (SLICE-1).....	114
Figure C-6. Test No. IBP-3 Results (SLICE-2).....	115
Figure C-7. Test No. IBP-4 Results (SLICE-1).....	116
Figure C-8. Test No. IBP-4 Results (SLICE-2).....	117

**LIST OF TABLES**

Table 1. Dynamic Testing Summary .....54  
Table 2. Dynamic Testing Results .....73

## 1 INTRODUCTION

### 1.1 Background

Combination bridge rails are commonly used by many state departments of transportation and often consist of a concrete parapet with an upper steel railing system. In the past, these types of bridge rails have typically been designed with the steel posts attached to the concrete parapet using a cast-in-place anchorage system. While cast-in-place anchors have performed well, they have several disadvantages, including added complexity and construction costs, as well as issues with dimensional tolerances regarding their placement in the parapet.

The Iowa Department of Transportation (IaDOT) was interested in investigating the use of epoxy adhesive anchorages for the attachment of posts used in combination bridge rails. IaDOT desired an alternative anchorage method for the attachment of the steel beam-and-post system to a concrete parapet on the BR27C combination bridge rail system. An alternative epoxy adhesive connection detail was proposed, as shown in Figure 1. The Midwest Roadside Safety Facility (MwRSF) performed initial calculations to evaluate the capacity of the epoxy anchorage based on a previous MwRSF research study involving the dynamic component testing of anchors [1] and applying the methodologies found in ACI 318-11 [2]. From this preliminary analysis, it was found that the capacity of the proposed anchorage was potentially insufficient. However, the methodology provides conservative results and may underestimate anchorage capacity. As such, it was noted that the best evaluation of this proposed alternative anchorage system may be to perform dynamic component testing of the epoxy adhesive system.

IaDOT indicated that they desired an alternative epoxy adhesive anchorage system for the BR27C combination bridge railing, as well as evaluation of an epoxy adhesive anchorage system for the BR27C previously used on an existing bridge on US-20 in Iowa.

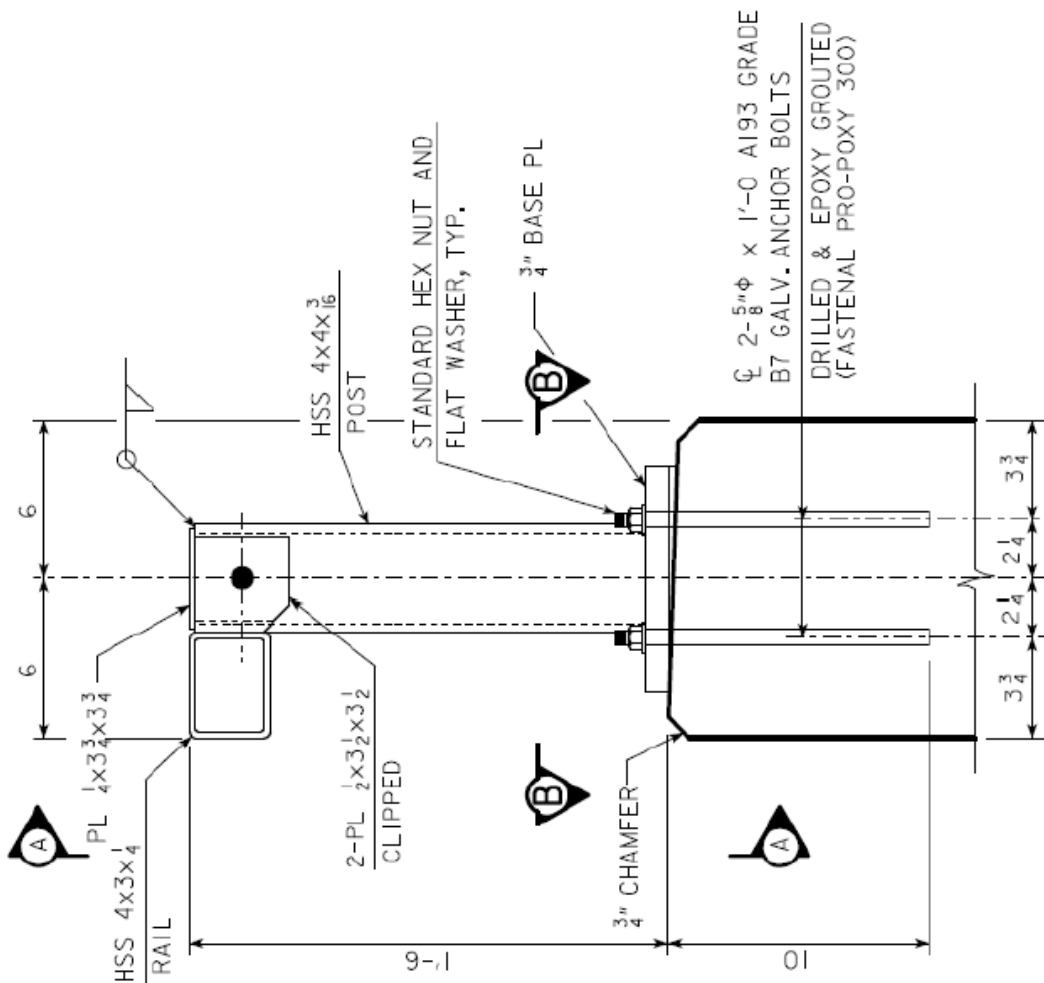


Figure 1. Proposed BR27C Combination Rail Attachment

## **1.2 Objective**

The research objective was to design and evaluate alternative epoxy adhesive anchorages for use in the IaDOT BR27C combination bridge rail system. The alternative epoxy adhesive anchorages were to have equal or greater capacity than the current cast-in-place anchorage, so that they can be used in new construction or as a retrofit to modify existing bridge railings. The proposed epoxy attachment designs were to be evaluated through dynamic component testing to verify their capacity.

## **1.3 Scope**

The research effort consisted of design, testing, and evaluation of alternative epoxy adhesive anchorages for attaching the beam and post system of the BR27C combination bridge railing to a concrete parapet. MwRSF researchers reviewed the current cast-in-place anchorage design and developed alternative epoxy adhesive anchorage configurations, including inline anchor systems and a four-anchor system similar to the cast in place configuration but with spacing more compatible with the epoxy adhesive. The alternative epoxy adhesive anchorage systems were submitted to IaDOT for review and selection of preferred systems to be tested and evaluated.

Dynamic component testing was used to evaluate the selected epoxy adhesive anchorages and to demonstrate that the capacities of the proposed epoxy anchorages were equal to or greater than the existing cast-in-place anchorage system. The capacity of the current cast-in-place anchorage had not been fully quantified with testing. Thus, one dynamic component test was performed on a bridge rail post using the current cast-in-place anchorage configuration. Additional dynamic component tests were performed on the proposed alternative epoxy adhesive anchorage systems. The target impact conditions for all tests would be identical, and the tests were configured so that the applied impact load occurred at a height on the post that produced a



bending moment and combined loading on the anchorage system similar to that provided during vehicle crash events. The force versus deflection, energy dissipated versus deflection, and failure modes were documented for each test and compared to one another. These comparisons were used to verify that the proposed anchorages provided equal or greater capacities than the current anchorage, and that the alternative anchorages did not display undesirable failure modes.

IaDOT also proposed an additional test to evaluate a currently installed epoxy adhesive anchorage for the BR27C bridge rail used on the US-20 bridge near Hardin, IA. This setup was tested and analyzed using the procedures described above for the cast-in-place design and the newly designed epoxy anchorages.

## **2 DESIGN OF ALTERNATIVE EPOXY ADHESIVE ANCHORAGE**

### **2.1 Design Methodology**

Limited prior research has been conducted related to the use of epoxy adhesive anchors for attachment of a beam-and-post railing system to the top of concrete parapets. In 2010, Texas A&M Transportation Institute (TTI) researchers conducted a study to develop two new retrofit combination steel and concrete bridge rail designs [3]. This effort included the design of a retrofit epoxy anchorage design and pendulum testing of the anchorage system on a short section of concrete parapet in order to verify the capacity of the connection. Thus, the methodology of evaluating the alternative epoxy anchorage systems through dynamic component testing has been previously accepted.

MwRSF researchers also conducted a related study for the Wisconsin Department of Transportation involving epoxy adhesive anchors for attachment of concrete barriers to bridge decks [1]. The objective of this research was to determine if epoxy adhesive anchors could be utilized to attach concrete barriers to bridge decks and to develop design procedures for implementing epoxy adhesive anchorages into concrete bridge railings. A series of 16 dynamic bogie tests and one static test were conducted to investigate the behavior of epoxy adhesive anchors under dynamic load. Additional dynamic tests were conducted on 1½-in. (29-mm) diameter ASTM A307 threaded rods.

Comparisons were made between the results from the component tests and analytical models for epoxy adhesive anchors. The cone or full uniform bond model [4-5] and ACI 318-11 [2] procedures were both compared with the component tests in order to verify their effectiveness. Review of the comparisons between the analytical models and the tensile component tests found that both the cone and full uniform bond model and ACI 318-11 provided reasonable predictions for the failure mode of the epoxy adhesive anchors, but both methods

were conservative for the prediction of capacities (i.e., underestimated strength). The shear testing results and predicted capacities were compared, but findings were limited due to the observed failure modes in the component tests. However, it was found that ACI 318-11 provided reasonable yet conservative estimates for shear capacity of the epoxy adhesive anchors. It was also found that the proposed dynamic increase factors for concrete breakout, steel fracture, and bond strength improved the prediction of the anchor failure modes and capacities. It was recommended that the ACI 318-11 procedures be combined with the proposed dynamic increase factors for designing epoxy adhesive anchors. Recommendations for future research were made to fill gaps in the existing research effort and to evaluate the conservative nature of the proposed design methodology.

Based on the previous research on epoxy adhesive anchorages, it was proposed to design several potential alternatives for the BR27C combination rail anchorage using the analytical procedures developed during the Wisconsin study. Then IaDOT could select the alternative anchorage designs they found most desirable, and dynamic component testing would be performed to verify their capacity.

## **2.2 IaDOT BR27C Combination Bridge Rail**

The BR27C combination bridge rail design was originally developed and tested at the Texas A&M Transportation Institute in 1993 [6]. The bridge rail design consisted of a 24-in. (610-mm) tall by 10-in. (254-mm) thick vertical concrete parapet, with the combination rail mounted on top of the parapet, as shown in Figure 2. Both the sidewalk- and bridge deck-mounted versions of the combination bridge rail were subjected to three full-scale crash tests according to Performance Level 2 (PL-2) of the *AASHTO Guide Specifications for Bridge Railings* [7]. The three full-scale crash tests included:

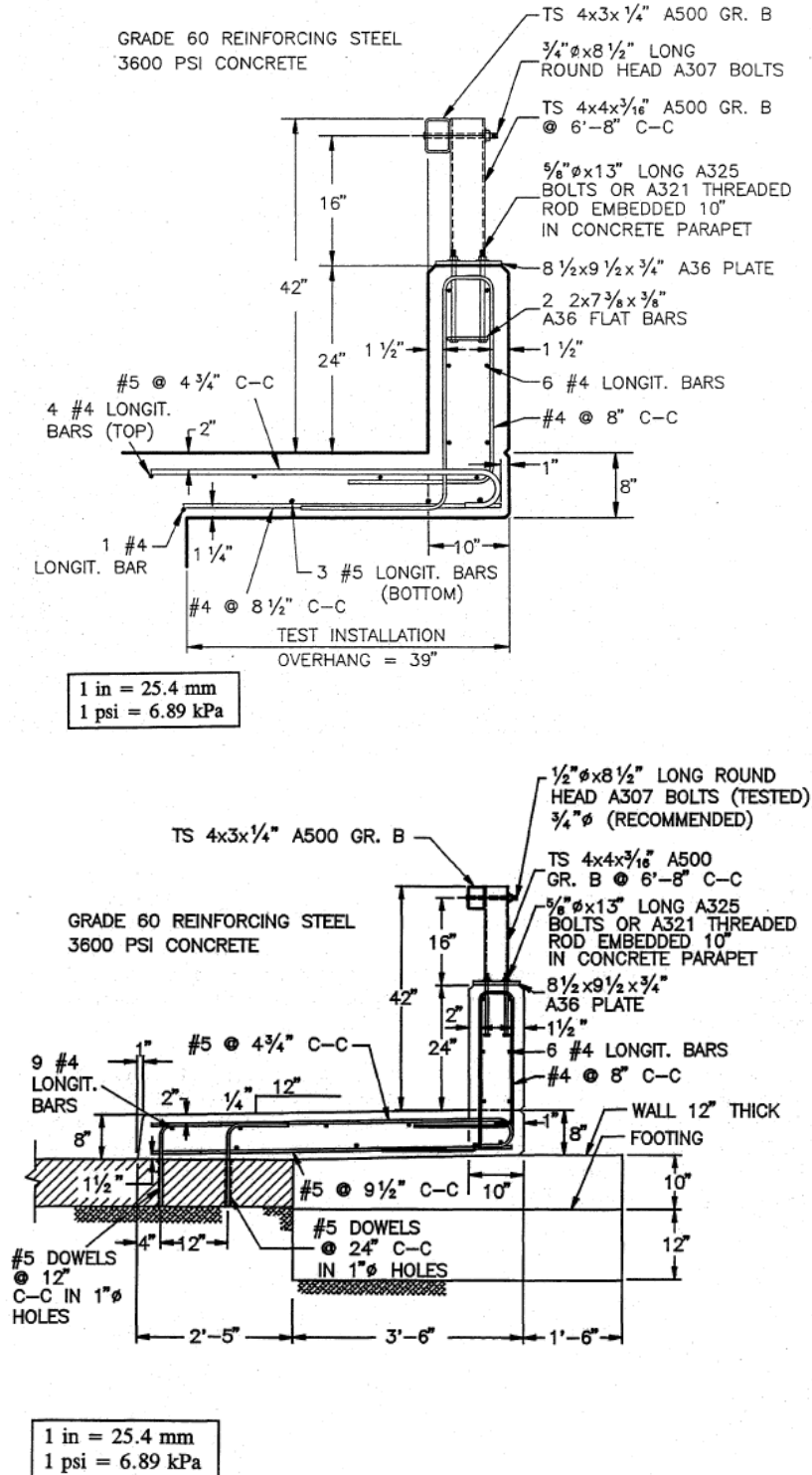


Figure 2. BR27C Design on Concrete Bridge Deck and Sidewalk

1. Impact of an 1,800-lb (817-kg) small car at 60 mph (96.6 km/h) and an angle of 20 degrees.
2. Impact of a 5,400-lb (2,452-kg) pickup truck at 60 mph (96.6 km/h) and an angle of 20 degrees.
3. Impact of an 18,000-lb (8,172-kg) single unit truck at 50 mph (80.5 km/h) and an angle of 15 degrees.

All six crash tests of the BR27C combination rail were successful and met the AASHTO PL-2 criteria. Damage to the combination rail and parapet was limited in the majority of the tests. One of the single-unit truck tests did show detachment of the rail from the support posts, but most of the bridge rail damage was minor, and the combination rail posts remained attached to the parapet in all of the tests.

Subsequent to the design and testing of the original BR27C combination bridge rail, the Federal Highway Administration (FHWA) released a memo regarding listings of bridge railing designs that were considered acceptable for use on federal aid projects by virtue of their previous crash test performance [8]. FHWA officials reviewed these listings and assigned each a rating that was relative to one of the six test levels suggested in NCHRP Report No. 350 [9]. In this memo, the BR27C design was listed as equivalent to NCHRP Report No. 350 Test Level 4 (TL-4).

Based on the previous testing and the FHWA memo, IaDOT has previously used the BR27C railing on their facilities. As part of recent updates to their bridge rail designs, IaDOT has switched to a slightly wider concrete parapet design that is 24 in. (610 mm) tall by 12 in. (305 mm) thick, as shown in Figure 3. As such, the revised parapet design was used for the alternative epoxy adhesive anchor designs developed as part of this research.

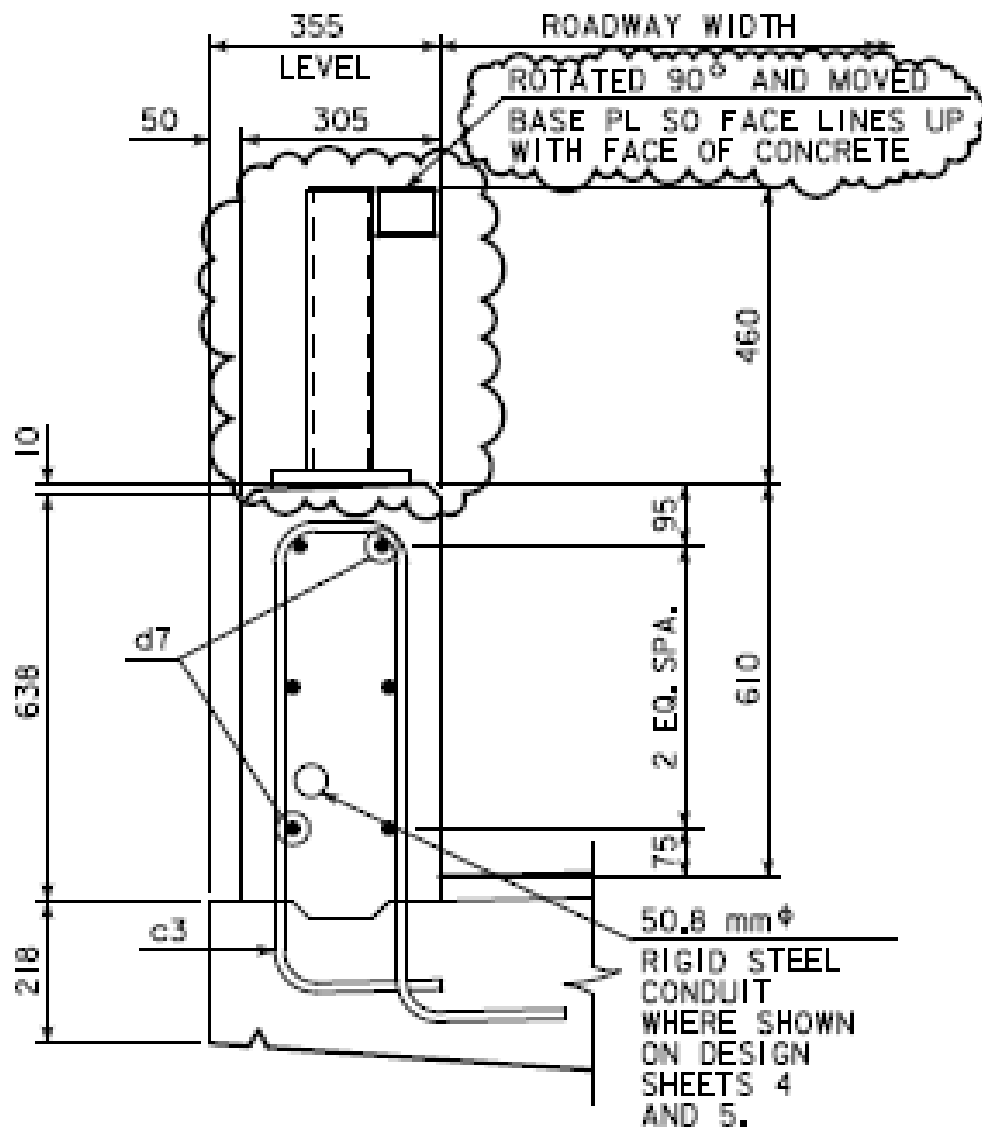


Figure 3. IaDOT Revised BR27C Parapet Design

## 2.3 Alternative Anchorage Design Calculations

The design of the epoxy adhesive anchorages began with determination of a design load for the post and baseplate of the BR27C combination rail. Because the exact impact loading of the BR27C rail during the original crash testing was unknown, it was assumed that the anchorage designs would need to develop the full-moment capacity of the bridge rail post. Designing the alternative anchorages to meet this load would ensure that the designs were as strong as the original cast-in-place anchorage that was tested and could develop the upper bound of the potential load imparted to the anchorage.

The BR27C railing uses a HSS 4-in. x 4-in. x  $\frac{3}{16}$ -in. (102-mm x 102-mm x 5-mm) A500 Grade B steel tube for the vertical support post attached to a  $\frac{3}{4}$ -in. (19-mm) thick A36 steel baseplate. The tube section has an area, section modulus, and plastic section modulus of 2.77 in<sup>2</sup> (1,787 mm<sup>2</sup>), 3.30 in<sup>3</sup> (54,077 mm<sup>3</sup>), and 3.91 in<sup>3</sup> (64,073 mm<sup>3</sup>), respectively. A500 Grade B steel has a minimum yield strength of 42 ksi (289.6 MPa). However, steel tube sections designed as A500 Grade B are regularly fabricated from higher-strength steel, occasionally up to the A500 Grade C minimum yield strength of 46 ksi (317.2 MPa). Assuming the potential for the higher-strength Grade C material, and using the plastic section modulus of the tube, gives a moment capacity of the post of 179.9 kip-in. (20.33 kN-m). This moment capacity was rounded to an even 180 kip-in. (20.34 kN-m) and used for the design calculations of the alternative epoxy adhesive anchorages.

As noted previously, the design of alternative epoxy adhesive anchorages for the BR27C combination bridge rail was developed using ACI 318-11 procedures for design of epoxy anchorages with modifications of dynamic increase factors for concrete breakout, steel fracture, and bond strength. Details of the design calculations for the final designs are provided in Appendix A, but some comments on the basic design procedures should be noted. First, for

concepts incorporating two rows of anchors, it was assumed the tensile loads to develop moment capacity would be supplied by the front anchors while the rear anchors would develop the shear loads. Anchorage concepts that used only a single row of bolts had to account for both tensile and shear loads in all anchors. The design calculations evaluated steel fracture, concrete breakout, and adhesive bond failure in tension. Shear calculations evaluated steel fracture, concrete breakout, and concrete pryout.

The calculations also accounted for reduction in anchor capacity due to the distance to the edge of the parapet and anchor spacing based on the area of influence for the concrete and bond failures. Anchorage area of influence defines a region of the concrete where the anchorage forces are distributed in order to develop load for both concrete breakout and bond strength. If these areas exceed the edge of the parapet or overlap the area of influence of other anchors, then the capacity of the anchor is reduced by the ratio of the unavailable area divided by the original assumed influence area. A simple example of area of influence for two anchors that exceed the concrete edge and interfere with adjacent anchors is shown in Figure 4. Note that for the simple two-anchor example, the purple area denotes where the area of influence exceeds beyond the parapet edges. The orange area indicates where the area of influence for anchors “A” and “B” overlap. In this area, only half of the overlapping area can be utilized by each anchor, so the anchor capacity must be reduced accordingly.

A final note should be made regarding an additional modification that was made to the ACI 318-11 calculations for this project. Initial calculations for tensile concrete breakout capacity indicated that extremely large embedment depths would be required to provide the desired anchorage, due to the edge distance of the anchors to the side of the parapet. These calculations assume a concrete cone failure of the parapet that extends diagonally from the base of the anchor to the edges of the area of influence.



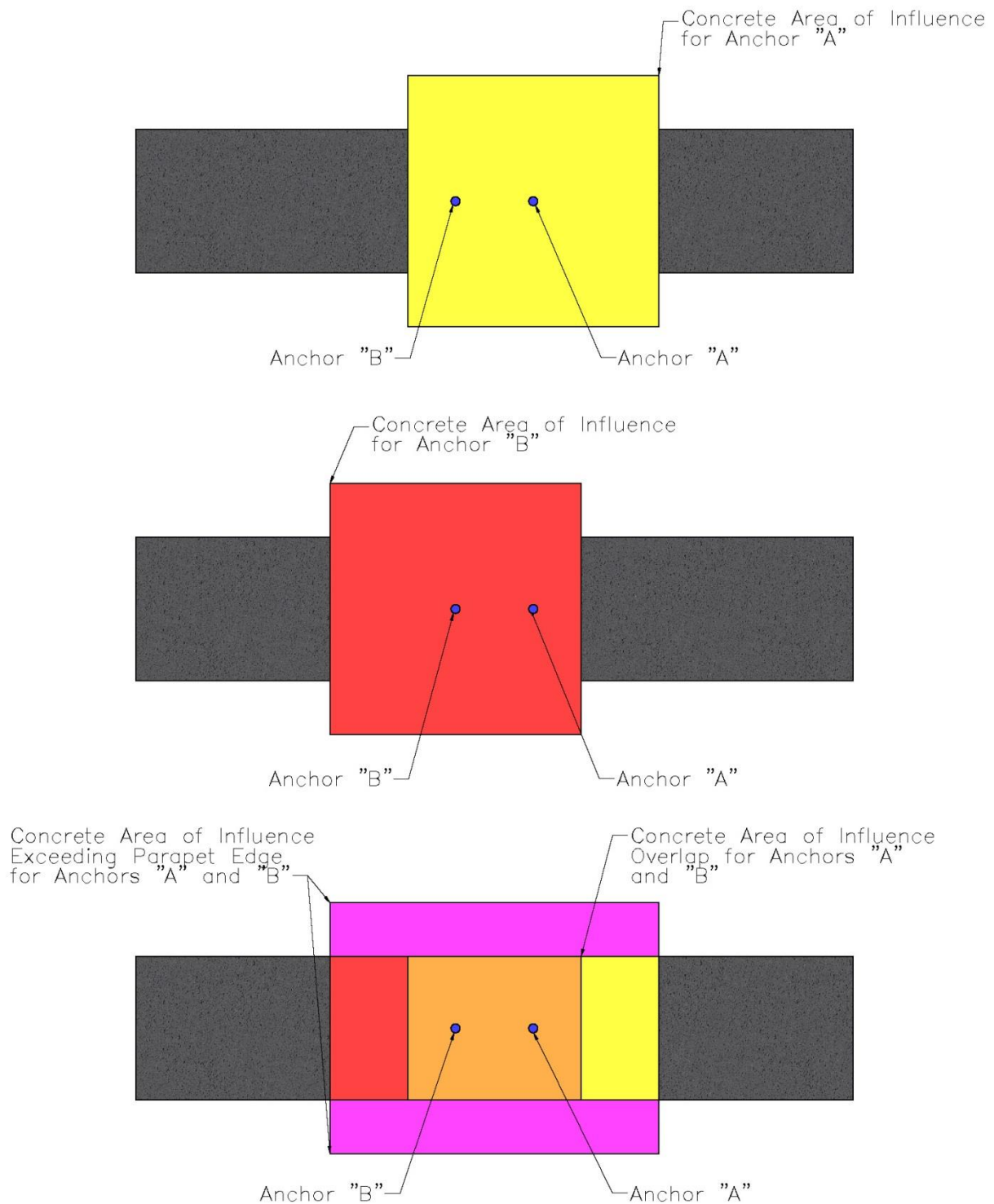
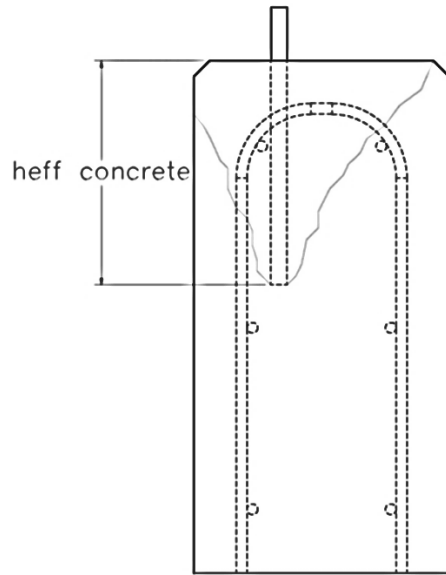


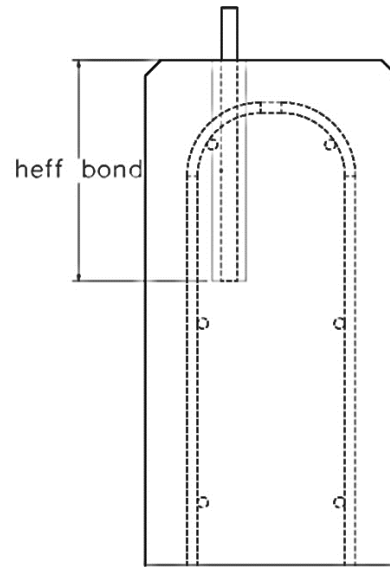
Figure 4. Concrete Area of Influence for Two Adjacent Anchors on Concrete Parapet

While this assumption may be true of large-area, unreinforced slabs, it was not believed to be accurate for the reinforced concrete parapet in this research. A more reasonable form of the failure mode was believed to be a hybrid concrete cone and adhesive bond failure, as shown in Figure 5. In this type of failure mode, the concrete cone failure is prevented from extending to the base of the anchor by the longitudinal rebar. The hybrid failure assumption was extended to the ACI 318-11 calculations by assuming that the upper half of the anchor embedment contributed to the concrete breakout and the lower half of the embedment contributed to a bond failure. Thus, the calculations for the concrete breakout and bond strength were performed with one-half of the actual anchor embedment and then summed to determine the tensile anchor capacity.

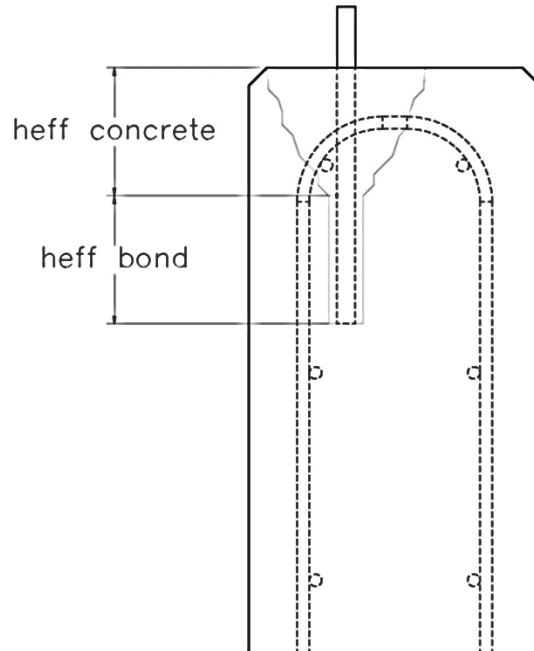
All calculations for the alternative adhesive anchorages were performed assuming the use of Hilti RE-500 epoxy adhesive, which has a bond strength of 1,800 psi (12.4MPa). It was assumed that other epoxy adhesives could also be used with the alternative anchorages, as long as the bond strength of the adhesive was equal to or greater than 1,800 psi (12.4MPa). The concrete compressive strength for the design calculations was assumed to be 4,000 psi (27.6 MPa).



ACI 318–11 Concrete  
Breakout Failure Assumption



ACI 318–11 Bond  
Failure Assumption



Hybrid Concrete and Bond  
Failure Assumption

Figure 5. Comparison of ACI 318-11 Concrete Breakout and Hybrid Failure Assumptions

## **2.4 Alternative Anchorage Concepts**

Multiple concepts were developed and evaluated as part of the design effort, but only four concepts were submitted to IaDOT for review. The four concepts varied the number, placement, and size of the anchors. It was believed that all of the designs would meet the design tensile and shear loads determined from the moment capacity of the post. Each of the concepts is reviewed in the subsequent sections. Details of the design calculations for the final designs are provided in Appendix A.

### **2.4.1 Four-Bolt Square Anchorage**

The four-bolt square anchorage concept used a rectangular bolt pattern of four bolts on a square plate, as shown in Figure 6. The four bolts allowed for a design where the front bolts develop the tensile loads and the back anchors accounted for the shear loads.

This concept was also similar in layout to the current cast-in-place design. The anchor bolts were  $\frac{5}{8}$  in. (16 mm) in diameter and embedded 10 in. (254 mm) into the parapet. All of the anchorage concepts were designed to have between  $\frac{3}{4}$  in. (19 mm) and 1 in. (25 mm) of clearance from the longitudinal parapet reinforcement to ensure that they were not impacted during installation of the epoxy anchors. This constrained the design somewhat, but the concept did meet the tension and shear load requirements as determined from the moment capacity of the vertical post. The main drawback of this concept was that the anchors were only 2.75 in. (70 mm) apart across the width of the parapet, which could make it difficult to install.

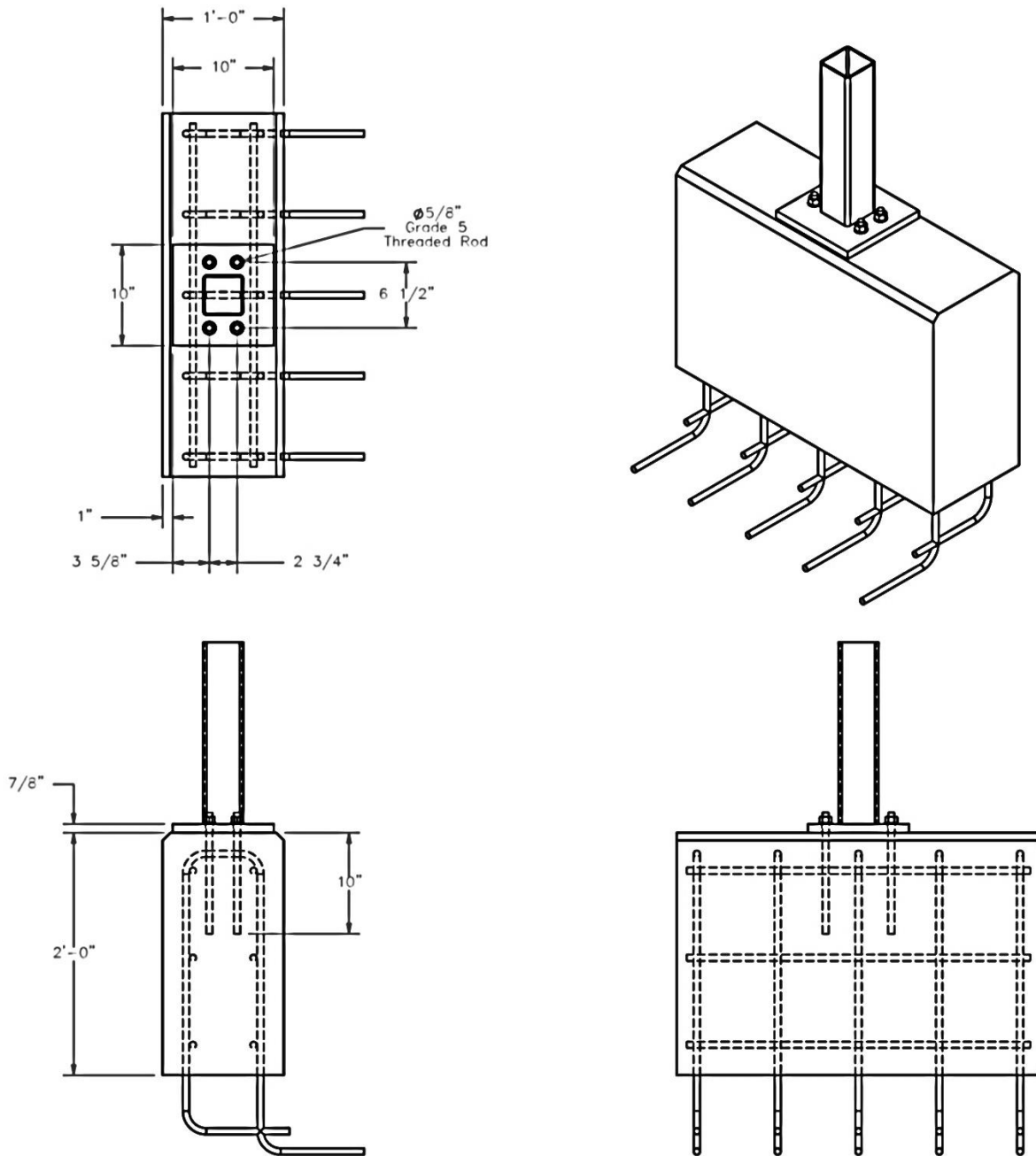


Figure 6. Four-Bolt Square Alternative Anchorage Concept

#### **2.4.2 Four-Bolt Spread Anchorage**

The four-bolt spread anchorage concept used the same anchor size and embedment depth, but it spread out the backside anchors to improve the anchor spacing for a four-bolt pattern, as shown in Figure 7. Design calculations indicated that the increased spacing of the anchors not only satisfied the design loads, but led to this configuration having a higher capacity than the four-bolt square anchorage concept.

#### **2.4.3 Two-Bolt Centered Anchorage**

The two-bolt centered anchorage concept used a linear bolt pattern of two bolts centered on a square baseplate, as shown in Figure 8. This concept reduced the number of anchors but required increased anchor diameter and embedment depth due to combined shear and tension loading of the anchors. The concept used  $\frac{3}{4}$ -in. (19-mm) diameter bolts with an embedment of 12 in. (305 mm). Design calculations for this concept showed that the anchorage can develop both the shear and the tensile loads when determined individually. However, the ACI code recommends a reduction for combined loading, where the sum of the applied design load divided by the total capacity in both shear and tension must be less than 1.2. For this concept, that sum was calculated to be 1.44. However, neither the general anchor calculations nor the combined loading calculation in ACI 318-11 account for the reinforcing steel and its contributions to the anchorage capacity. As such, this design would potentially work under combined loads when including these other factors.

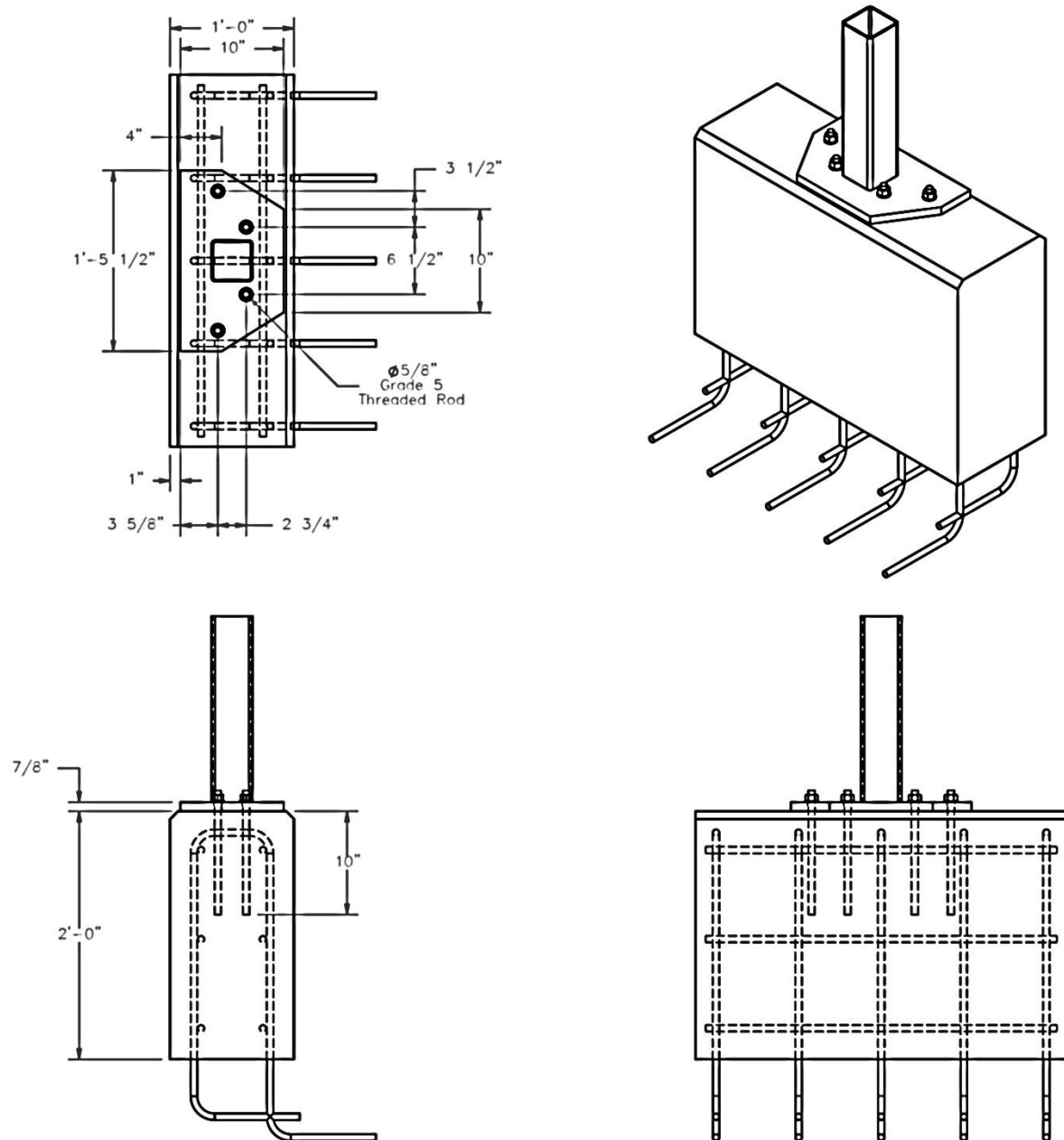


Figure 7. Four-Bolt Spread Alternative Anchorage Concept

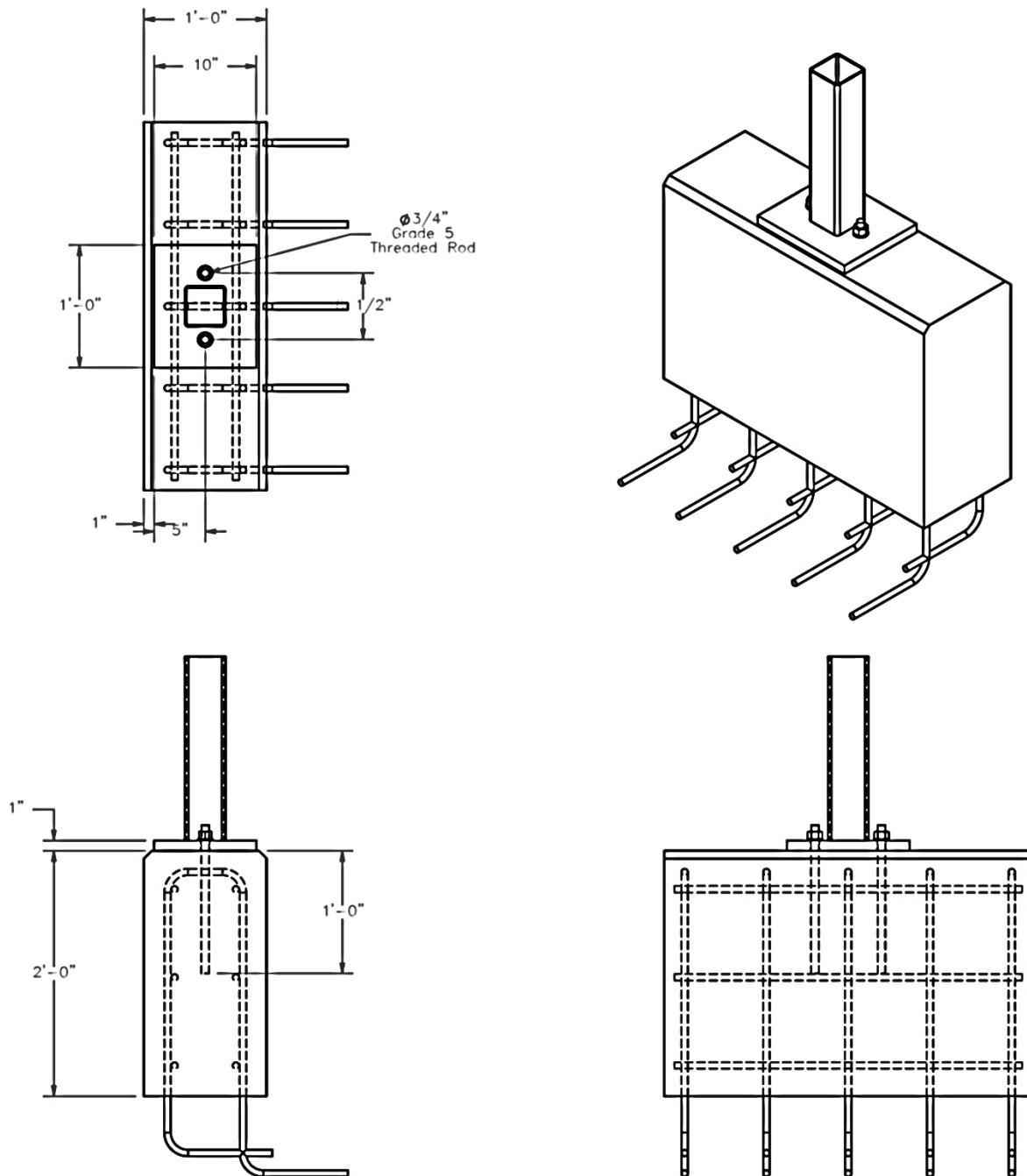


Figure 8. Two-Bolt Centered Alternative Anchorage Concept



#### **2.4.4 Two-Bolt Offset Anchorage**

The two-bolt offset anchorage concept used two bolts offset towards the front of the square baseplate, as shown in Figure 9. The design was identical to the centered concept, except that the bolts were offset towards the front of the parapet to increase the shear capacity sufficiently to meet the combined loading requirement in the ACI code. Thus, it was a more conservative design. Drawbacks to this design were the offset of the anchors and the potential for reverse bending loads. The researchers believed that the centered concept may be easier to install due to the bolts being centered on the rail rather than offset. Additionally, if the potential exists for significant reverse bending loads, then this concept would have reduced capacity in that regard. However, it was believed that the reverse bending loads on the BR27C combination rail were lower than the primary impact loads. Thus, the concern with respect to reverse bending overloading the anchorage was limited. In order to alleviate that concern, a smaller anchor could be placed on the backside of the post.

#### **2.5 Selection of Preferred Alternative Anchorage Concepts for Evaluation**

IaDOT representatives reviewed the four proposed alternative anchorage concepts and selected the four-bolt spread anchorage and the two-bolt offset anchorage as the preferred designs for evaluation through dynamic component testing. In addition to these two proposed configurations, IaDOT also requested that the researchers conduct dynamic testing on a third option that had been previously installed on the US-20 bridge near Hardin, IA, as shown in Figures 10 through 13. IaDOT was interested in evaluating whether this specific configuration meets/exceeds the capacity of the FHWA-approved cast-in-place BR27C combination bridge rail, and they wished to verify its performance as constructed.

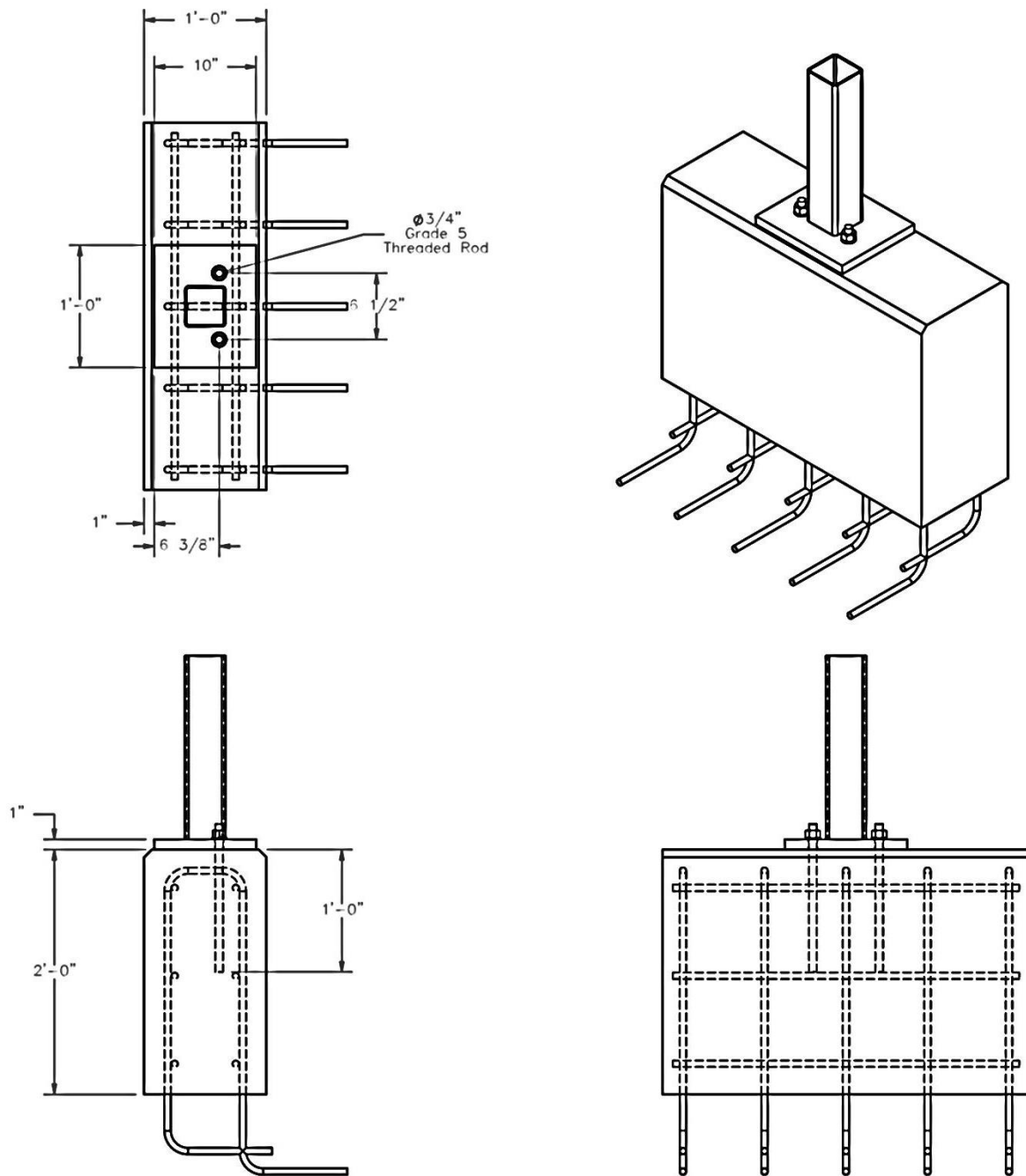


Figure 9. Two-Bolt Offset Alternative Anchorage Concept

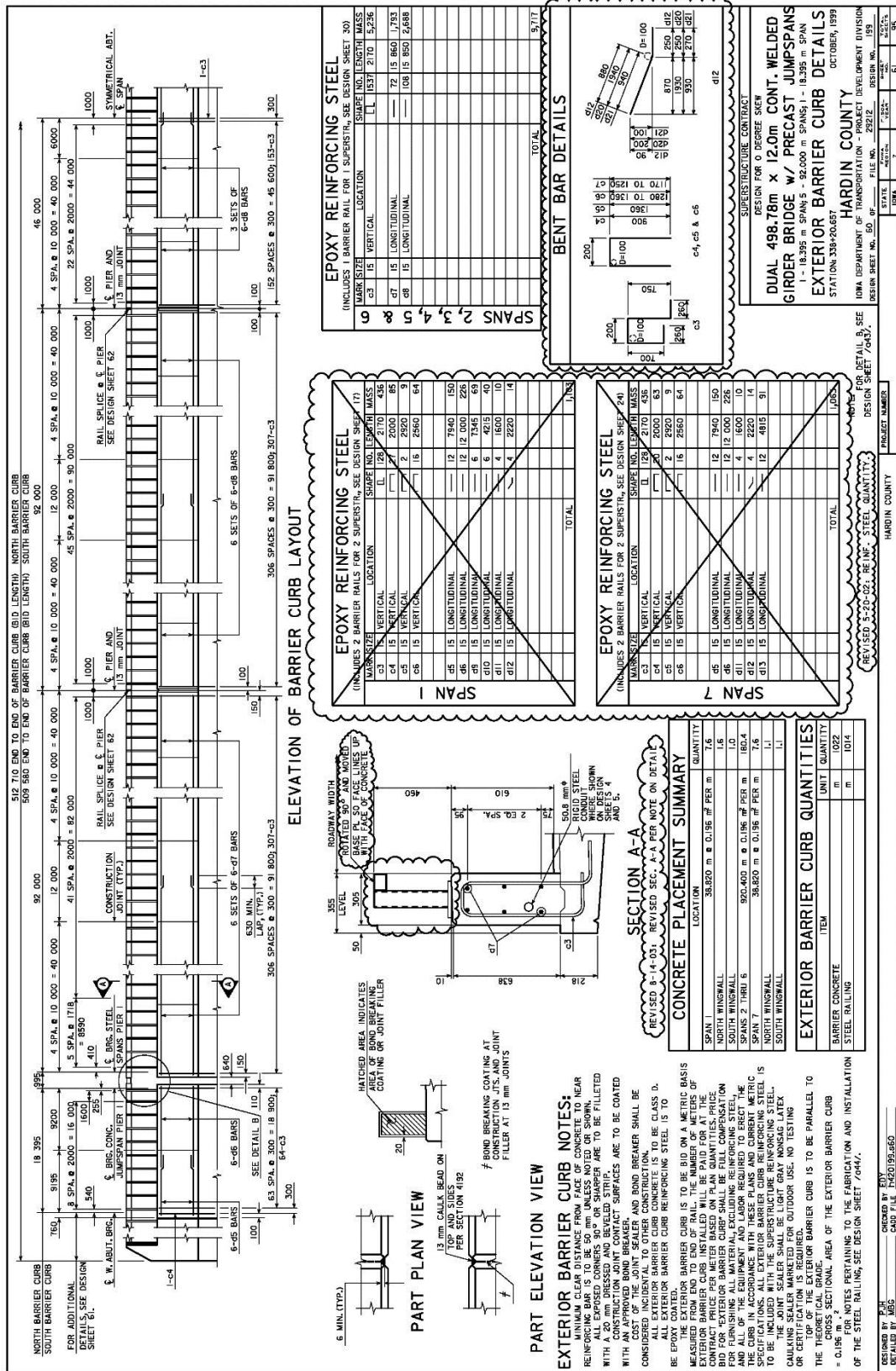


Figure 10. BR27C Installation on US-20 Bridge Near Hardin, IA

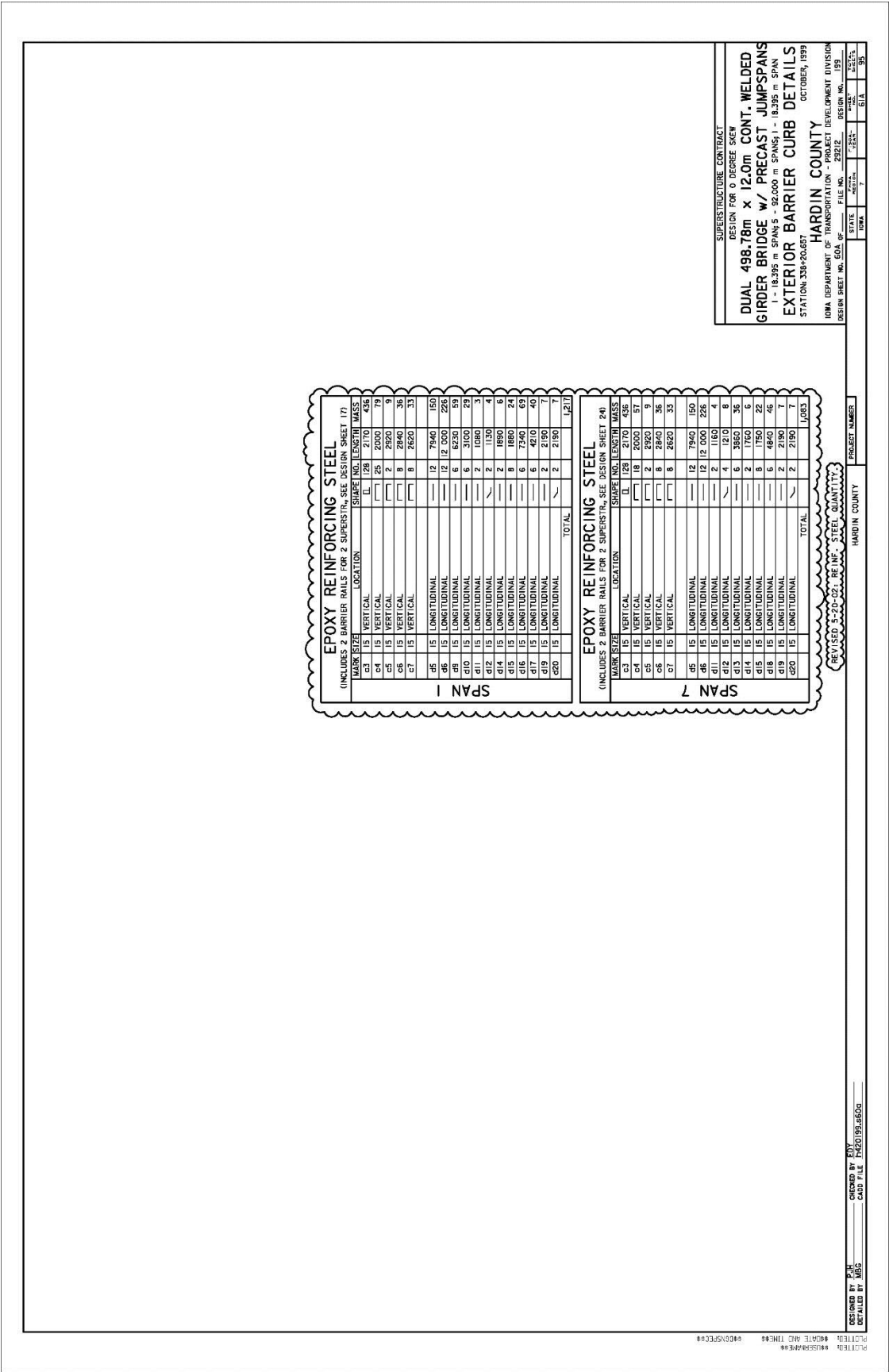
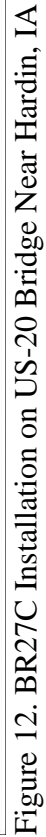


Figure 11. BR27C Installation on US-20 Bridge Near Hardin, IA



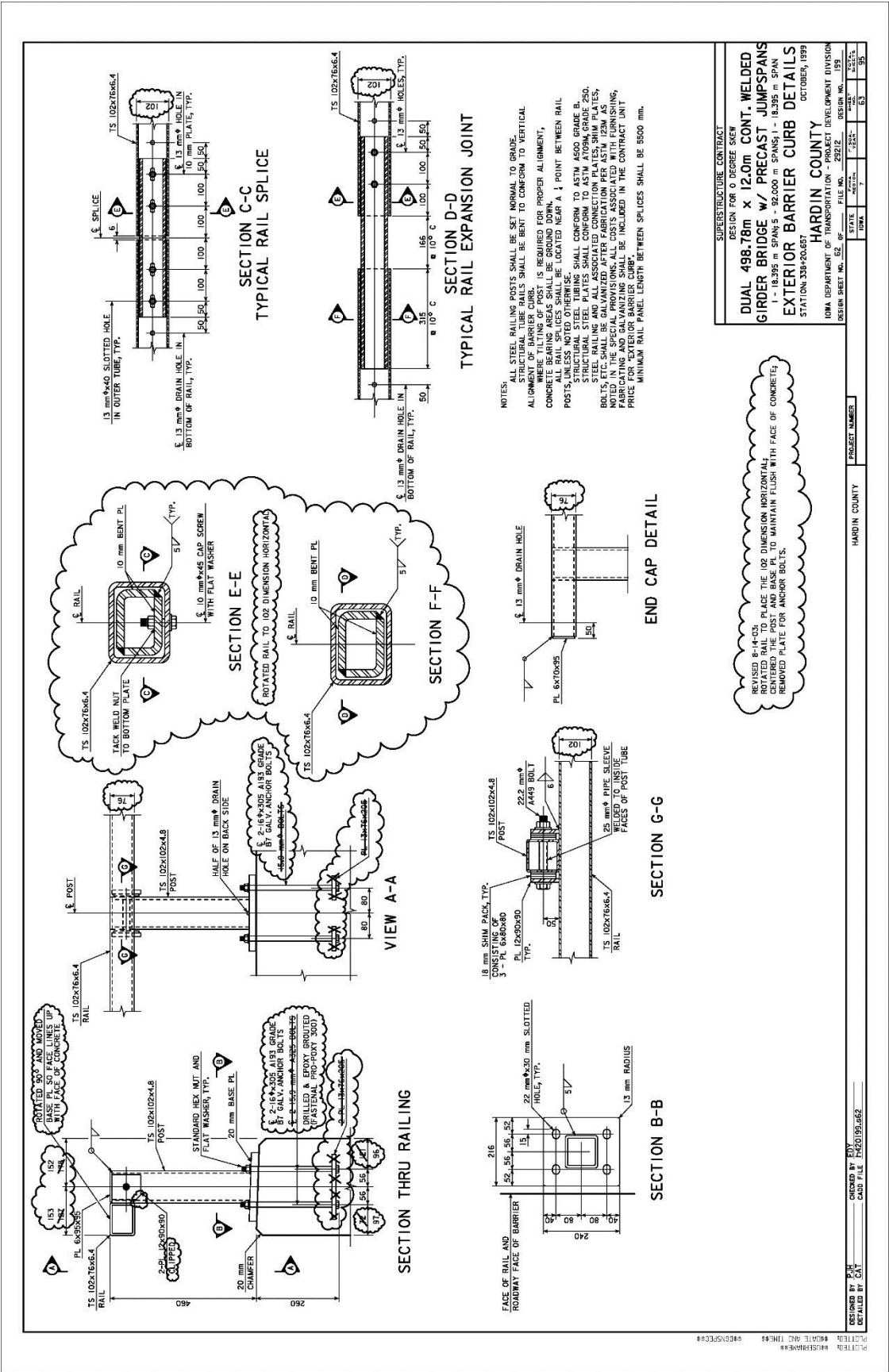


Figure 13. BR27C Installation on US-20 Bridge Near Hardin, IA

### **3 POST TESTING CONDITIONS**

#### **3.1 Purpose**

A series of four dynamic bogie tests were conducted on the original BR27C combination bridge rail post and three alternative epoxy adhesive anchorage designs. The purposes of these tests were to establish the baseline capacity of the original BR27C cast-in-place anchorage and compare this capacity with the proposed alternative designs. The target impact conditions for all tests were identical. The tests were configured so that the applied impact load would occur at a height of 16 in. (406 mm) above the top of the parapet on the post/rail in order to produce a bending moment in the post and combined loading on the anchorage system similar to that provided during vehicle crash events. The force versus deflection, energy dissipated versus deflection, and failure modes were documented for each test and compared to one another. These comparisons were then used to verify that the proposed anchorages provided equal or greater capacity than the full-scale crash tested anchorage. The tests required construction of a short section of simulated bridge rail for attachment of the post, baseplate, and anchor hardware. All dynamic tests were conducted at the MwRSF proving grounds in Lincoln, Nebraska.

#### **3.2 Scope**

Four dynamic bogie tests were conducted on HSS 4-in. x 4-in. x  $\frac{3}{16}$ -in. (102-mm x 102-mm x 5-mm) steel tubes with baseplates mounted on top of a reinforced concrete parapet. The reinforced concrete parapet was installed below grade, such that the top of the parapet was essentially level with the concrete apron at the test site. Installation of the parapet below grade allowed the researchers to impact the post assembly at the desired height to produce similar post loading to the horizontal bridge rail tube during an impact event. The concrete parapet layout was based on the parapet design used in the original full-scale crash testing of the BR27C combination bridge rail and the revised parapet design provided by IaDOT. As such, the parapet

was 10 in. (254 mm) wide on one end and was then widened to 12 in. (305 mm) for the remainder of the parapet. All parapet reinforcement was made consistent with the original and revised parapet designs that were provided. The concrete used for the parapet was selected to be a 3,600-psi (24.8-MPa) mix meeting IaDOT Class C-4 concrete specification. This mix design was consistent with the concrete strength of the parapet used in the original BR27C combination bridge rail crash testing. IaDOT typically uses a 4,000-psi (27.6-MPa) concrete mix for their concrete parapets, but the lower-strength concrete was selected for all the component tests in order to provide accurate data for the baseline test of the original cast-in-place anchorage and to provide a consistent comparison of anchorage capacity using the same concrete strength. It was believed that if the alternative anchorages provided equal or greater capacity to the original anchorage in the 3,600-psi (24.8-MPa) concrete, it would be acceptable in higher-strength concrete as well.

The posts and baseplates used in the dynamic component tests were developed based on details of the original BR27C combination bridge rail, the alternative anchorages developed in the previous chapter, and details provided by IaDOT for the US-20 bridge installation. All of the test setups used the same HSS 4-in. x 4-in. x  $\frac{3}{16}$ -in. (102-mm x 102-mm x 5-mm) steel tube welded to baseplates that were anchored to the concrete parapet. Baseplates for the four-bolt spread and two-bolt offset anchorages were designed based on the anchorage system and moment capacity of the post. The two remaining designs used baseplates based on the provided details. The two alternative anchor concepts developed in the previous chapter were installed using Hilti RE-500 SD epoxy adhesive. The anchorage for the US-20 bridge was installed with Fastenal Pro-Poxy 300, per the IaDOT details.


The target impact conditions were a speed of 15 mph (24.1 km/h) and an angle of 90 degrees, creating a “head-on” or full-frontal impact and strong-axis bending. Target impact



height for the testing was 16 in. (406 mm) above the ground line. The posts were impacted 17 in. (432 mm) above the top of the parapet due to the concrete parapet being 1 in. (25 mm) lower than grade.

The test matrix is shown in Figure 14, and the test setup is shown in Figures 15 through 29. Test installation photographs are shown in Figures 30 through 34. Material specifications, mill certifications, and certificates of conformity for the combination rails attached to concrete parapets are shown in Appendix B.

<p>Notes: (1) Instrumentation          –DTS SLICE 1 and 2          –High-speed cameras perpendicular, offset behind, and offset front          (2) Document parapet cracking and damage before and after test.          (3) Need concrete cylinders from the pour (ø6"x12" [ø152x305])          –12 from start of pour and 12 at end of pour          (4) Concrete parapet and grade beam may be constructed by subcontractor.</p>	Test No.	Test Article	Impact Height	Impact Speed mph [km/h]	Angle Degrees
	1	Cast-in-Place Anchorage	16" [406]	15 [24.1]	90
	2	Four Spread Epoxy Anchors	16" [406]	15 [24.1]	90
	3	Two Offset Epoxy Anchors	16" [406]	15 [24.1]	90
	4	US-20/Hardin Bridge	16" [406]	15 [24.1]	90



Midwest Roadside Safety Facility

Iowa Bridge Rail

Test Matrix

DWG. NAME: IowaBR27C\_R3

SCALE: 1:30  
UNITS: in, [mm]

SHEET: 1 of 16

DATE: 4/30/2014

DRAWN BY: SDB

REV. BY: RWB/KAL

Figure 14. Bogie Testing Matrix and Setup

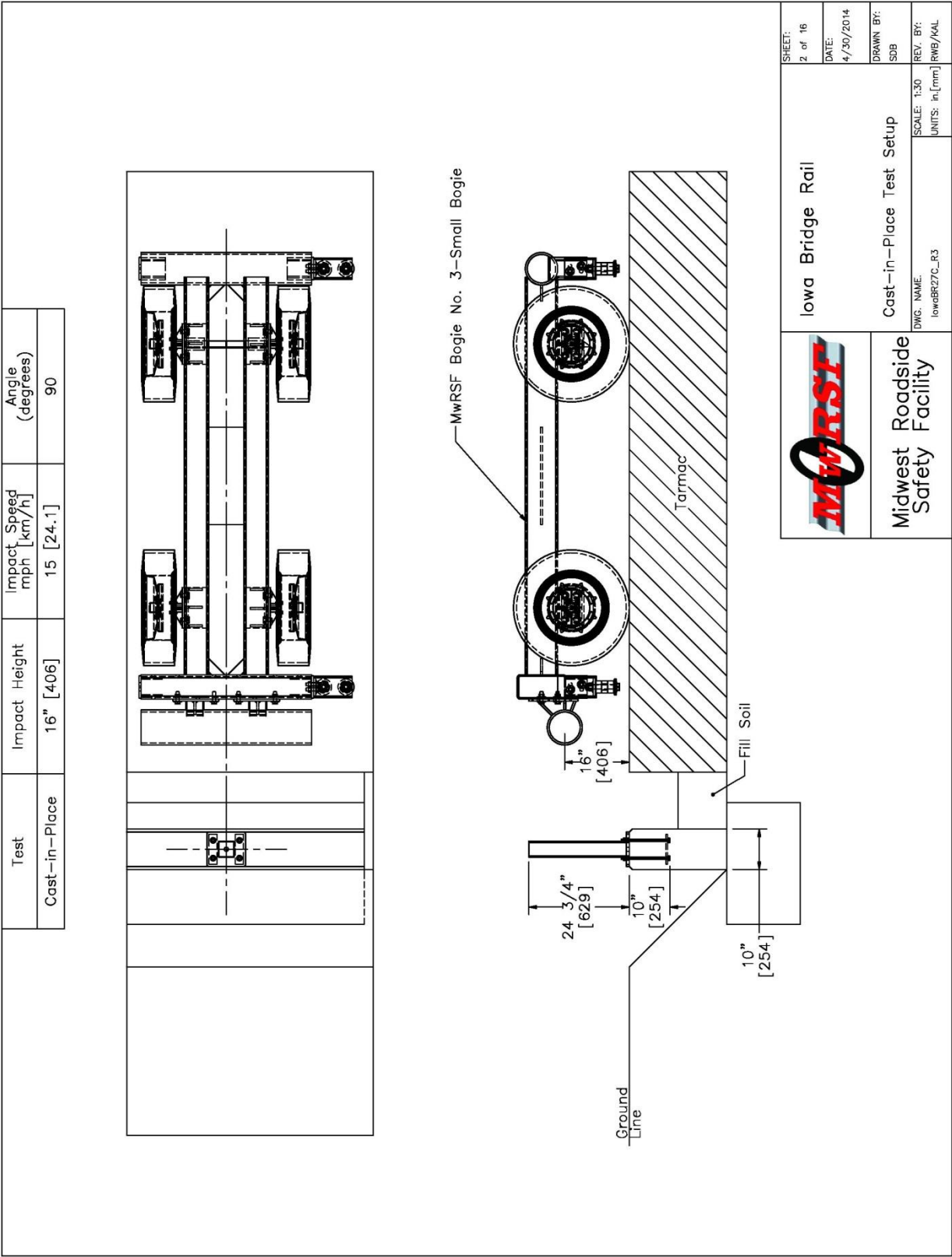


Figure 15. Cast-in-Place Test Setup, Test No. IBP-1

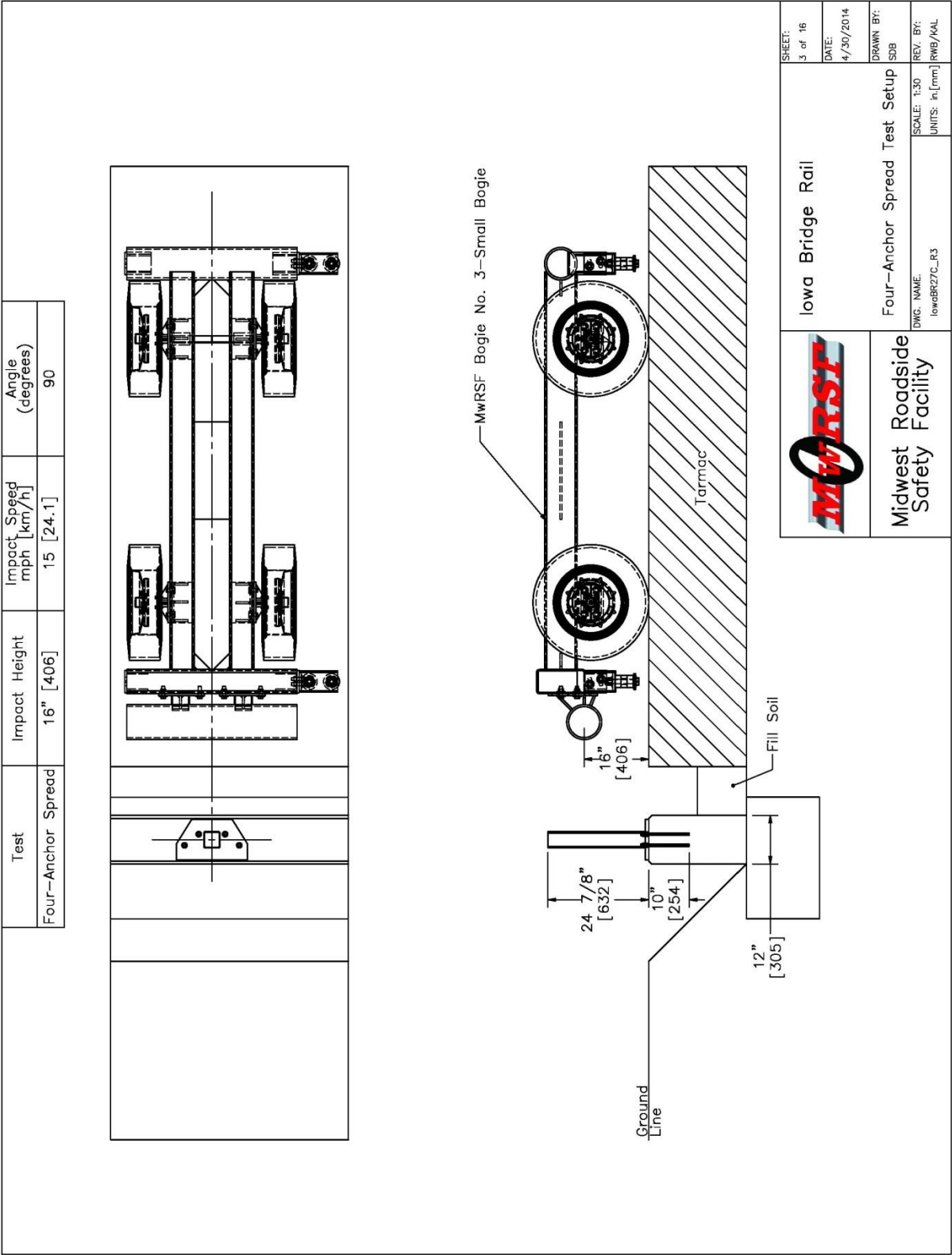


Figure 16. Four-Anchor Test Setup, Test No. IBP-2

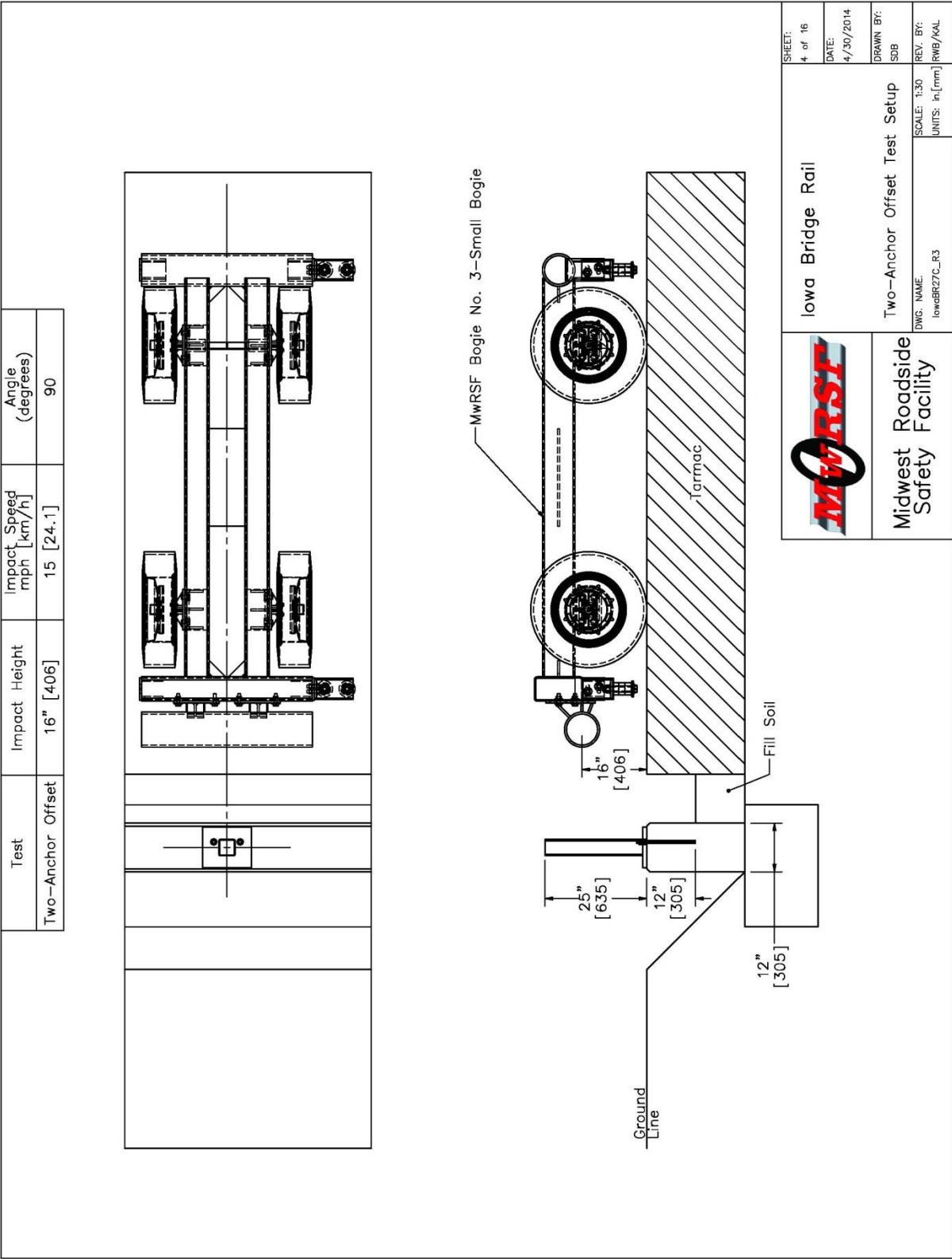


Figure 17. Two-Anchor Offset Test Setup, Test No. IBP-3

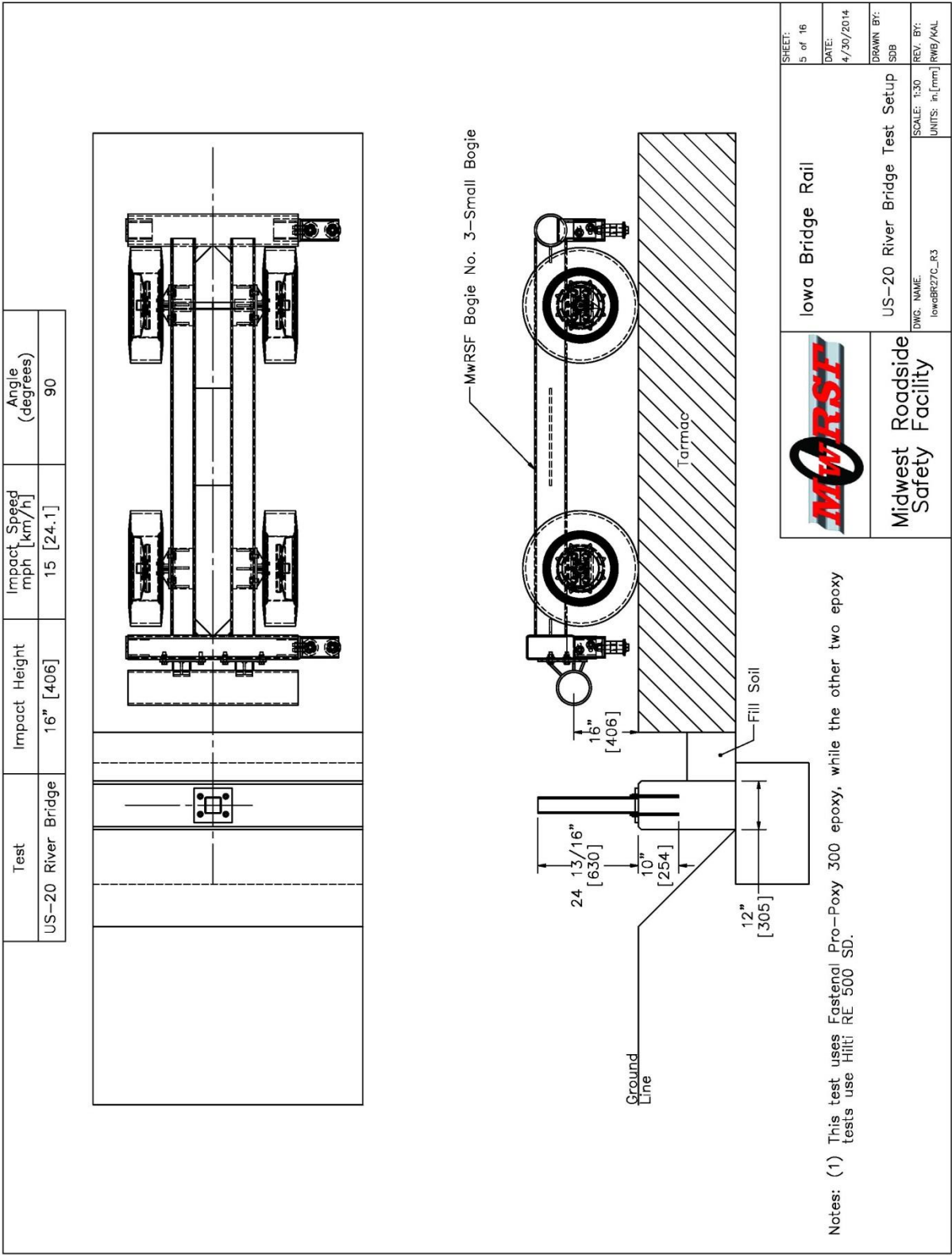


Figure 18. US-20 River Bridge Test Setup, Test No. IBP-4

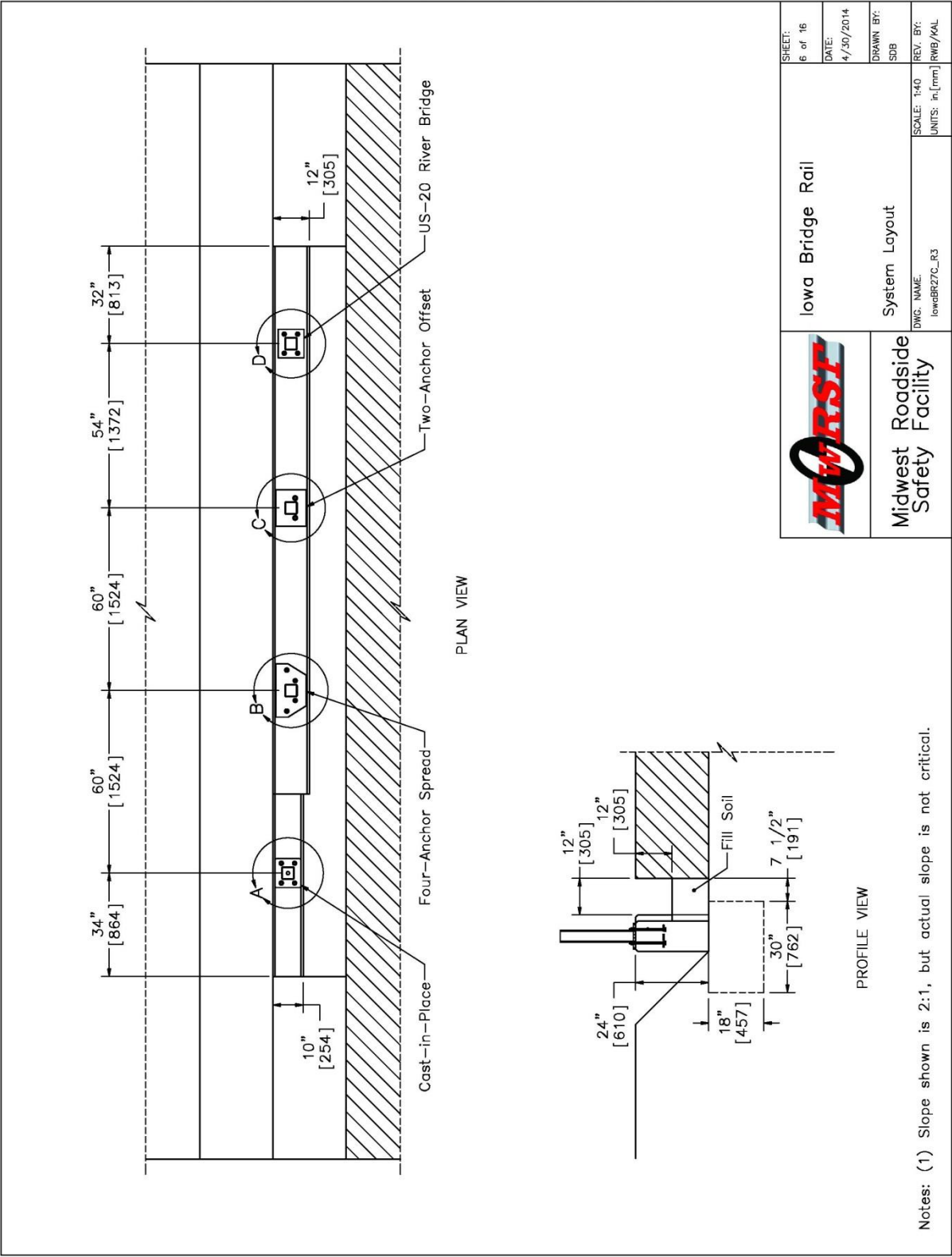


Figure 19. System Layout

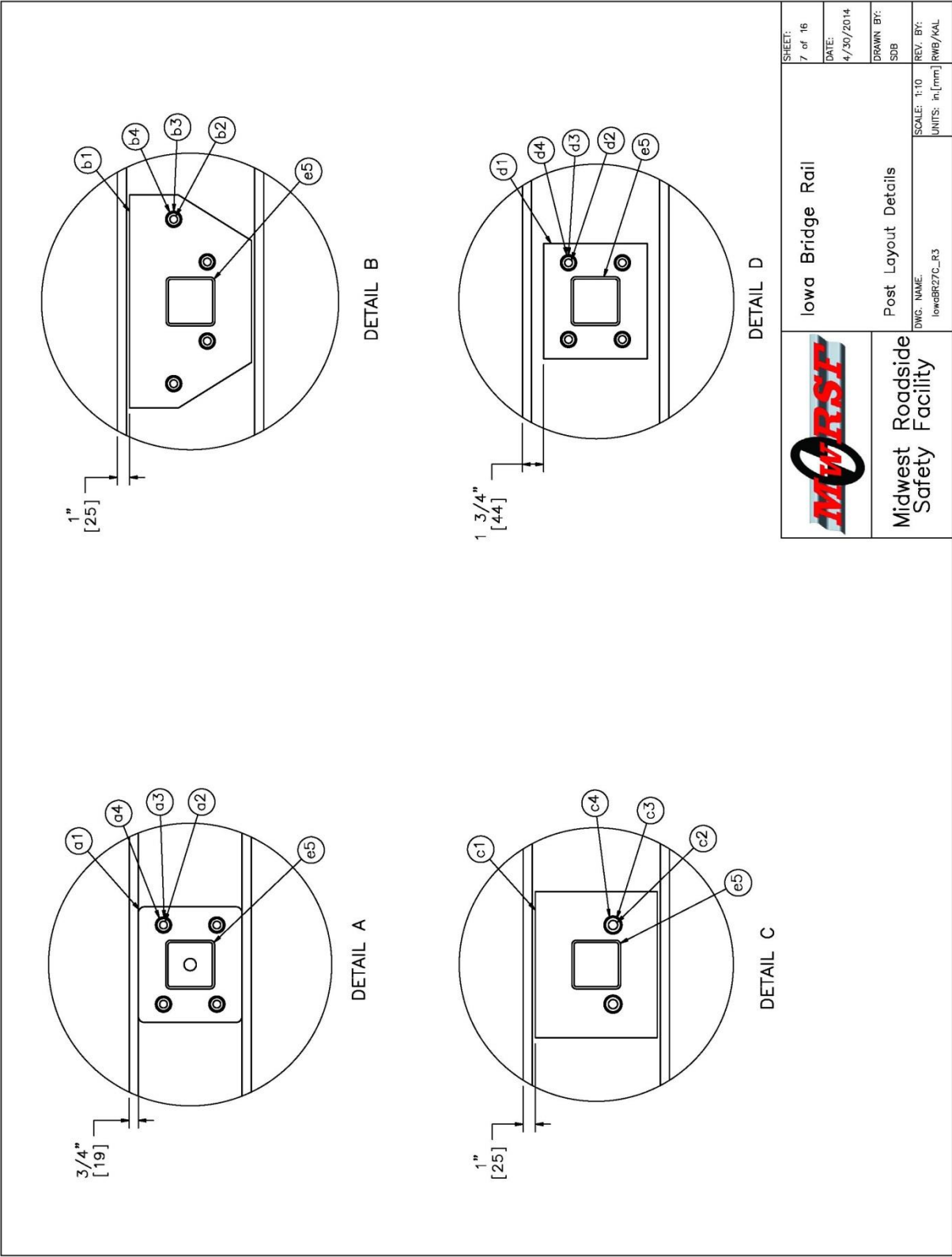


Figure 20. Post Layout Details



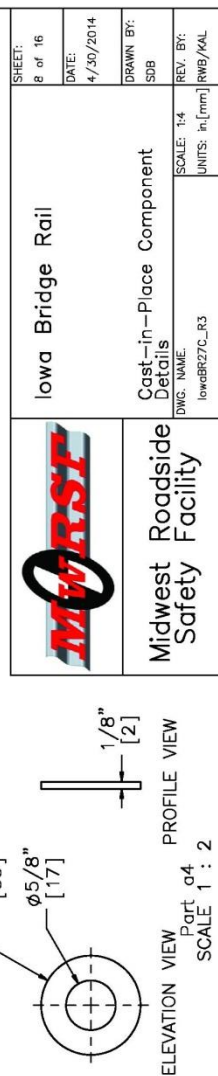


Figure 21. Cast-in-Place Component Details, Test No. IBP-1

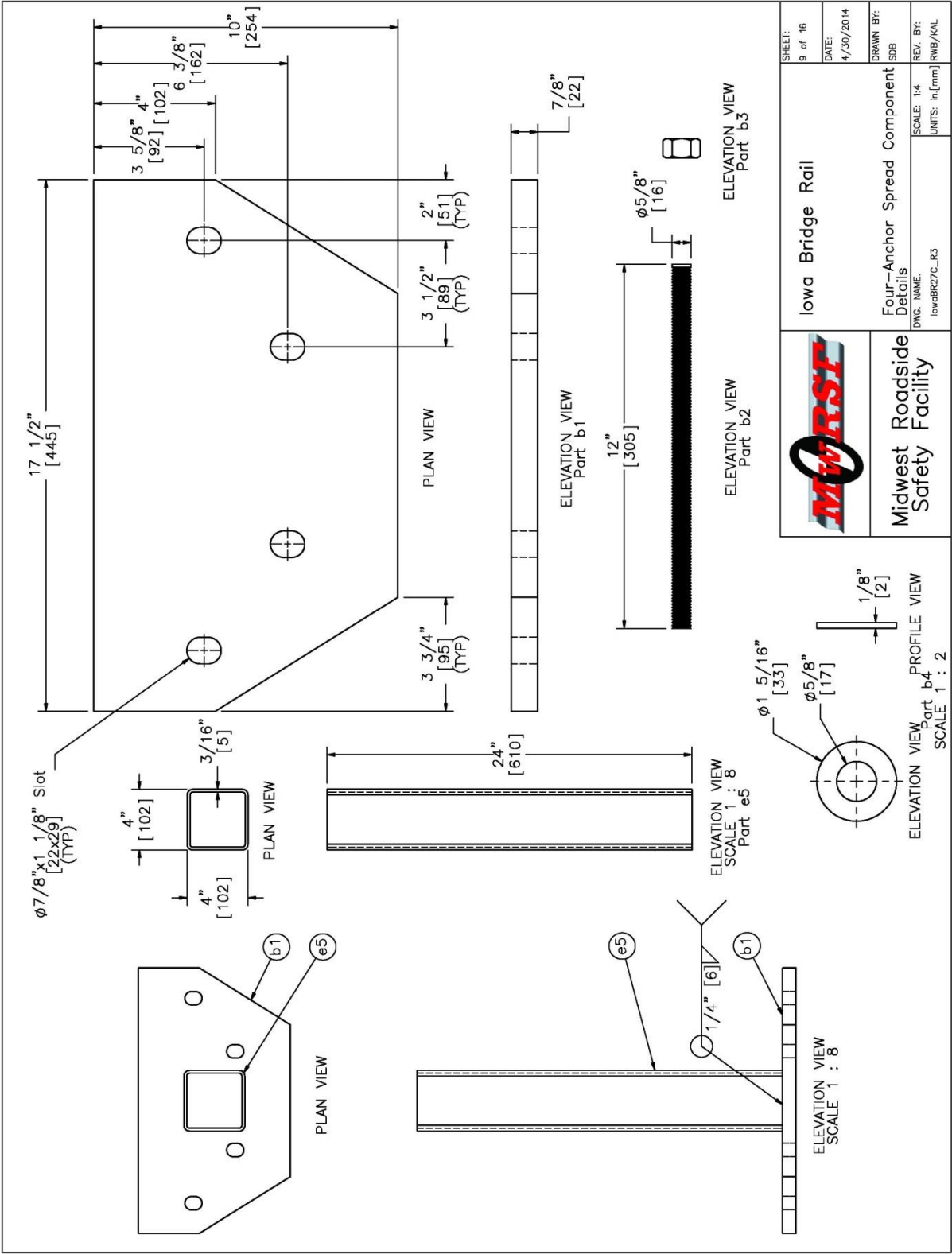


Figure 22. Four-Anchor Spread Component Details, Test No. IBP-2

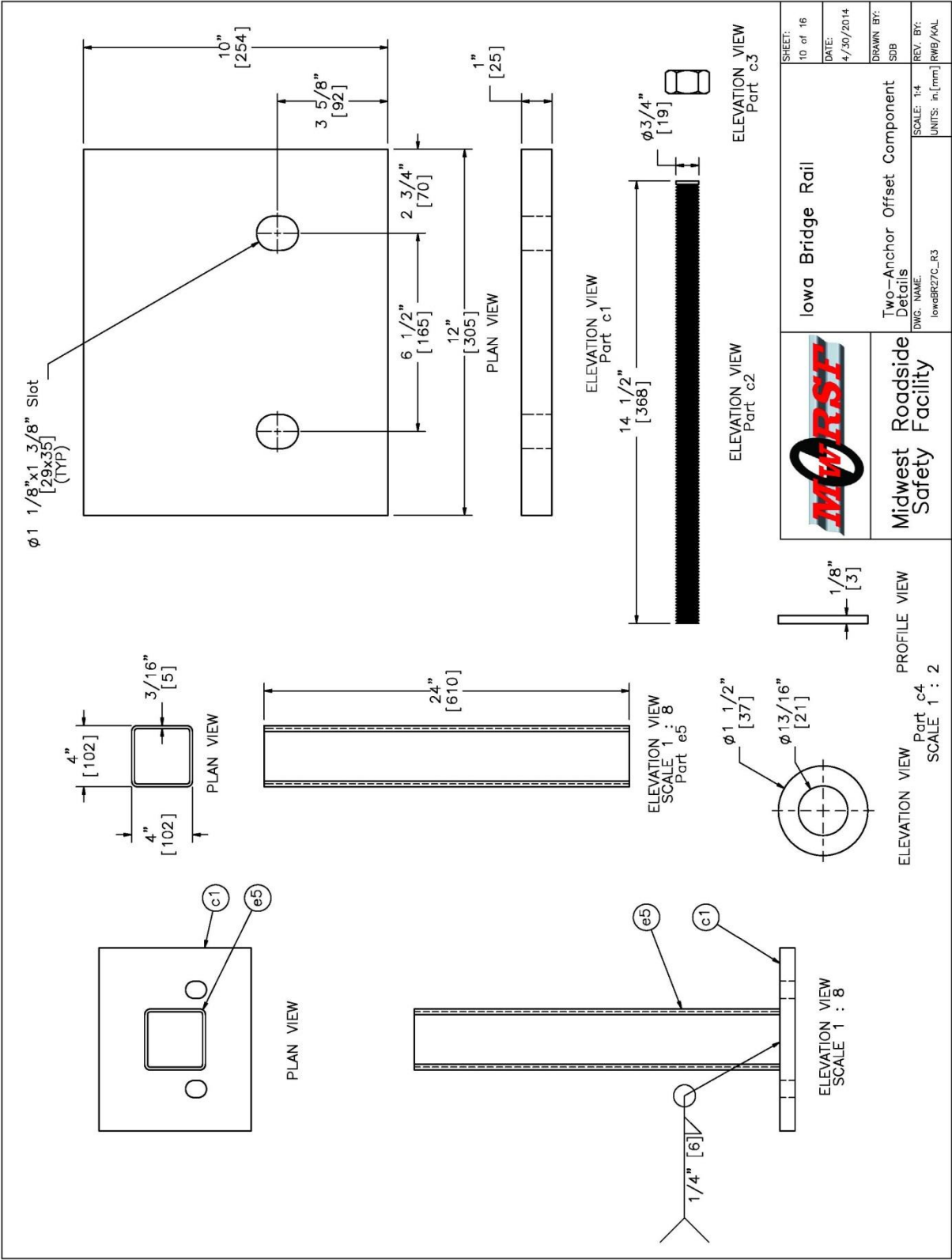


Figure 23. Two-Anchor Offset Component Details, Test No. IBP-3

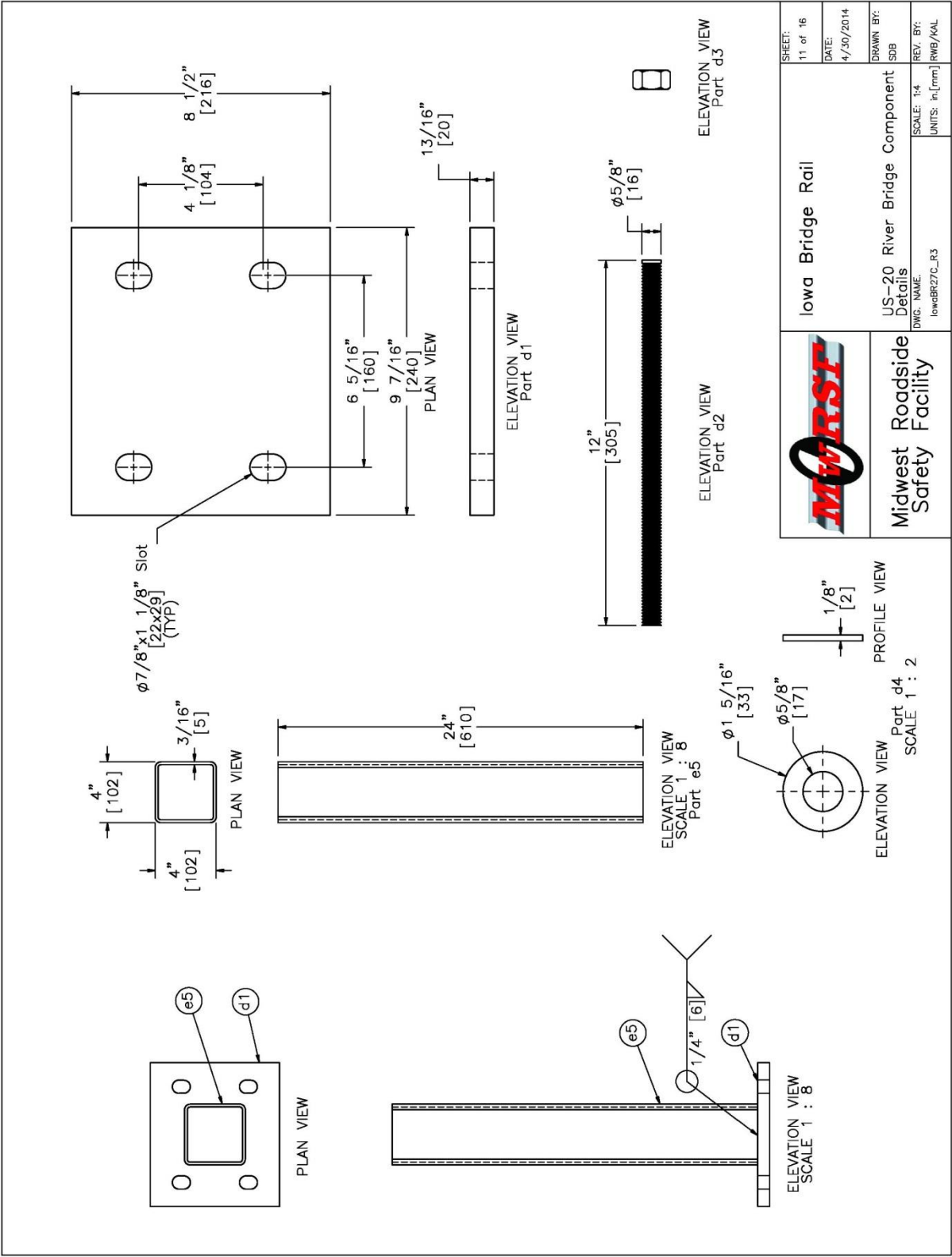


Figure 24. US-20 River Bridge Component Details, Test No. IBP-4

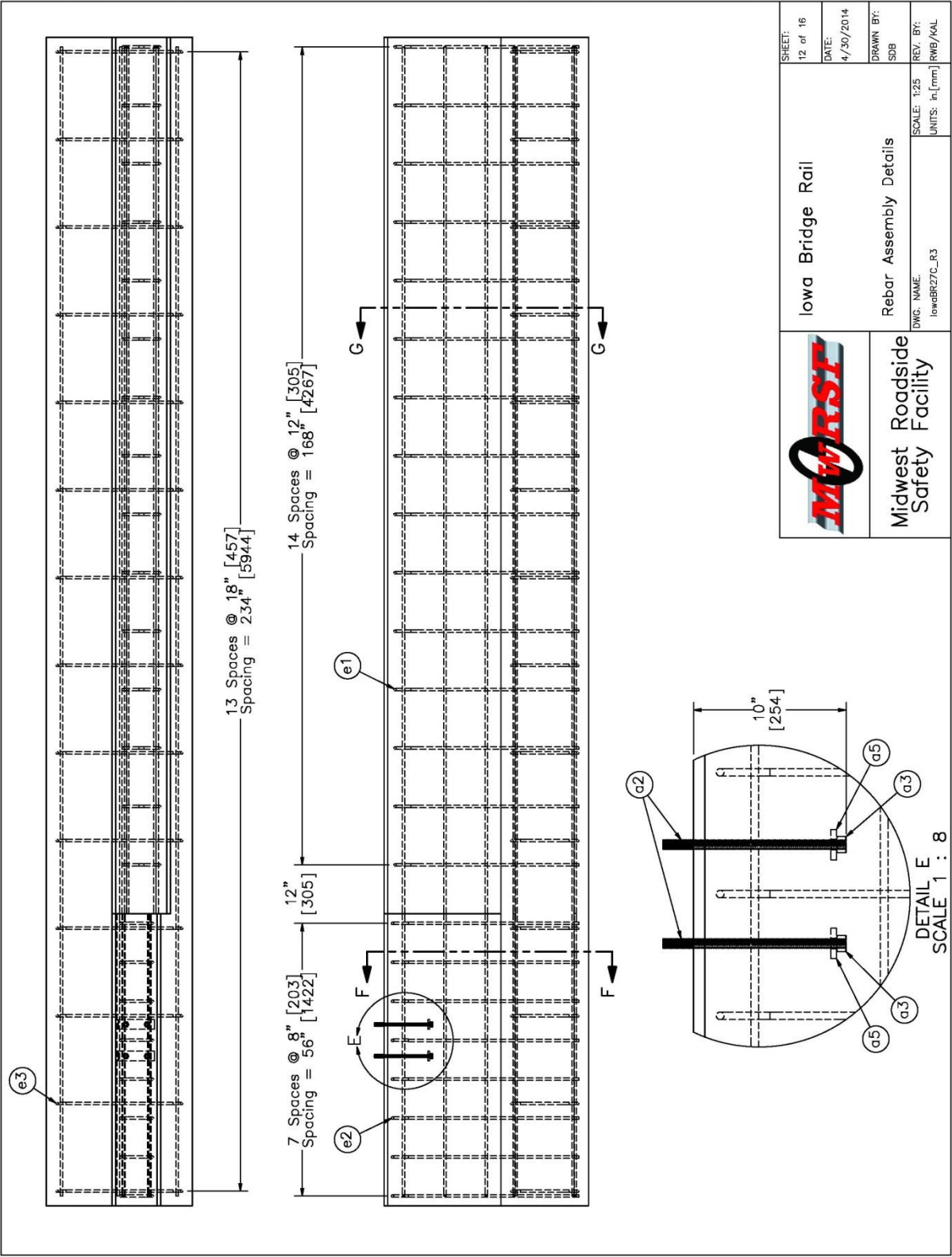


Figure 25. Rebar Assembly Details

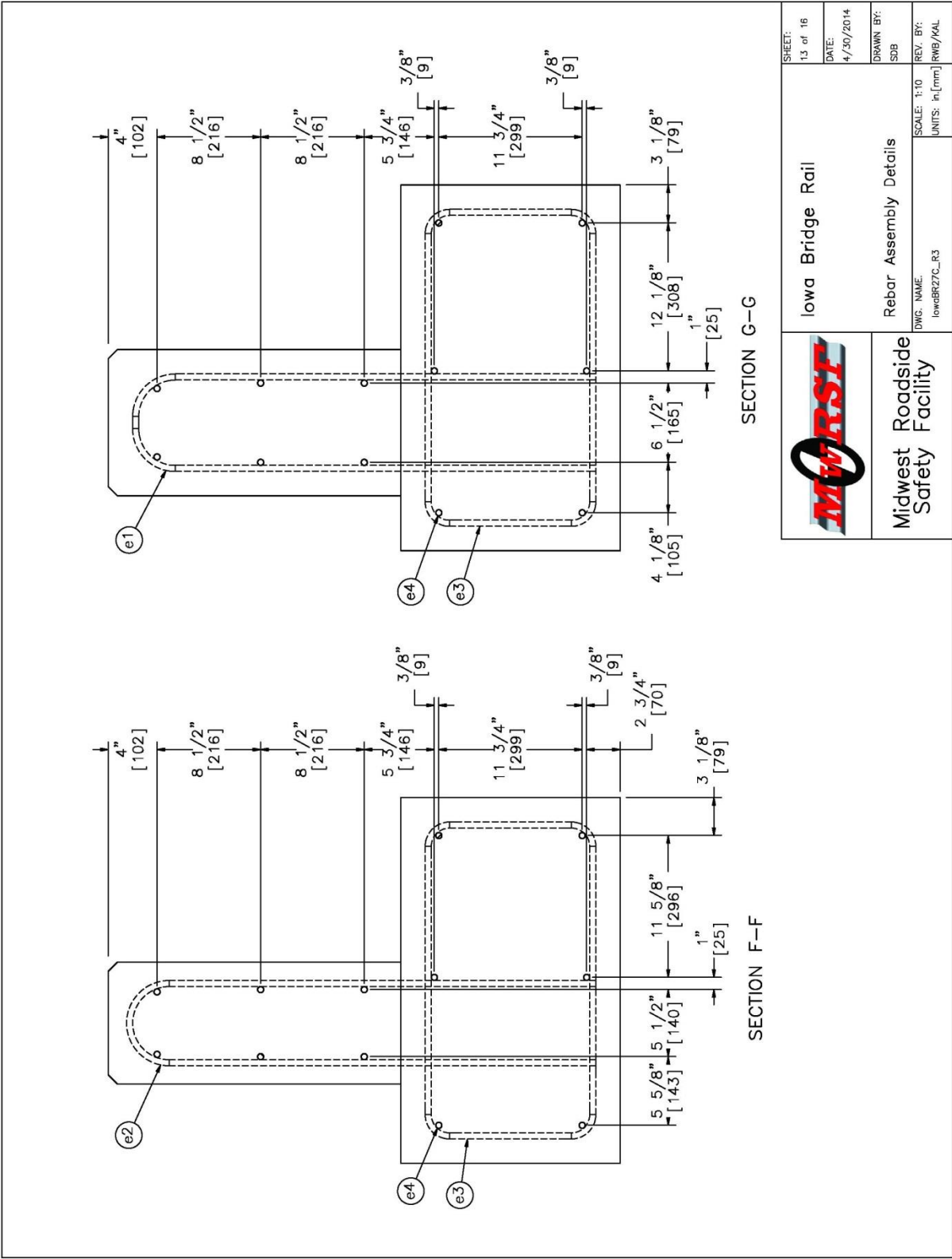


Figure 26. Additional Rebar Assembly Details

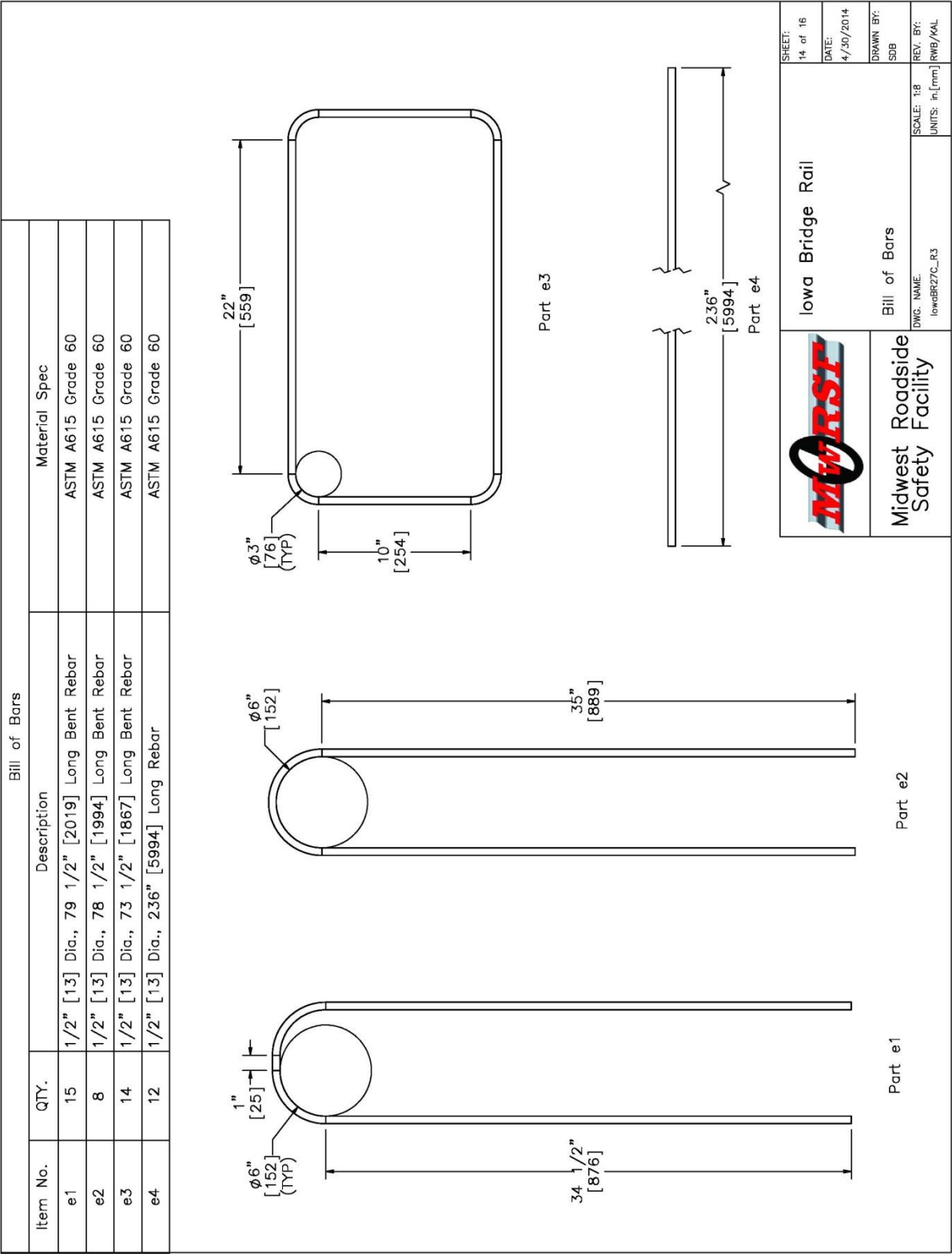


Figure 27. Bill of Bars



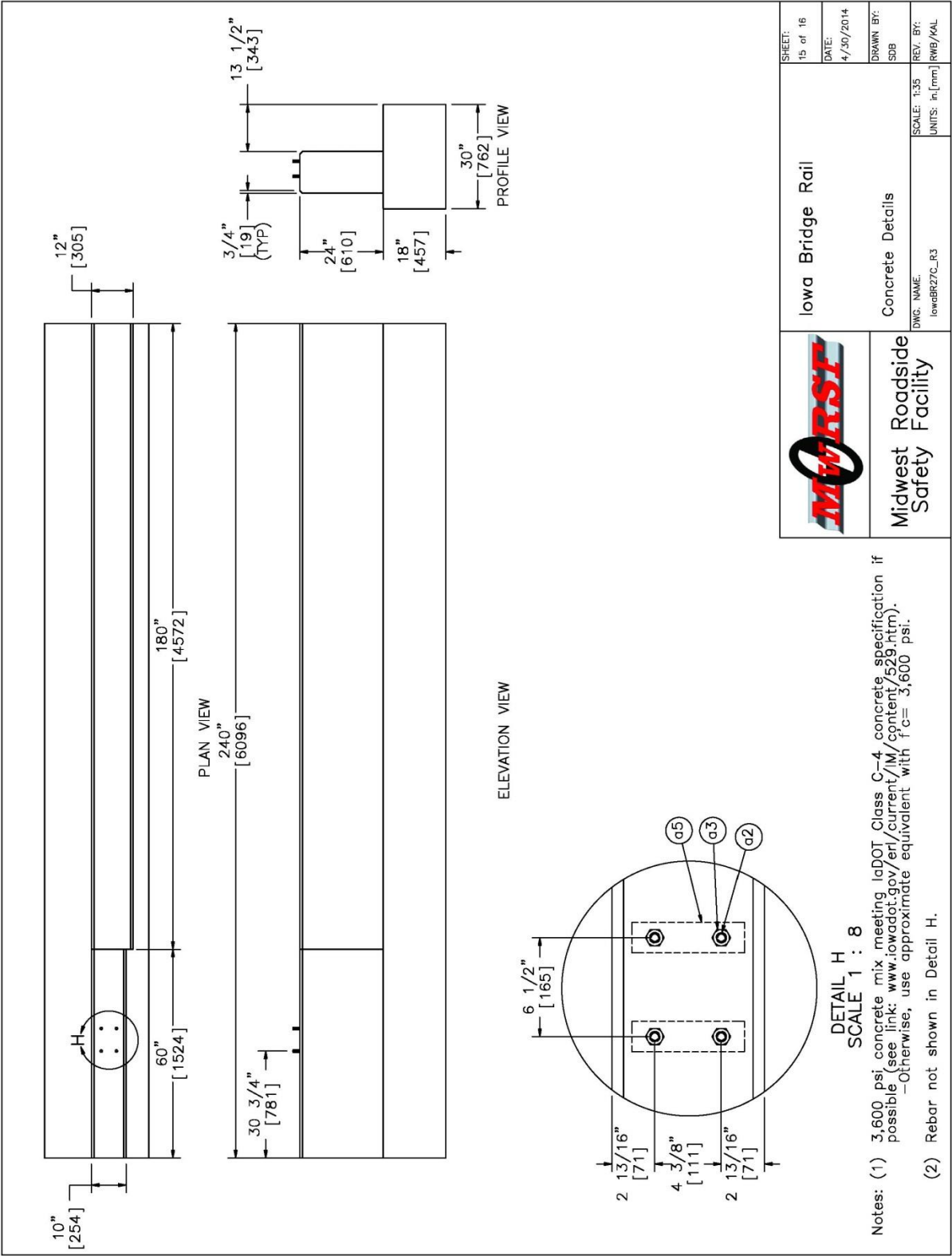


Figure 28. Concrete Details



Cast-in-Place			
Item No.	QTY.	Description	Material Spec
a1	1	Baseplate	ASTM A36
a2	4	5/8" [16] Dia. UNC, 12" [305] Long Threaded Rod	ASTM A193 Grade B7
a3	8	5/8" [16] Dia. Hex Nut	ASTM A563 DH
a4	4	5/8" [16] Dia. SAE Flat Washer	ASTM F436
a5	2	2"x7 3/8"x3/8" [51x187x10] Washer Plate	ASTM A36
e5	4	HSS 4"x4"x3/16" [102x102x5] Steel Tube	ASTM A500 Grade B
Four-Anchor Spread			
Item No.	QTY.	Description	Material Spec
b1	1	Baseplate	ASTM A36
b2	4	5/8" [16] Dia. UNC, 12" [305] Long Threaded Rod	ASTM A193 Grade B7
b3	4	5/8" [16] Dia. Hex Nut	ASTM A563 DH
b4	4	5/8" [16] Dia. SAE Flat Washer	ASTM F436
e5	1	HSS 4"x4"x3/16" [102x102x5] Steel Tube	ASTM A500 Grade B
e6	–	Epoxy	Hilti RE-500 SD Epoxy
Two-Anchor Offset			
Item No.	QTY.	Description	Material Spec
c1	1	Baseplate	ASTM A36
c2	2	3/4" [19] Dia. UNC, 14 1/2" [368] Long Threaded Rod	ASTM A193 Grade B7
c3	2	3/4" [19] Dia. Hex Nut	ASTM A563 DH
c4	2	3/4" [19] Dia. SAE Flat Washer	ASTM F436
e5	1	HSS 4"x4"x3/16" [102x102x5] Steel Tube	ASTM A500 Grade B
e6	–	Epoxy	Hilti RE-500 SD Epoxy
US-20 River Bridge			
Item No.	QTY.	Description	Material Spec
d1	1	Baseplate	ASTM A36
d2	4	5/8" [16] Dia. UNC, 12" [305] Long Threaded Rod	ASTM A193 Grade B7
d3	4	5/8" [16] Dia. Hex Nut	ASTM A563 DH
d4	4	5/8" [16] Dia. SAE Flat Washer	ASTM F436
e5	1	HSS 4"x4"x3/16" [102x102x5] Steel Tube	ASTM A500 Grade B
e6	–	Epoxy	Fastenal Pro-Poxy 300


	Iowa Bridge Rail	
	Bill of Materials	
DWG. NAME: LOWBR27C_R4		SCALE: 1/8" = 1'-0"
DRAWN BY: SDB/JAH		REV. BY: RWB/KAL/DPM
DATE: 7/21/2015		SHEET: 16 of 16

Figure 29. Bill of Materials



Figure 30. Test Installation Photographs





Figure 31. Pre-Test Installation Photographs, Test No. IBP-1





Figure 32. Pre-Test Installation Photographs, Test No. IBP-2





Figure 33. Pre-Test Installation Photographs, Test No. IBP-3





Figure 34. Pre-Test Installation Photographs, Test No. IBP-4

### 3.3 Equipment and Instrumentation

Equipment and instrumentation utilized to collect and record data during the dynamic bogie tests included a bogie vehicle, accelerometers, a retroreflective speed trap, high-speed digital video, standard-speed digital video, and still cameras.

#### 3.3.1 Bogie Vehicle

A rigid-frame bogie was used to impact the posts. A variable-height, detachable impact head was used in the testing. The bogie head was constructed of 8-in. (203-mm) diameter, ½-in. (13-mm) thick standard steel pipe, with ¾-in. (19-mm) neoprene belting wrapped around the pipe to prevent local damage to the post from the impact. The impact head was bolted to the bogie vehicle, creating a rigid frame with an impact height of 16 in. (406 mm). The bogie with the impact head is shown in Figure 35. The total weight of the bogie with the addition of the mountable impact head and accelerometers was 1,808 lb (820 kg).



Figure 35. Rigid-Frame Bogie on Guidance Track

The tests were conducted using a steel corrugated-beam guardrail to guide the tire of the bogie vehicle. A pickup truck was used to push the bogie vehicle to the required impact velocity. After reaching the target velocity, the push vehicle braked, allowing the bogie to be free-rolling

as it came off the track. A remote braking system was installed on the bogie, allowing it to be brought safely to rest after the test.

### **3.3.2 Accelerometers**

Two environmental shock and vibration sensor/recorder systems were used to measure the accelerations in the longitudinal, lateral, and vertical directions. However, only the longitudinal acceleration was processed and reported. All of the accelerometers were mounted near the centers of gravity of the test vehicles. The electronic accelerometer data obtained in dynamic testing was filtered using the SAE Class 60 and the SAE Class 180 Butterworth filters conforming to SAE J211/1 specifications [10].

The two systems, the SLICE-1 and SLICE-2 units, were modular data acquisition systems manufactured by Diversified Technical Systems, Inc. (DTS) of Seal Beach, California. The acceleration sensors were mounted inside the bodies of custom-built SLICE 6DX event data recorders and recorded data at 10,000 Hz to the onboard microprocessor. Each SLICE 6DX was configured with 7 GB of non-volatile flash memory, a range of  $\pm 500$  g's, a sample rate of 10,000 Hz, and a 1,650 Hz (CFC 1000) anti-aliasing filter. The "SLICEWare" computer software program and a customized Microsoft Excel worksheet were used to analyze and plot the accelerometer data.

### **3.3.3 Retroreflective Optic Speed Trap**

Retroreflective optic speed trap was used to determine the speed of the bogie vehicle before impact. Three retroreflective targets, spaced at approximately 18-in. (457-mm) intervals, were applied to the side of the bogie vehicle. When the emitted beam of light was reflected by the targets and returned to the Emitter/Receiver, a signal was sent to the data acquisition computer, recording at 10,000 Hz, as well as the external LED box activating the LED flashes. The speed was then calculated using the spacing between the retroreflective targets and the time



between the signals. LED lights and high-speed digital video analysis are only used as a backup in the event that vehicle speeds cannot be determined from the electronic data.

### **3.3.4 Digital Photography**

Three AOS high-speed digital video cameras and three GoPro digital video cameras were used to document each test. The AOS high-speed camera had a frame rate of 500 frames per second, and the GoPro video camera had a frame rate of 120 frames per second. The cameras were placed laterally from the post, with a view perpendicular to the bogie's direction of travel, as well as diagonally from the post. A Nikon D50 digital still camera was used to document pre- and post-test conditions for all tests.

### **3.4 End of Test Determination**

When the impact head initially contacts the test article, the force exerted by the surrogate test vehicle is directly perpendicular. However, as the post rotates, the surrogate test vehicle's orientation and path moves farther from perpendicular. This introduces two sources of error: (1) the contact force between the impact head and the post has a vertical component, and (2) the impact head slides upward along the test article. Therefore, only the initial portion of the accelerometer trace should be used, since variations in the data become significant as the system rotates and the surrogate test vehicle overrides the system. Additionally, guidelines were established to define the end of test time using the high-speed video of the impact. The first occurrence of either of the following events was used to determine the end of the test: (1) the test article fractures, or (2) the surrogate vehicle overrides/loses contact with the test article.

### **3.5 Data Processing**

The electronic accelerometer data obtained in dynamic testing was filtered using the SAE Class 60 Butterworth filter conforming to SAE J211/1 specifications [10]. The pertinent acceleration signal was extracted from the bulk data signals. The processed acceleration data was

then multiplied by the mass of the bogie to get the impact force using Newton's Second Law. Next, the acceleration trace was integrated to find the change in velocity versus time. Initial velocity of the bogie, calculated from the pressure tape switch data, was then used to determine the bogie velocity, and the calculated velocity trace was integrated to find the bogie's deflection. This deflection is also the deflection of the post. Combining the previous results, a force versus deflection curve was plotted for each test. Finally, integration of the force versus deflection curve provided the energy versus deflection curve for each test.

## 4 COMPONENT TESTING RESULTS AND DISCUSSION

### 4.1 Results

Results from the dynamic component testing of the four anchorage systems for the BR27C combination bridge rail are detailed in the subsequent section. In each test, acceleration data, high-speed video, and post-test documentation of the system damage were used to evaluate the anchorages. The accelerometer data for each test was processed in order to obtain acceleration, velocity, and deflection curves, as well as force versus deflection and energy versus deflection curves. Although the individual transducers produced similar results, the values described herein were calculated from the SLICE-2 data curves in order to provide common basis for comparing results from multiple tests. Test results for all transducers are provided in Appendix C. A summary of the four dynamic component tests is shown in Table 1.

Table 1. Dynamic Testing Summary

Test No.	Design Configuration	Target Impact Velocity (mph) [km/h]	Impact Height (in.) [mm]	Impact Angle (degrees)
IBP-1	Original BR27C Cast-In-Place	15.0 [24.1]	16 [406]	90
IBP-2	Four-Bolt Spread	15.0 [24.1]	16 [406]	90
IBP-3	Two-Bolt Offset	15.0 [24.1]	16 [406]	90
IBP-4	US-20 Bridge	15.0 [24.1]	16 [406]	90

#### **4.1.1 Test No. IBP-1**

During test no. IBP-1, the bogie impacted the HSS 4-in. x 4-in. x  $\frac{3}{16}$ -in. (102-mm x 102-mm x 5-mm) steel post at a speed of 16.1 mph (25.9 km/h), causing the post to deflect backward. During the test, shear cracks formed starting at the front anchors that propagated to the backside of the parapet. This concrete failure caused significant damage to the parapet but did not cause the yielding of the post. The post continued to rotate backwards, causing additional fracture and disengagement of the concrete parapet behind the post. The two front anchor rods on the post fractured in tension approximately 66 msec after impact, causing the loading of the bogie vehicle to drop to zero at a deflection of 13 in. (330 mm). The bogie overrode the top of the post at approximately 224 msec, as determined from the high-speed film data. Sequential photographs of the test are shown in Figure 36.

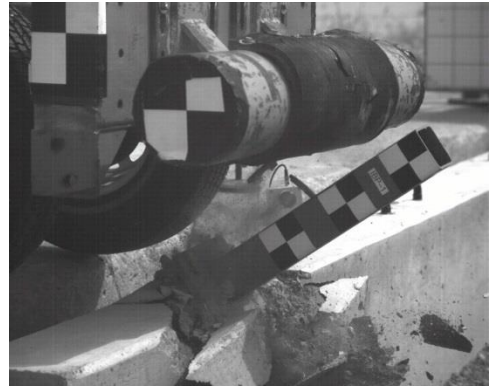
Damage to the system consisted of major damage to the concrete parapet and the cast-in-place anchorage, as shown in Figure 37. The concrete parapet displayed shear cracking along the top of the parapet and disengagement of a large section of concrete on the backside of the parapet. Lesser amounts of concrete were disengaged on the top and front sides of the parapet. The post and baseplate assembly were largely undamaged. The post and baseplate displayed minimal local deformations due to the impact, and the post did not form a plastic hinge. The threaded rod anchors on the front of the parapet fractured during the test, and the rear anchors were bent backward due to the rotation of the post.

Force versus deflection and energy versus deflection curves were created from the accelerometer data and are shown in Figure 38. A peak force of 22.9 kips (101.9 kN) was reached at a deflection of 1.5 in. (38 mm), prior to the disengagement of sections of the concrete parapet. The post continued to develop load as the post deflected until the fracture of the front

two anchor rods. At a maximum deflection of 13 in. (330 mm), the post assembly absorbed 146 kip-in. (16.5 kJ) of energy.



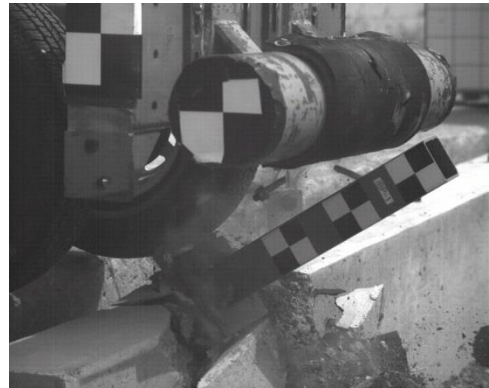
0.000 sec



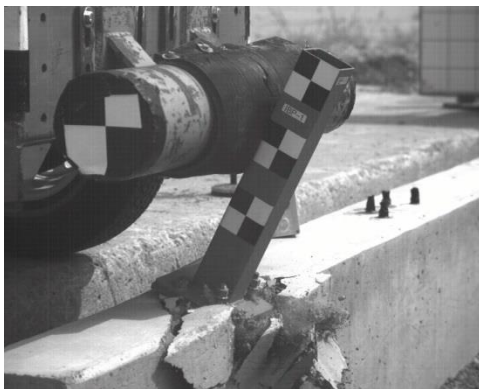
0.100 sec



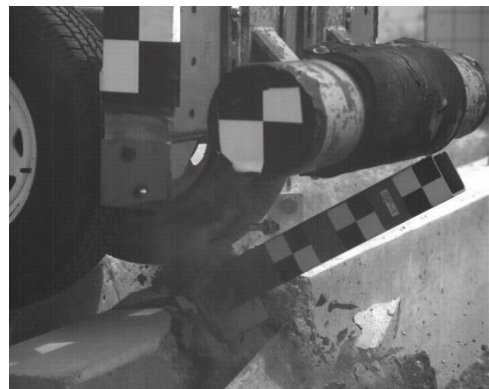
0.025 sec



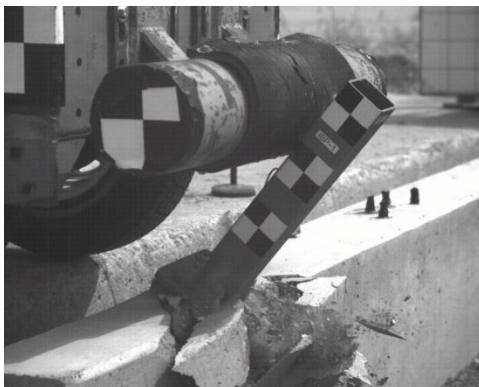
0.125 sec



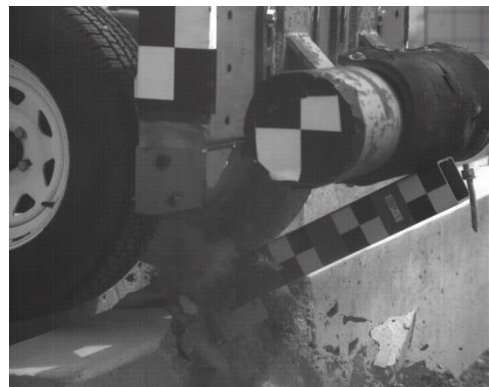
0.050 sec



0.150 sec



0.075 sec



0.175 sec

Figure 36. Sequential Photographs, Test No. IBP-1



Figure 37. Post-Impact Photographs, Test No. IBP-1



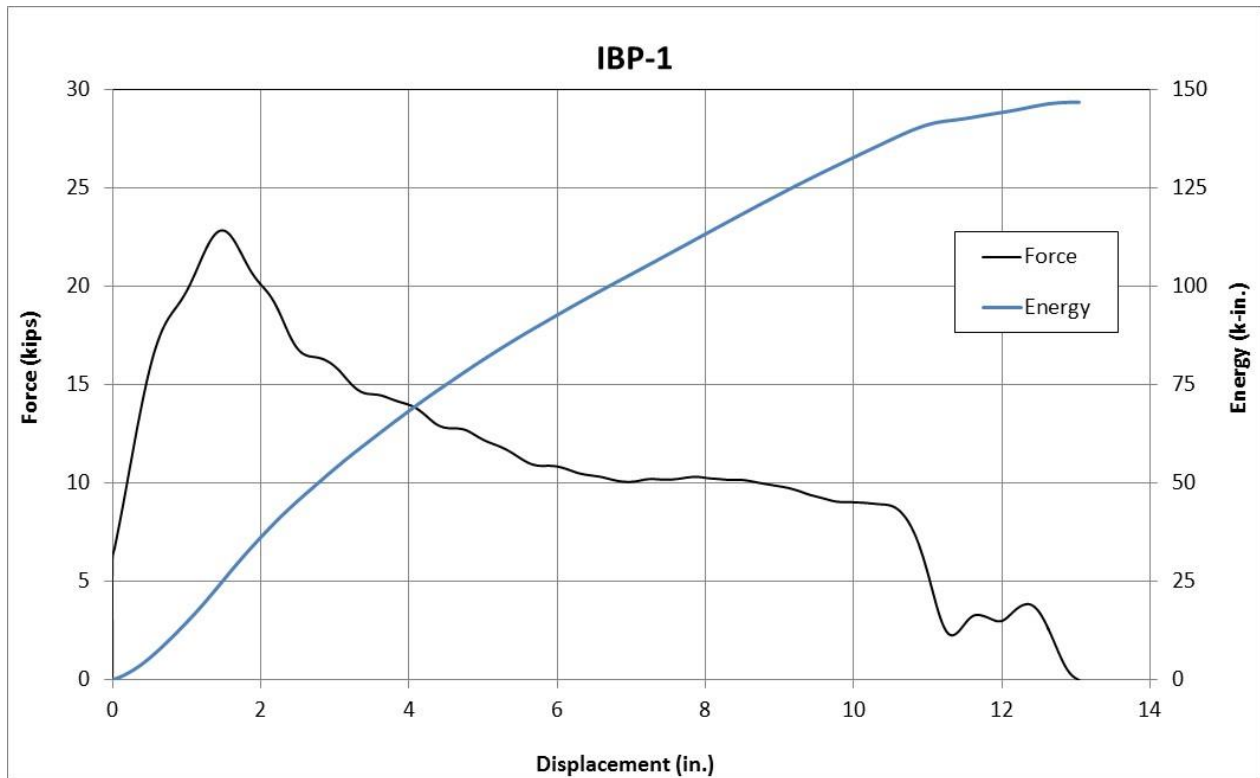


Figure 38. SLICE-2 Force vs. Deflection and Energy vs. Deflection, Test No. IBP-1



#### **4.1.2 Test No. IBP-2**

During test no. IBP-2, the bogie impacted the HSS 4-in. x 4-in. x  $\frac{3}{16}$ -in. (102-mm x 102-mm x 5-mm) steel post at a speed of 16.2 mph (26.1 km/h), causing the post to deflect backward. During the test, shear cracks formed starting at the rear anchors that propagated to the backside of the parapet, and which disengaged a large section of the rear face of the parapet. At the same time, loading of the front two anchors caused cracking and concrete disengagement on the top-front of the parapet. The impact loads caused concrete failure and significant damage to the parapet but did not cause the yielding of the post. As the post continued to rotate, all four anchor rods were pried from the fracture parapet. The force on the bogie vehicle dropped to zero at a deflection of 11.9 in. (302 mm). The bogie overrode the top of the post at approximately 156 msec, as determined from the high-speed film data. Sequential photographs of the test are shown in Figure 39.

Damage to the system consisted primarily of damage to the concrete parapet, as shown in Figure 40. The concrete parapet displayed shear cracking along the top and disengagement of a large section of concrete on the backside. Lesser amounts of concrete were disengaged on the top and front sides of the parapet. The post and baseplate assembly were largely undamaged. The post and baseplate displayed minimal local deformations due to the impact, and the post did not form a plastic hinge. The four threaded rod anchors were all disengaged from the parapet due to the impact loads and fracture of the surrounding concrete.

Force versus deflection and energy versus deflection curves were created from the accelerometer data and are shown in Figure 41. A peak force of 24.9 kips (110.8 kN) was reached at a deflection of 1.4 in. (36 mm), prior to the disengagement of sections of the concrete parapet. The post continued to develop load as the post deflected until the disengagement of the

anchor rods from the parapet. At a maximum deflection of 11.9 in. (302 mm), the post assembly absorbed 69.6 kip-in. (7.9 kJ) of energy.

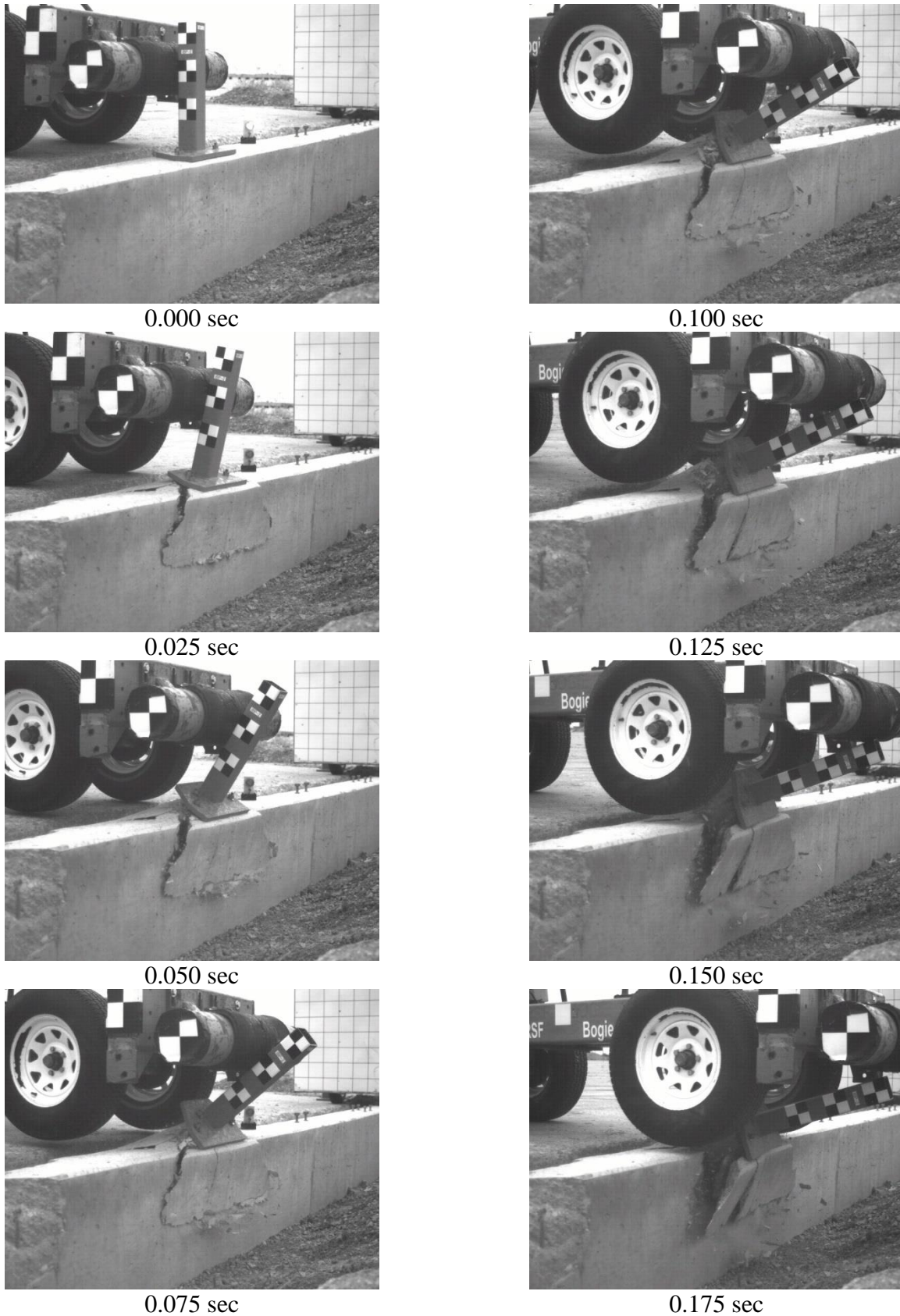


Figure 39. Sequential Photographs, Test No. IBP-2



Figure 40. Four-Anchor Post-Impact Photographs, Test No. IBP-2

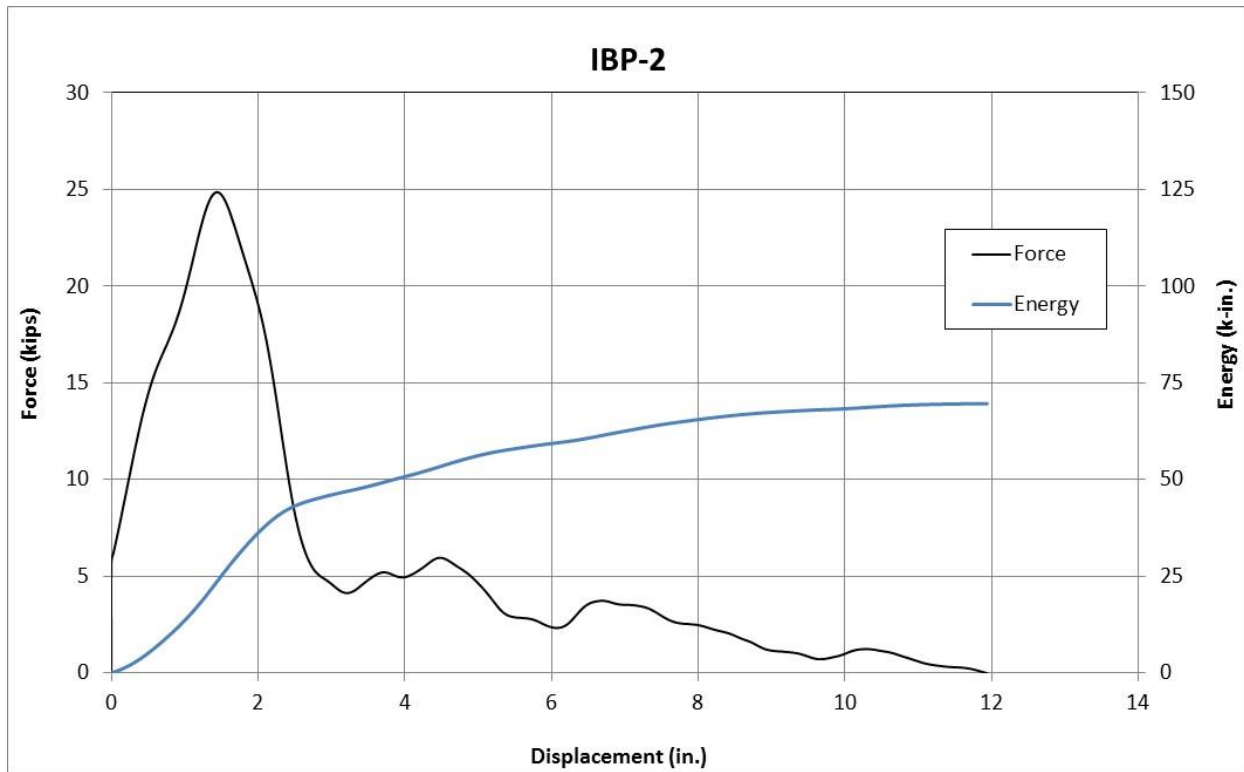


Figure 41. SLICE-2 Force vs. Deflection and Energy vs. Deflection, Test No. IBP-2

#### **4.1.3 Test No. IBP-3**

During test no. IBP-3, the bogie impacted the HSS 4-in. x 4-in. x  $\frac{3}{16}$ -in. (102-mm x 102-mm x 5-mm) steel post at a speed of 16.3 mph (26.2 km/h), causing the post to deflect backward. During the test, shear cracks formed starting at the anchors and propagated to the backside of the parapet. As the bogie continued to load the post, the weld between the post and the baseplate fractured on the front-side of the post approximately 10 msec after impact. As the post continued to deflect, the weld between the post and the baseplate fractured along both sides of the post, allowing the post to rotate backward. The force on the bogie vehicle dropped to zero at a deflection of 2.7 in. (69 mm). The post completely disengaged from the baseplate at approximately 112 msec, as determined from the high-speed film data. Sequential photographs of the test are shown in Figure 42.

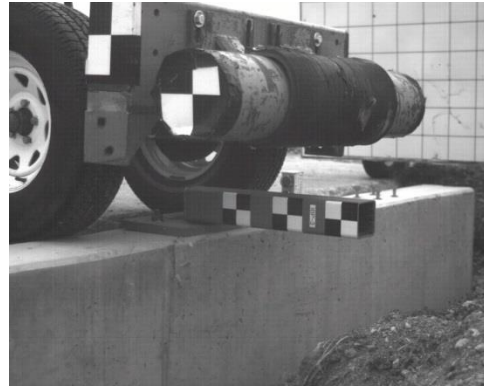
Damage to the system consisted of damage to the concrete parapet and the weld between the post and the baseplate, as shown in Figure 43. The concrete parapet displayed shear cracking along the top of the parapet as well as some cracking of the top of the rear face of the parapet. No significant sections of concrete were disengaged from the parapet in this test. The post and baseplate assembly were not deformed, but the weld between them was completely fractured at the base of the post. The two threaded rod anchors remained embedded in the concrete.

Force versus deflection and energy versus deflection curves were created from the accelerometer data and are shown in Figure 44. A peak force of 28.3 kips (125.9 kN) was reached at a deflection of 1.4 in. (36 mm). The post continued to develop load as the post deflected until the fracture of the weld between the post and the baseplate. At a maximum deflection of 2.7 in. (69 mm), the post assembly absorbed 48.3 kip-in. (5.5 kJ) of energy.





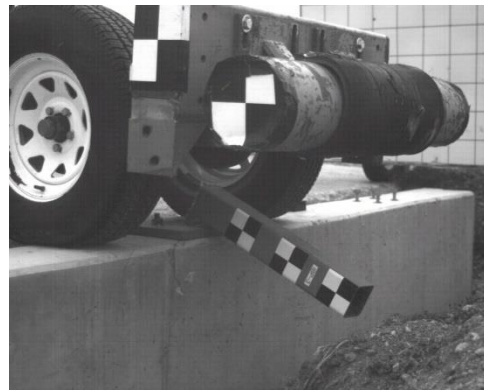
0.000 sec



0.100 sec



0.025 sec



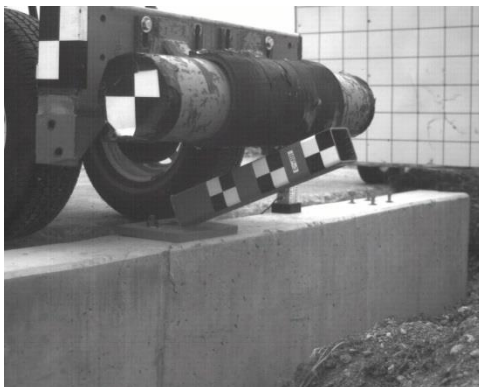
0.125 sec



0.050 sec



0.150 sec



0.075 sec



0.175 sec

Figure 42. Sequential Photographs, Test No. IBP-3



Figure 43. Post-Impact Photographs, Test No. IBP-3



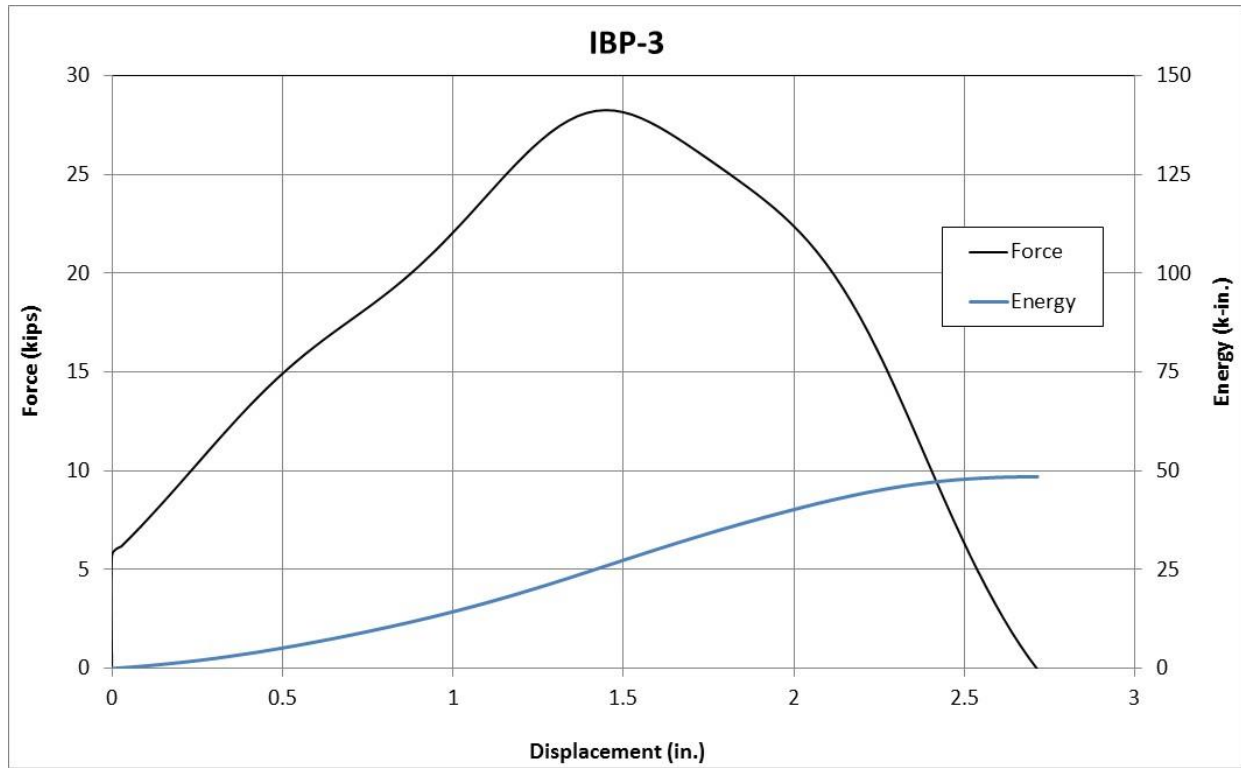


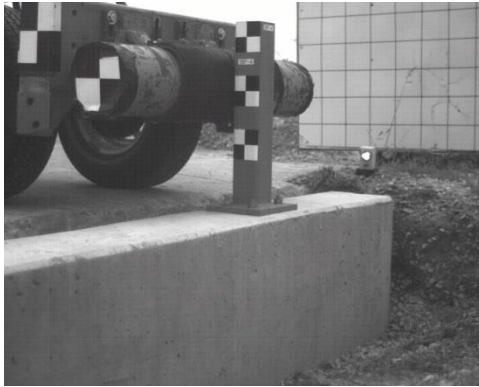
Figure 44. SLICE-2 Force vs. Deflection and Energy vs. Deflection, Test No. IBP-3

#### **4.1.4 Test No. IBP-4**

During test no. IBP-4, the bogie impacted the HSS 4-in. x 4-in. x  $\frac{3}{16}$ -in. (102-mm x 102-mm x 5-mm) steel post at a speed of 15.4 mph (24.8 km/h), causing the post to deflect backward. During the test, the deflection of the post caused uplift of the front of the baseplate, which caused the front two threaded anchors to fail in tension approximately 12 msec after impact. The post continued to rotate backwards, causing shear cracks to form at the two back anchors and propagate towards the backside of the parapet. The shear cracks and the continued rotation of the steel baseplate caused disengagement of a section of the back of the concrete parapet. The loading of the bogie vehicle dropped to zero at a deflection of 3.4 in. (86 mm). The bogie overrode the top of the post at approximately 166 msec, as determined from the high-speed film data. Sequential photographs of the test are shown in Figure 45.

Damage to the system consisted of damage to the concrete parapet and the anchor rods, as shown in Figure 46. The concrete parapet displayed cracking on the top and disengagement of a section of concrete on the backside. The post and baseplate assembly were largely undamaged. The post and baseplate displayed minimal local deformations due to the impact, and the post did not form a plastic hinge. The threaded rod anchors on the front of the parapet fractured during the test, and the rear anchors were bent backward due to the rotation of the post.

Force versus deflection and energy versus deflection curves were created from the accelerometer data and are shown in Figure 47. A peak force of 23.2 kips (103.2 kN) was reached at a deflection of 1.4 in. (36 mm), prior to the fracture of the two front anchor rods. At a maximum deflection of 3.4 in. (86 mm), the post assembly absorbed 60.3 kip-in. (6.8 kJ) of energy.



0.000 sec



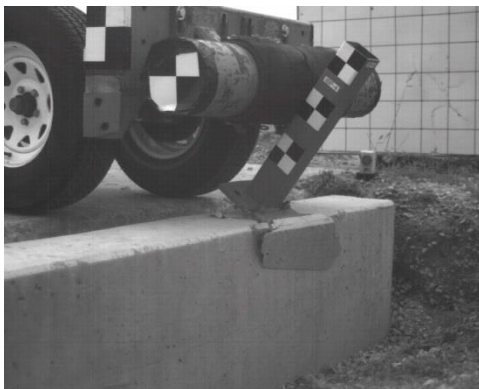
0.100 sec



0.025 sec



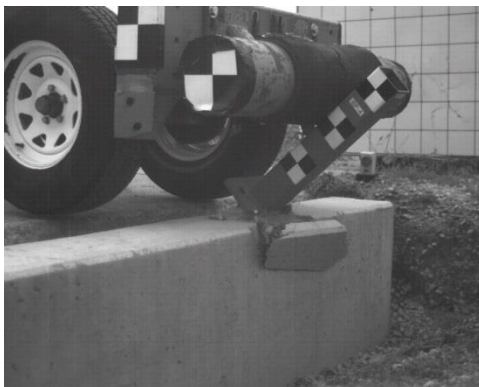
0.125 sec



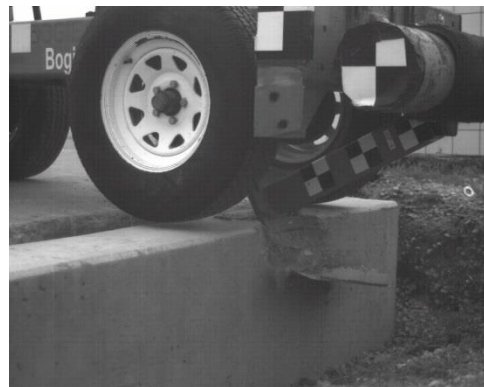
0.050 sec



0.150 sec



0.075 sec



0.175 sec

Figure 45. Sequential Photographs, Test No. IBP-4



Figure 46. US-20 River Bridge Post-Impact Photographs, Test No. IBP-4

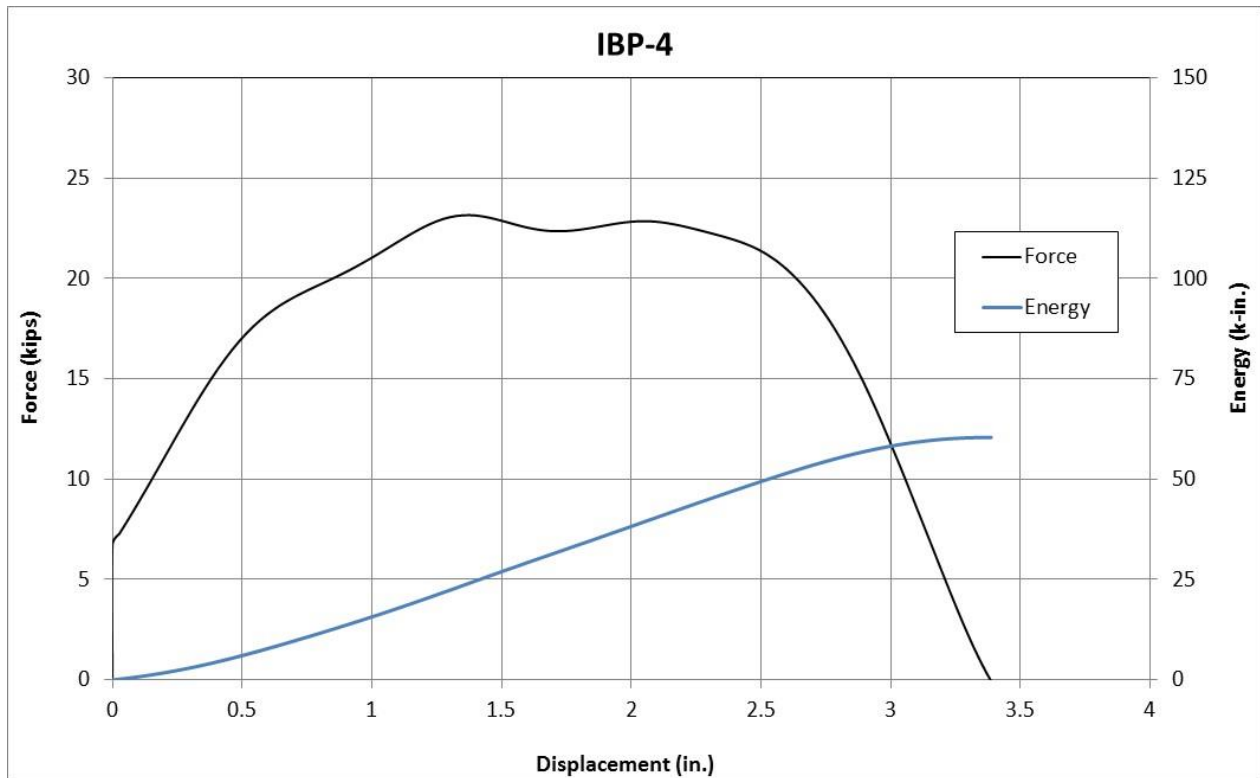


Figure 47. SLICE-2 Force vs. Deflection and Energy vs. Deflection, Test No. IBP-4

## 4.2 Discussion

The purpose of the dynamic component testing was to determine if two proposed and one currently installed alternative epoxy adhesive anchorages for the BR27C combination bridge rail had sufficient capacity to be used in lieu of the cast-in-place anchorage that was used in the original full-scale crash-tested design. Thus, the dynamic tests were used to evaluate and compare the force versus deflection behavior and the failure modes of the proposed designs to the baseline cast-in-place anchorage. A summary of all dynamic component testing results is shown in Table 2.

Table 2. Dynamic Testing Results

Test No.	Design Configuration	Impact Velocity (mph) [km/h]	Peak Force (kips) [kN]	Max Deflection (in.) [mm]	Total Energy Absorbed (k-in.) [kJ]
IBP-1	Original BR27C Cast-In-Place	16.1 [25.9]	22.9 [101.9]	13.0 [330]	146.0 [16.5]
IBP-2	Four-Bolt Spread	16.2 [26.1]	24.9 [110.8]	11.9 [302]	69.6 [7.9]
IBP-3	Two-Bolt Offset	16.3 [26.2]	28.3 [125.9]	2.7 [69]	48.3 [5.5]
IBP-4	US-20 Bridge	15.4 [24.8]	23.2 [103.2]	3.4 [86]	60.3 [6.8]

The force versus deflection data for the four dynamic component tests as derived from SLICE-2 acceleration transducer, is shown in Figures 48 and 49. Comparison of the results from the four tests found that all three of the alternative epoxy adhesive anchorage designs exceeded the peak force of the original cast-in-place anchorage. The cast-in-place anchorage evaluated in test no. IBP-1 developed the lowest peak force of all the anchorages with a value of 22.9 kips

(101.9 kN) at a deflection of 1.5 in. (38 mm). The US-20 bridge design evaluated in test no. IBP-4 had the next highest peak force with a value of 23.2 kips (103.2 kN) at a deflection of 1.4 in. (36 mm). The four-bolt spread anchorage evaluated in test no. IBP-2 had the third highest peak force with a value of 24.9 kips (110.8 kN) at a deflection of 1.4 in. (36 mm). The two-bolt offset anchorage evaluated in test no. IBP-3 developed the highest peak force with a value of 28.3 kips (125.9 kN) at a deflection of 1.4 in. (36 mm). The forces after the peak force was reached differ for the four anchorages, depending on the failure mode of the anchorage.

The energy versus deflection data for the four dynamic component tests is shown in Figures 50 and 51. Energy levels for all four of the tested anchorages were similar through the first 2 in. (51 mm) of post deflection, but diverged similar to the force levels after that point due to variation in the failure modes.

These results were reviewed to determine the feasibility of the alternative anchorage designs. The original cast-in-place anchorage for the BR27C generated the lowest peak load of the four anchorages. The failure modes observed for this design were a combination of tensile failure of the front anchor rods and breakout of the concrete on the rear of the parapet. This level of damage was much higher than the damage observed in full-scale crash testing. In the full-scale tests, no failure of anchor rods or the concrete parapet was noted. This would indicate that the damage and force levels developed in the component testing were significantly higher than the loading of the post and anchorage during full-scale testing. Thus, alternative designs that exceeded the peak force of the original cast-in-place anchorage should be considered acceptable.

The four-bolt spread anchorage design developed higher peak loads than the original cast-in-place anchorage. Energy levels for the two designs differed, as the cast-in-place anchorage did not completely disengage from the concrete and developed load longer after the initial peak load was reached. Higher peak loads were expected for the four-bolt spread

anchorage based on the increased anchor spacing providing reduction of the overlapped area of influence for the epoxy adhesive anchors, but the peak forces developed in testing found those gains to be minimal. Review of the failure of the anchorage showed that orienting the front and rear anchors for this design diagonal to one another may have allowed shear stresses and cracking to develop along the same plane for both the front and rear anchor simultaneously. This may have contributed to the lower-than-expected improvement in force level of the four-bolt spread anchorage. However, the four-bolt spread anchorage did possess improved capacity to the original cast-in-place anchorage and would be considered an acceptable alternative.

The two-bolt offset anchorage design developed the highest peak load of all of the tested designs. This design also exhibited less damage to the concrete parapet, as the increased offset from the rear face of the parapet increased the shear capacity of the anchorage over the other alternatives. The failure mode for this design was rupture of the weld between the baseplate and the post. Thus, it is the only design tested that did not result in failure of the anchorage itself. The two-bolt offset anchorage was also considered to be an acceptable alternative anchorage. The two-bolt offset anchorage also posed an advantage, in that it required fewer anchors and would be easier to install.

The US-20 bridge anchorage displayed a peak force and failure modes that were quite similar to the original cast-in-place anchorage design. This was not unexpected, as the two designs were similar in terms of the layout and anchor size. The US-20 bridge anchorage was considered to be an acceptable alternative anchorage.

Thus, all three of the alternative anchorage designs were considered to be acceptable alternatives to the original cast-in-place anchorage design. The peak force levels for the alternative anchorages indicated greater capacities than the original anchorage, and the damage levels observed in the dynamic component testing far exceeded the levels observed in full-scale



crash tests. As such, there was no reason to believe that the alternative anchorages would not perform safely. Of the three alternative designs, the two-bolt offset design was deemed the best option due to its potential to reduce parapet damage and improved its ease of installation.

It should be noted that all of the alternative designs were developed and tested on the 12-in. (305-mm) wide version of the IaDOT concrete parapet. These results would likely change if the alternative epoxy anchorages were evaluated on the narrower parapet used with the original cast-in-place anchorage. It should also be noted that the four-bolt spread and two-bolt offset anchorages were designed to develop the full plastic moment capacity of the support post. Based on the test results, the four-bolt spread anchorage was not capable of developing the moment capacity of the post due to concrete breakout in shear. The two-bolt offset design may have had the potential to develop the moment capacity, but the post-to-baseplate weld failed prior to reaching that load. This does not affect the suitability of the alternative anchorages as replacements for the cast-in-place design, but it does suggest that the design calculations for concrete breakout in shear may need further development when considering anchorage for dynamic impact on narrow parapets.

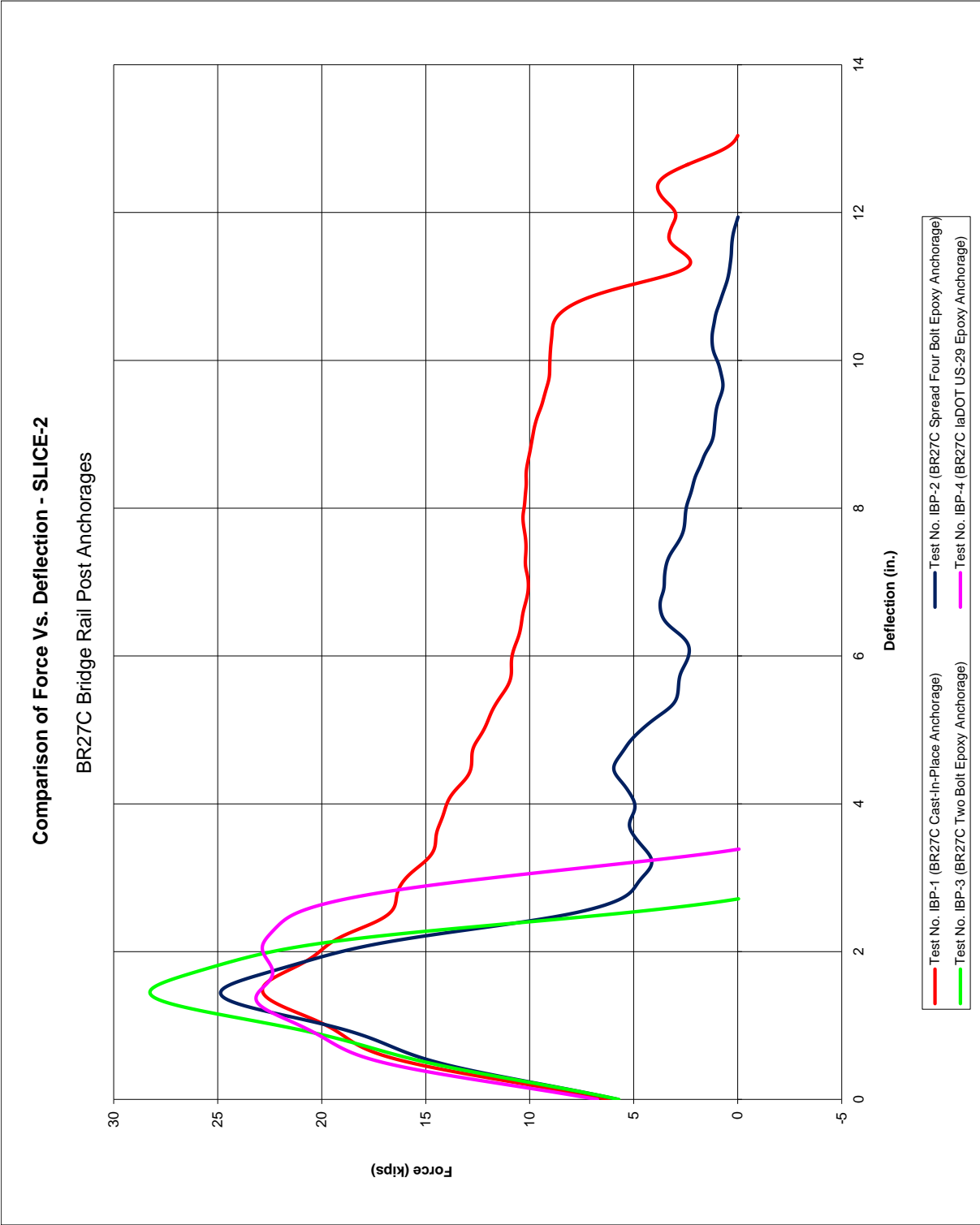


Figure 48. SLICE-2 Force vs. Deflection Comparison, All Bogie Tests

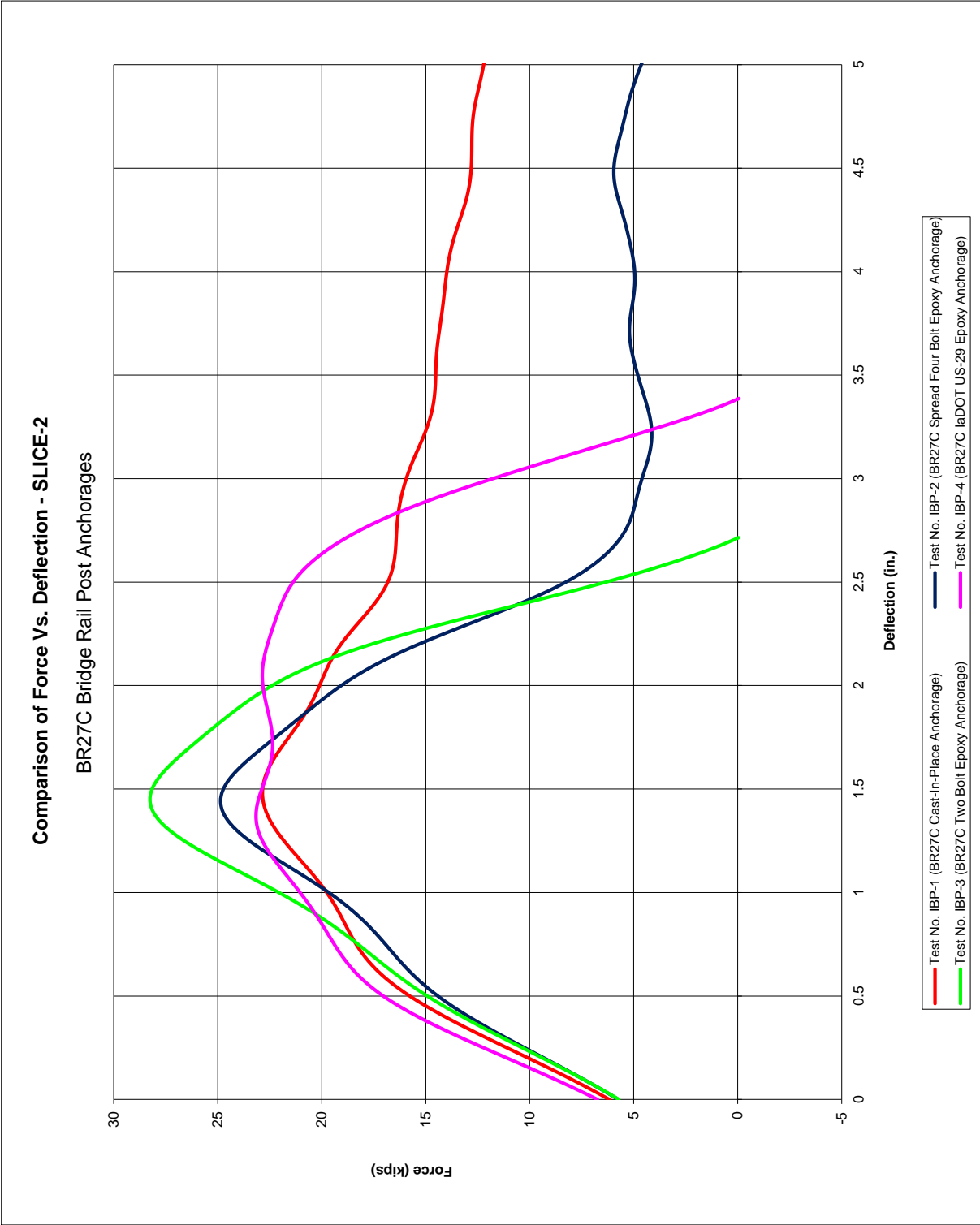


Figure 49. SLICE-2 Force vs. Deflection Comparison Zoom, All Bogie Tests

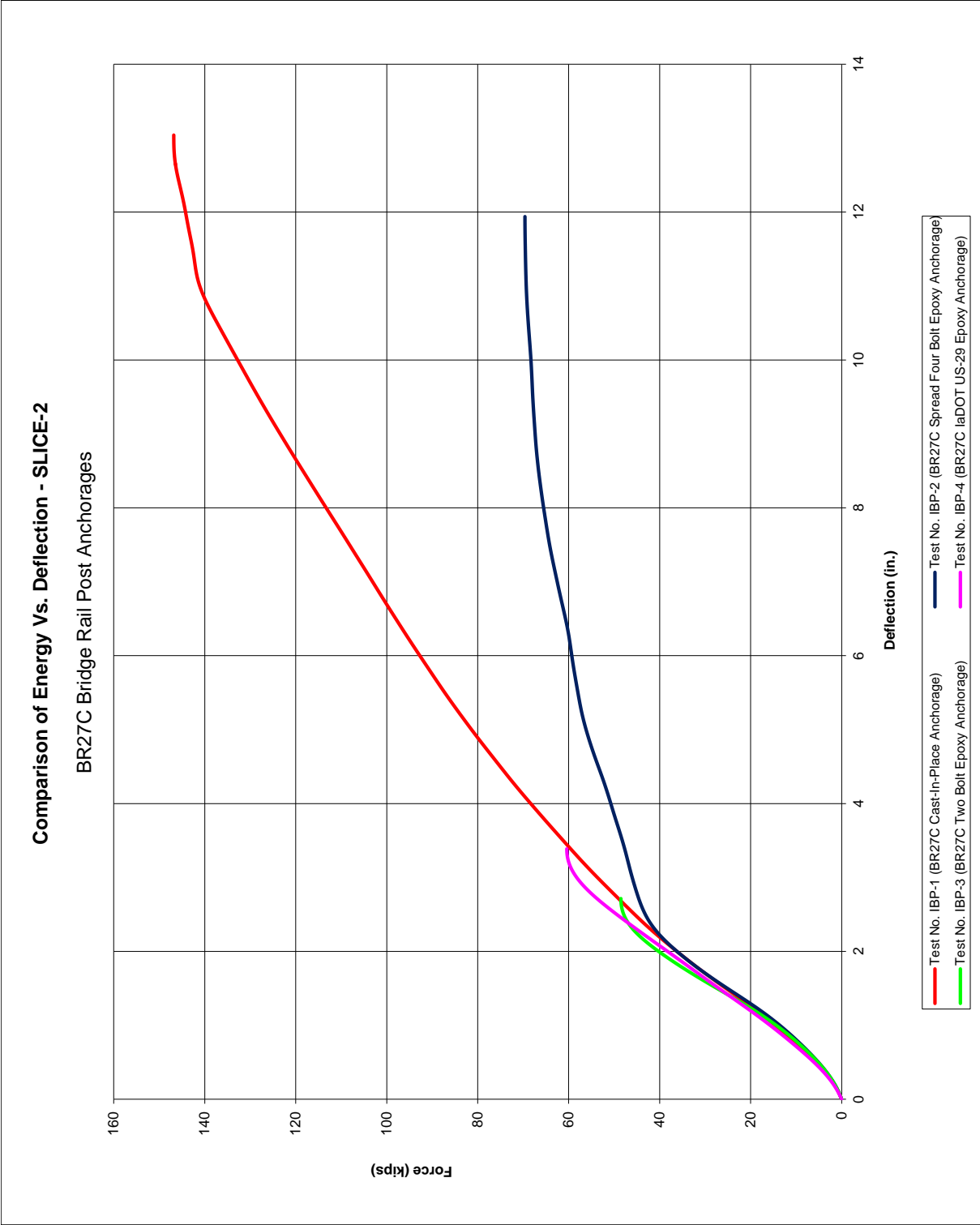


Figure 50. SLICE-2 Energy vs. Deflection Comparison, All Bogie Tests

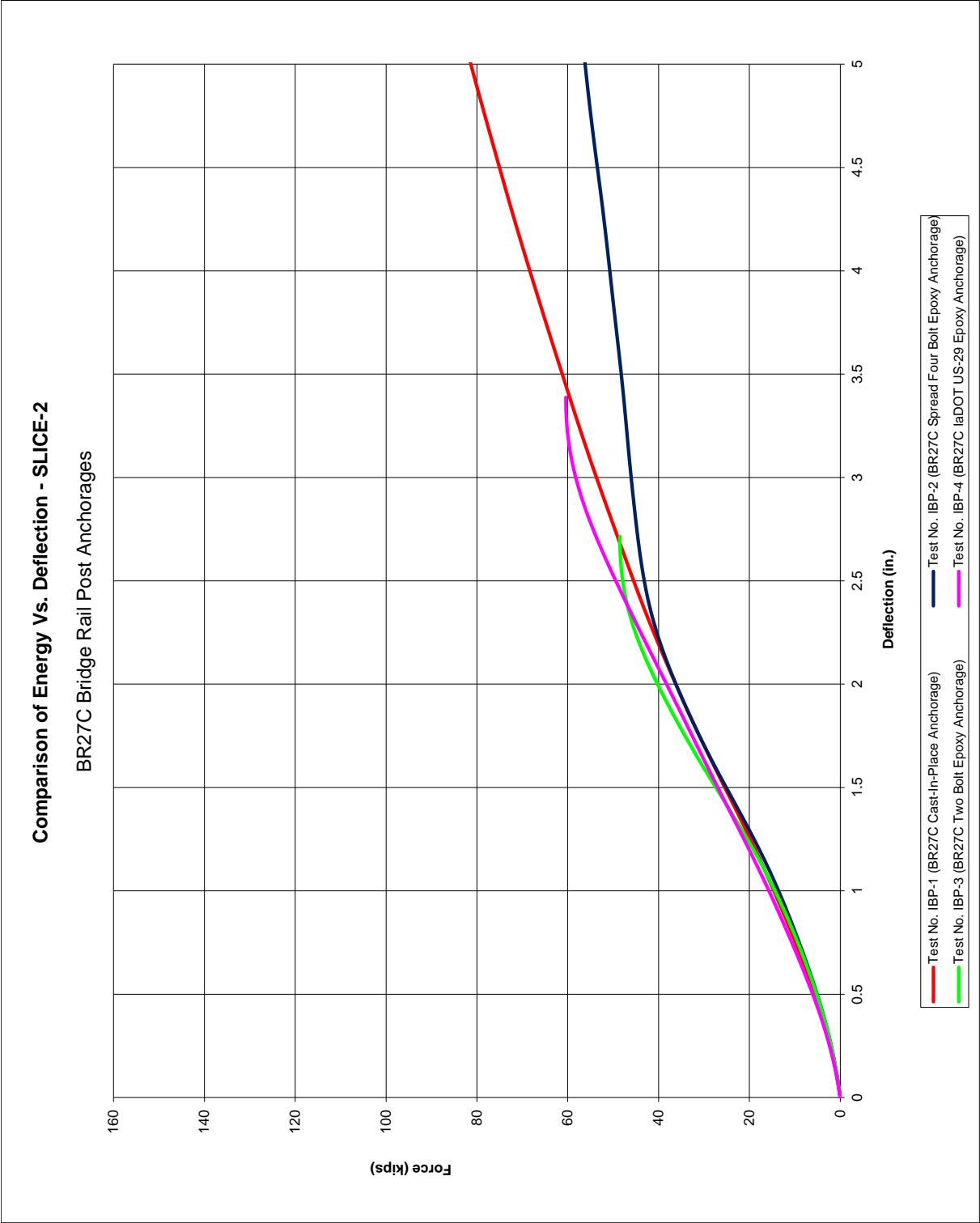


Figure 51 SLICE-2 Energy vs. Deflection Comparison Zoom, All Bogie Tests

## **5 SUMMARY, CONCLUSIONS, AND RECOMMENDATIONS**

The objective of this research was to develop and evaluate alternative epoxy adhesive anchorage systems for the BR27C combination bridge rail system. The BR27C combination bridge rail was originally designed and tested with a 24-in. (610-mm) tall by 10-in. (254-mm) wide vertical concrete parapet with a steel post-and-rail system mounted on top. The steel posts in the combination rail were attached to the concrete parapet with cast-in-place concrete anchors. IaDOT desired an alternative epoxy adhesive anchor design that would be easier to install.

The research effort began with development of several proposed alternative anchorage concepts. The concepts were designed using a modified version of the ACI 318-11 procedures for adhesive anchor design with modifications for dynamic increase factors and the expected failure modes. All of the concepts were designed to develop the full plastic moment capacity of the post. Four design concepts were developed for review by IaDOT, including: (1) a four-bolt, square anchorage, (2) a four-bolt, spread anchorage, (3) a two-bolt, centered anchorage, and (4) a two-bolt, offset anchorage. IaDOT representatives selected the four-bolt spread anchorage and the two-bolt offset anchorage as the preferred designs for evaluation. In addition to these two proposed configurations, IaDOT also requested that the researchers evaluate a third option that had been previously installed on the US-20 bridge near Hardin, IA.

In order to evaluate the performance of the proposed alternative anchorages, dynamic component testing was conducted on the original cast-in-place anchorage as well as the three alternative anchorages using a simulated bridge rail parapet. The test of the original cast-in-place anchorage test no. IBP-1 was used as a baseline for comparison with the alternative designs and developed a peak load of 22.9 kips (101.9 kN) at a deflection of 1.5 in. (38 mm). All three of the tested alternative anchorages provided greater load capacity than the original cast-in-place design and were deemed acceptable surrogates. Of the three alternative designs, the two-bolt offset

design was deemed the best option due to its developing the highest peak loads, the potential for reduced parapet damage, and improved ease of installation. It was also noted that the alternative designs were developed and tested on a 12-in. (305-mm) wide version of the IaDOT concrete parapet. Thus, the alternative anchorages would not be recommended for use on the narrower parapet used with the original cast-in-place anchorage.

## 6 REFERENCES

1. Dickey, B.J., Faller, R.K., Rosenbaugh, S.K., Bielenberg, R.W., Lechtenberg, K.A., and Sicking, D.L., *Development of a Design Procedure for Concrete Traffic Barrier Attachments to Bridge Decks Utilizing Epoxy Concrete Anchors*, Final Report to the Wisconsin Department of Transportation, Transportation Research Report No. TRP 03-264-12, Project No.: TPF-5(193) Supplement #14, Project Code: RPFP WISC-3, Midwest Roadside Safety Facility, University of Nebraska-Lincoln, Lincoln, Nebraska, November 26, 2012.
2. ACI Committee 318, *Building Code Requirements for Structural Concrete (ACI 318-11) and Commentary*, Farmington Hills, MI, American Concrete Institute, August 2011.
3. Williams, W. and Boyd, C. "Design and Construction of Two New Retrofit Combination Steel and Concrete Bridge Rail Designs," *Transportation Research Record: Journal of the Transportation Research Board* 2251 (2011): 34-43.
4. Collins, D.M., Klingner, R.E., Polyzois, D., *Load-Deflection Behavior of Cast-in-Place and Retrofit Concrete Anchors Subjected to Static, Fatigue, and Impact Tensile Loads*, Report No. FHWA/TX-89+1126-1, Center for Transportation Research, University of Texas, Austin, TX, February 1989.
5. Cook, R.A., *Behavior of Chemically Bonded Anchors*, *Journal of Structural Engineering*, American Society of Civil Engineers, September, 1993.
6. Buth, E.B., Hirsh, T.J., and Menges, W.L., *Testing of New Bridge Rail and Transition Designs, Volume VIII: Appendix G, BRs7C Bridge Railing*, Final Report for FHWA Safety and Traffic Operations R&D, FHWA-RD-93-065, Contract No. DTFH61-86-C-00071, Texas Transportation Institute, Texas A&M University, College Station, Texas, June 1997.
7. *Guide Specifications for Bridge Railings*, American Association of State Highway Transportation Officials, Washington, D.C., 1989.
8. Hatton, J.H., *Bridge Railing Design And Testing*, A Discussion with the AASHTO Highway Subcommittee on Bridges and Structures Technical Committee (T-7) for Guardrail and Bridge Rail, Federal Highway Administration (FHWA), U.S. Department of Transportation, FHWA HNG-10, May 7, 1996.
9. Ross, H.E., Sicking, D.L., Zimmer, R.A., and Michie, J.D., *Recommended Procedures for the Safety Performance Evaluation of Highway Features*, National Cooperative Research Program (NCHRP) Report No. 350, Transportation Research Board, Washington, D.C., 1993.
10. Society of Automotive Engineers (SAE), *Instrumentation for Impact Test – Part 1 – Electronic Instrumentation*, SAE J211/1 MAR95, New York City, NY, July, 2007.



## **7 APPENDICES**

## **Appendix A. Alternative Epoxy Adhesive Anchor Design Calculations**

The anchorage calculations used during the development of the four design concepts presented in this research are detailed herein. The calculations were based on development of the full-plastic moment capacity of the BR27C combination bridge rail post and the corresponding shear and tensile loads when used with the 12-in. (305-mm) wide parapet design provided by IaDOT. Details of the design of the baseplates for the posts are not included.

### TENSION ANCHORS (FRONT FACE)

Embedment Depth, $h_{ef}$ :	5 in.
Steel Bar Diameter, $d_b$ :	0.625 in.
Area of Steel, $A_s$ :	0.226 in. <sup>2</sup>
Front (Tension) Anchor Spacing, $s$ :	6.5 in.
Front (Tension) Anchor to deck edge, $c_{a,min}$ :	4.625 in.
Bond Strength, $\tau_{cr}$ :	1800 psi
Steel Ultimate Strength, $f_{uta}$ :	120 ksi
Concrete Strength, $f_c$ :	4000 psi
Deck Reinforced? ( $\gamma/n$ ):	$\gamma$
Steel DIF, $\psi_{sd}$ :	1.18
Concrete DIF, $\psi_{cd}$ :	1.88
Adhesive/Bond DIF, $\psi_{bd}$ :	1.484

### Tension Strengths

Failure Mode	Load (kips)
Steel Fracture:	24.00
Concrete Breakout:	10.43
Bond Failure:	7.86
Hybrid:	18.29

	Tension	Shear
ACI Steel Strength Reduction Factor, $\phi_s$ :	0.75	0.65
ACI Concrete Strength Reduction Factor, $\phi_c$ :	0.65	0.75
ACI Adhesive Strength Reduction Factor, $\phi_a$ :	0.65	NA

### TENSION CAPACITY

Steel Fracture:  $\Phi N_s = A_s N_s f_{uta} \psi_{sd}$

$\Phi N_s = 24.00$  kips

Concrete Breakout:  $\Phi N_{cb} = A_{Nc}/A_{Nco} * \psi_{ed,N} \psi_{cp,N} \psi_{cd} * N_b$

$N_b = k_c * h_{ef}^{1.5} \sqrt{f_c}$   
 $k_c = 17$  (24 for cast in place, 17 for post installed)  
 $\psi_{cp,N} = 1.4$  (1.25 for cast in anchors, 1.4 for post installed, 1.0 if kc taken from external document without further instructions)

$N_b = 12.02$  kips

$c_{ac} = 10$

$\psi_{cp,N} = 1$

$\psi_{ed,N} = 0.885$

$A_{Nco} = 9 * h_{ef}^2 = 225$  in.<sup>2</sup>

$A_{Nc} = 129$  in.<sup>2</sup>

$A_{Nc}/A_{Nco} = 0.573333$

Note - Calculated based on influence area per anchor

$\Phi N_{cb} = 10.43$  kips

Adhesive / Bond Failure:  $\Phi N_a = A_{Na}/A_{Nao} * \psi_{ed,Na} \psi_{cp,Na} \psi_{bd} * N_{ba}$

$N_{ba} = \tau_{cr} \pi d_b h_{ef}$

$N_{ba} = 17.67$  kips

$A_{Nao} = (2 * C_{Na})^2$

$C_{Na} = 10 * d_b * \sqrt{\tau_{cr}/1100}$

$C_{Na} = 8.00$  in.

$A_{Nao} = 255.68$  in.<sup>2</sup>

$A_{Na} = 134.9403$  in.<sup>2</sup>

$A_{Na}/A_{Nao} = 0.527767$

Note - Calculated based on influence area per anchor

$\psi_{cp,Na} = 1$  (should be the same as  $\psi_{cp,N}$ )

$\psi_{ed,Na} = 0.873545$

$\Phi N_a = 7.86$  kips

Figure A-1. Tensile Adhesive Anchorage Calculations, Four-Bolt Square Anchorage Concept

### SHEAR ANCHORS (BACK FACE)

Embedment Depth, $h_{ef}$ :	10 in.
Steel Bar Diameter, $d_b$ :	0.625 in.
Area of Steel, $A_s$ :	0.226 in. <sup>2</sup>
Anchor Spacing, $s$ :	6.5 in.
Anchor to Deck Edge Distance, $c_{ad}$ :	4.625 in.
Steel Ultimate Strength, $f_{tsa}$ :	120 ksi
Concrete Strength, $f'_c$ :	4000 psi
Deck Thickness, $h_a$ :	26 in.
Deck Reinforced? (y/n):	y
Bond Strength, $\tau_{cr}$ :	1800 psi

### Shear Strengths

Failure Mode	Load (kips)
Steel Fracture:	12.48
Concrete Breakout:	7.65
Concrete Pryout:	15.25

Total Anchor Shear for Barrier

LCR: 20 ft

$\Phi V_{s, barrier} = 282.38$  kips

### SHEAR CAPACITY

Steel Fracture:  $\Phi V_{sa} = 0.6 A_s f_{tsa} \Psi_{sa}$

$\Phi V_{sa} = 12.48$  kips

Concrete Breakout:  $\Phi V_{cb} = A_{vc}/A_{vc0} \Psi_{ed,v} \Psi_{c,v} \Psi_{h,v} \Psi_{ed} V_b$

$$V_{b1} = 7 \cdot (l_e/d_b)^{0.2} \cdot \sqrt{d_b} \cdot \sqrt{f'_c} \cdot C_{a1}^{1.5}$$

$$l_e = 5.00$$

$$V_{b1} = 5.28 \text{ kips}$$

$$V_{b2} = 9 \cdot C_{a1}^{1.5} \cdot \sqrt{f'_c}$$

$$5.66 \text{ kips}$$

$$V_b = \min(V_{b1}, V_{b2}) = 5.28 \text{ kips}$$

$$\Psi_{ed,v} = 1 \text{ (only reduced for anchor adjacent to deck discontinuity)}$$

$$\Psi_{c,v} = 1.4 \text{ (1.4 for uncracked deck, 1.2 for cracked reinforced, 1.0 for cracked unreinforced deck)}$$

$$\Psi_{h,v} = 1.00$$

$$A_{vc0} = 4.5 \cdot (c_{ad})^2 = 96.25781 \text{ in.}^2$$

$$A_{vc} = 70.67578 \text{ in.}^2$$

$$A_{vc0}/A_{vc} = 0.734234$$

$\Phi V_{cb} = 7.65$  kips

Concrete Pryout Strength:  $\Phi V_{cp} = k_{cp} N_q$

$$k_{cp} = 2$$

$$N_q = \min(N_{cb}, N_a)$$

$$N_b = A_{N0}/A_{N00} \cdot \Psi_{ed,N} \Psi_{c,N} \Psi_{cp,N} \Psi_{ed} \cdot N_b$$

$$N_b = k_c \cdot h_{ef}^{1.5} \cdot \sqrt{f'_c}$$

$$k_c = 17$$

$$\Psi_{c,N} = 1.4$$

$$N_b = 34.00 \text{ kips}$$

$$c_{ac} = 20$$

$$\Psi_{cp,N} = 1$$

$$\Psi_{ed,N} = 0.7925$$

$$A_{N00} = 9 \cdot h_{ef}^2 = 900 \text{ in.}^2$$

$$A_{Nc} = 129 \text{ in.}^2$$

$$A_{Nc}/A_{N00} = 0.143333$$

$$N_a = 10.17$$

$$N_q = 10.17$$

$\Phi V_{cp} = 15.25$  kips

$$N_a = A_{Na}/A_{Na0} \cdot \Psi_{ed,Na} \Psi_{cp,Na} \Psi_{bd} \cdot N_{ba}$$

$$N_{ba} = \tau_{cr} \cdot \pi \cdot d_b \cdot h_{ef}$$

$$N_{ba} = 35.34 \text{ kips}$$

$$A_{Na0} = (2 \cdot C_{Na})^2$$

$$C_{Na} = 10 \cdot d_b \cdot \sqrt{\tau_{cr}/1100}$$

$$C_{Na} = 8.00$$

$$A_{Na0} = 255.68 \text{ in.}^2$$

$$A_{Na} = 134.9403 \text{ in.}^2$$

$$A_{Na}/A_{Na0} = 0.527767$$

$$\Psi_{cp,Na} = 1 \text{ (should be the same as } \Psi_{cp,N})$$

$$\Psi_{ed,Na} = 0.873545$$

$$N_a = 24.18$$

Figure A-2. Shear Adhesive Anchorage Calculations, Four-Bolt Square Anchorage Concept

### TENSION ANCHORS (FRONT FACE)

Embedment Depth, $h_{ef}$ :	5 in.
Steel Bar Diameter, $d_b$ :	0.625 in.
Area of Steel, $A_s$ :	0.226 in. <sup>2</sup>
Front (Tension) Anchor Spacing, $s$ :	6.5 in.
Front (Tension) Anchor to deck edge, $c_{a,min}$ :	4.625 in.
Bond Strength, $\tau_{cr}$ :	1800 psi
Steel Ultimate Strength, $f_{uta}$ :	120 ksi
Concrete Strength, $f'_c$ :	4000 psi
Deck Reinforced? ( $\gamma/n$ ):	Y
Steel DIF, $\psi_{sd}$ :	1.18
Concrete DIF, $\psi_{cd}$ :	1.88
Adhesive/Bond DIF, $\psi_{bd}$ :	1.484

### Tension Strengths

Failure Mode	Load (kips)
Steel Fracture:	24.00
Concrete Breakout:	10.43
Bond Failure:	7.86
Hybrid:	18.29

	Tension	Shear
ACI Steel Strength Reduction Factor, $\phi_s$ :	0.75	0.65
ACI Concrete Strength Reduction Factor, $\phi_c$ :	0.65	0.75
ACI Adhesive Strength Reduction Factor, $\phi_a$ :	0.65	NA

### TENSION CAPACITY

Steel Fracture:  $\phi N_s = A_s N f_{uta} \psi_{sd}$

$\phi N_s = 24.00$  kips

Concrete Breakout:  $\phi N_{cb} = A_{Nc}/A_{Nco} * \psi_{ed,N} \psi_{c,N} \psi_{cp,N} \psi_{cd} * N_b$

$N_b = k_c * h_{ef}^{1.5} \sqrt{f'_c}$

$k_c = 17$

(24 for cast in place, 17 for post installed)

$\psi_{c,N} = 1.4$

(1.25 for cast in anchors, 1.4 for post installed, 1.0 if  $k_c$  taken from external document without further instructions)

$N_b = 12.02$  kips

$c_{ac} = 10$

$\psi_{cp,N} = 1$

$\psi_{ed,N} = 0.885$

$A_{Nco} = 9 * h_{ef}^2 = 225$  in.<sup>2</sup>

$A_{Nc} = 129$  in.<sup>2</sup>

$A_{Nc}/A_{Nco} = 0.573333$

Note - Calculated based on influence area per anchor

$\phi N_{cb} = 10.43$  kips

Adhesive / Bond Failure:  $\phi N_a = A_{Na}/A_{Na0} * \psi_{ed,Na} \psi_{cp,Na} \psi_{bd} * N_{ba}$

$N_{ba} = \tau_{cr} \pi d_b h_{ef}$

$N_{ba} = 17.67$  kips

$A_{Na0} = (2 * C_{Na})^2$

$C_{Na} = 10 * d_b * \sqrt{\tau_{cr}/1100}$

$C_{Na} = 8.00$  in.

$A_{Na0} = 255.68$  in.<sup>2</sup>

$A_{Na} = 134.9403$  in.<sup>2</sup>

Note - Calculated based on influence area per anchor

$A_{Na}/A_{Na0} = 0.527767$

$\psi_{cp,Na} = 1$  (should be the same as  $\psi_{cp,N}$ )

$\psi_{ed,Na} = 0.873545$

$\phi N_a = 7.86$  kips

Figure A-3. Tensile Adhesive Anchorage Calculations, Four-Bolt Spread Anchorage Concept

### SHEAR ANCHORS (BACK FACE)

Embedment Depth, $h_{ef}$ :	10 in.
Steel Bar Diameter, $d_b$ :	0.625 in.
Area of Steel, $A_s$ :	0.225 in. <sup>2</sup>
Anchor Spacing, $s$ :	13.5 in.
Anchor to Deck Edge Distance, $c_{ad}$ :	4.625 in.
Steel Ultimate Strength, $f_{uta}$ :	120 ksi
Concrete Strength, $f'_c$ :	4000 psi
Deck Thickness, $h_d$ :	26 in.
Deck Reinforced? (y/n):	y
Bond Strength, $\tau_{cr}$ :	1800 psi

### Shear Strengths

Failure Mode	Load (kips)
Steel Fracture:	12.48
Concrete Breakout:	10.28
Concrete Pryout:	30.85

Total Anchor Shear for Barrier

LCR:	20 ft
$\Phi V_{barrier}$ :	182.67 kips

### SHEAR CAPACITY

Steel Fracture:  $\Phi V_{sa} = 0.6 * A_s * f_{uta} * \Psi_{sa}$   
 $\Phi V_{sa} = 12.48$  kips

Concrete Breakout:  $\Phi V_{cb} = A_{vc} / A_{vco} * \Psi_{ed,v} \Psi_{c,v} \Psi_{h,v} \Psi_{cd} * V_b$

$$V_{b1} = 7 * (l_e / d_b)^{0.2} * \sqrt{d_b} * \sqrt{f'_c} * C_{ad}^{1.5}$$

$$l_e: 5.00$$

$$V_{b1} = 5.28$$
 kips

$$V_{b2} = 9 * C_{ad}^{1.5} * \sqrt{f'_c}$$

$$5.66$$
 kips

$$V_b = \min(V_{b1}, V_{b2}) = 5.28$$
 kips

$$\Psi_{ed,v}: 1 \text{ (only reduced for anchor adjacent to deck discontinuity)}$$

$$\Psi_{c,v}: 1.4 \text{ (1.4 for uncracked deck, 1.2 for cracked reinforced, 1.0 for cracked unreinforced deck)}$$

$$\Psi_{h,v}: 1.00$$

$$A_{vco} = 4.5 * (c_{ad})^2 = 96.25781 \text{ in.}^2$$

$$A_{vc} = 94.95703 \text{ in.}^2$$

$$A_{vco} / A_{vc} = 0.986486$$

$$\Phi V_{cb} = 10.28$$
 kips

Concrete Pryout Strength:  $\Phi V_{cp} = K_{cp} * N_{cp}$

$$K_{cp} = 2$$

$$N_{cp} = \min(N_{cb}, N_a)$$

$$N_{cb} = A_{Ncb} / A_{Nco} * \Psi_{ed,N} \Psi_{c,N} \Psi_{cp,N} \Psi_{cd} * N_b$$

$$N_b = k_c * h_{ef}^{1.5} * \sqrt{f'_c}$$

$$k_c: 17$$

$$\Psi_{c,N}: 1.4$$

$$N_b = 34.00$$
 kips

$$C_{ac}: 20$$

$$\Psi_{cp,N}: 1$$

$$\Psi_{ed,N}: 0.7925$$

$$A_{Nco} = 9 * h_{ef}^2: 900 \text{ in.}^2$$

$$A_{Nc}: 261 \text{ in.}^2$$

$$A_{Nc} / A_{Nco}: 0.29$$

$$N_{cb} = 20.57$$

$$N_a = A_{Na} / A_{Nao} * \Psi_{ed,Na} \Psi_{c,Na} \Psi_{cp,Na} \Psi_{cd} * N_{ba}$$

$$N_{ba} = \tau_{cr} * \pi * d_b * h_{ef}$$

$$N_{ba} = 35.34$$
 kips

$$A_{Nao} = (2 * C_{Na})^2$$

$$C_{Na} = 10 * d_b * \sqrt{(\tau_{cr} / 1100)}$$

$$C_{Na} = 8.00$$

$$A_{Nao} = 255.68 \text{ in.}^2$$

$$A_{Na} = 176.9403 \text{ in.}^2$$

$$A_{Na} / A_{Nao}: 0.692033$$

$$\Psi_{cp,Na}: 1 \text{ (should be the same as } \Psi_{cp,N} \text{)}$$

$$\Psi_{ed,Na}: 0.873545$$

$$N_a = 31.71$$

$$N_{cp} = 20.57$$

$$\Phi V_{cp} = 30.85$$
 kips

Figure A-4. Shear Adhesive Anchorage Calculations, Four-Bolt Spread Anchorage Concept

### TENSION ANCHORS (FRONT FACE)

Embedment Depth, $h_{ef}$ :	6 in.
Steel Bar Diameter, $d_b$ :	0.75 in.
Area of Steel, $A_s$ :	0.334 in. <sup>2</sup>
Front (Tension) Anchor Spacing, $s$ :	6.5 in.
Front (Tension) Anchor to deck edge, $c_{a,min}$ :	6 in.
Bond Strength, $\tau_{cr}$ :	1800 psi
Steel Ultimate Strength, $f_{uta}$ :	120 ksi
Concrete Strength, $f'_c$ :	4000 psi
Deck Reinforced? (y/n):	y
Steel DIF, $\psi_{sd}$ :	1.18
Concrete DIF, $\psi_{cd}$ :	1.88
Adhesive/Bond DIF, $\psi_{bd}$ :	1.484

### Tension Strengths

Failure Mode	Load (kips)
Steel Fracture:	35.47
Concrete Breakout:	11.04
Bond Failure:	9.12
Hybrid:	20.16

	Tension	Shear
ACI Steel Strength Reduction Factor, $\phi_s$ :	0.75	0.65
ACI Concrete Strength Reduction Factor, $\phi_c$ :	0.65	0.75
ACI Adhesive Strength Reduction Factor, $\phi_a$ :	0.65	NA

### TENSION CAPACITY

Steel Fracture:  $\phi N_s = A_s f_{uta} \psi_{sd}$

$\phi N_s = 35.47$  kips

Concrete Breakout:  $\phi N_{cb} = A_{Nc}/A_{Nco} * \psi_{ed,N} \psi_{cp,N} \psi_{cd} * N_b$

$N_b = k_c * h_{ef}^{1.5} \sqrt{f'_c}$

$k_c = 17$  (24 for cast in place, 17 for post installed)

$\psi_{cp,N} = 1.4$  (1.25 for cast in anchors, 1.4 for post installed, 1.0 if  $k_c$  taken from external document without further instructions)

$N_b = 15.80$  kips

$C_{ac} = 12$

$\psi_{cp,N} = 1$

$\psi_{ed,N} = 0.9$

$A_{Nco} = 9 * h_{ef}^2 = 324$  in.<sup>2</sup>

$A_{Nc} = 147$  in.<sup>2</sup>

$A_{Nc}/A_{Nco} = 0.453704$

Note - Calculated based on influence area per anchor

$\phi N_{cb} = 11.04$  kips

Adhesive / Bond Failure:  $\phi N_a = A_{Na}/A_{Na0} * \psi_{ed,Na} \psi_{cp,Na} \psi_{bd} * N_{ba}$

$N_{ba} = \tau_{cr} \pi d_b h_{ef}$

$N_{ba} = 25.45$  kips

$A_{Na0} = (2 * C_{Na})^2$

$C_{Na} = 10 * d_b * \sqrt{\tau_{cr}/1100}$

$C_{Na} = 9.59$  in.

$A_{Na0} = 368.18$  in.<sup>2</sup>

$A_{Na} = 154.1284$  in.<sup>2</sup>

$A_{Na}/A_{Na0} = 0.41862$

Note - Calculated based on influence area per anchor

$\psi_{cp,Na} = 1$  (should be the same as  $\psi_{cp,N}$ )

$\psi_{ed,Na} = 0.887617$

$\phi N_a = 9.12$  kips

Figure A-5. Tensile Adhesive Anchorage Calculations, Two-Bolt Centered Anchorage Concept

### SHEAR ANCHORS (BACK FACE)

Embedment Depth, $h_{ef}$ :	12 in.
Steel Bar Diameter, $d_b$ :	0.75 in.
Area of Steel, $A_s$ :	0.334 in. <sup>2</sup>
Anchor Spacing, $s$ :	6.5 in.
Anchor to Deck Edge Distance, $c_{ad}$ :	6 in.
Steel Ultimate Strength, $f_{ut}$ :	120 ksi
Concrete Strength, $f'_c$ :	4000 psi
Deck Thickness, $h_d$ :	26 in.
Deck Reinforced? (y/n):	y
Bond Strength, $\tau_{cr}$ :	1800 psi

### Shear Strengths

Failure Mode	Load (kips)
Steel Fracture:	18.44
Concrete Breakout:	11.24
Concrete Pryout:	16.01

Total Anchor Shear for Barrier

LCR:	20 ft
$\Phi V_{barrier}$ :	414.96 kips

### SHEAR CAPACITY

**Steel Fracture:**  $\Phi V_{sa} = 0.6 * A_s * f_{ut} * \Psi_{ed}$   
 $\Phi V_{sa} = 18.44$  kips

**Concrete Breakout:**  $\Phi V_{cb} = A_{vc} / A_{vco} * \Psi_{ed,v} \Psi_{c,v} \Psi_{h,v} \Psi_{ed} * V_b$

$$V_{b1} = 7 * (l/d_b)^{0.2} * \sqrt{d_b} * \sqrt{f'_c} * c_{ad}^{1.5}$$

$$l_c = 6.00$$

$$V_{b1} = 8.54 \text{ kips}$$

$$V_{b2} = 9 * c_{ad}^{1.5} * \sqrt{f'_c}$$

$$8.37 \text{ kips}$$

$$V_b = \min(V_{b1}, V_{b2}) = 8.37 \text{ kips}$$

$$\Psi_{ed,v} = 1 \text{ (only reduced for anchor adjacent to deck discontinuity)}$$

$$\Psi_{c,v} = 1.4 \text{ (1.4 for uncracked deck, 1.2 for cracked reinforced, 1.0 for cracked unreinforced deck)}$$

$$\Psi_{h,v} = 1.00$$

$$A_{vco} = 4.5 * (c_{ad})^2 = 162 \text{ in.}^2$$

$$A_{vc} = 110.25 \text{ in.}^2$$

$$A_{vc} / A_{vco} = 0.680556$$

$$\Phi V_{cb} = 11.24 \text{ kips}$$

**Concrete Pryout Strength:**  $\Phi V_{cp} = k_{cp} N_{cp}$

$$k_{cp} = 2$$

$$N_{cp} = \min(N_{cb}, N_a)$$

$$N_{cb} = A_{Nc} / A_{Nco} * \Psi_{ed,N} \Psi_{c,N} \Psi_{cp,N} \Psi_{ed} * N_b$$

$$N_b = k_c * h_{ef}^{1.5} * \sqrt{f'_c}$$

$$k_c = 17$$

$$\Psi_{c,N} = 1.4$$

$$N_b = 44.69 \text{ kips}$$

$$c_{ac} = 24$$

$$\Psi_{cp,N} = 1$$

$$\Psi_{ed,N} = 0.8$$

$$A_{Nco} = 9 * h_{ef}^2 = 1296 \text{ in.}^2$$

$$A_{Nc} = 147 \text{ in.}^2$$

$$A_{Nc} / A_{Nco} = 0.113426$$

$$N_{cb} = 10.67$$

$$N_{cp} = 10.67$$

$$\Phi V_{cp} = 16.01 \text{ kips}$$

$$N_a = A_{Na} / A_{Nao} * \Psi_{ed,Na} \Psi_{c,Na} \Psi_{cp,Na} \Psi_{ed} * N_{ba}$$

$$N_{ba} = \tau_{cr} * \pi * d_b * h_{ef}$$

$$N_{ba} = 50.89 \text{ kips}$$

$$A_{Nao} = (2 * C_{Na})^2$$

$$C_{Na} = 10 * d_b * \sqrt{(\tau_{cr} / 1100)}$$

$$C_{Na} = 9.59$$

$$A_{Na} = 368.18 \text{ in.}^2$$

$$A_{Na} = 154.1284 \text{ in.}^2$$

$$A_{Na} / A_{Nao} = 0.41862$$

$$\Psi_{cp,Na} = 1 \text{ (should be the same as } \Psi_{cp,N})$$

$$\Psi_{ed,Na} = 0.887617$$

$$N_a = 28.06$$

Figure A-6. Shear Adhesive Anchorage Calculations, Two-Bolt Centered Anchorage Concept



### TENSION ANCHORS (FRONT FACE)

Embedment Depth, $h_{ef}$ :	6 in.
Steel Bar Diameter, $d_b$ :	0.75 in.
Area of Steel, $A_s$ :	0.334 in. <sup>2</sup>
Front (Tension) Anchor Spacing, $s$ :	6.5 in.
Front (Tension) Anchor to deck edge, $c_{a,min}$ :	4.625 in.
Bond Strength, $\tau_{cr}$ :	1800 psi
Steel Ultimate Strength, $f_{uts}$ :	120 ksi
Concrete Strength, $f'_c$ :	4000 psi
Deck Reinforced? (Y/N):	Y

### Tension Strengths

Failure Mode	Load (kips)
Steel Fracture:	35.47
Concrete Breakout:	10.48
Bond Failure:	8.68
Hybrid:	19.16

Steel DIF, $\psi_{sd}$ :	1.18
Concrete DIF, $\psi_{cd}$ :	1.88
Adhesive/Bond DIF, $\psi_{bd}$ :	1.484

	Tension	Shear
ACI Steel Strength Reduction Factor, $\phi_s$ :	0.75	0.65
ACI Concrete Strength Reduction Factor, $\phi_c$ :	0.65	0.75
ACI Adhesive Strength Reduction Factor, $\phi_a$ :	0.65	NA

### TENSION CAPACITY

Steel Fracture:  $\phi N_s = A_s N_f \psi_{sd}$   
 $\phi N_s = 35.47$  kips

Concrete Breakout:  $\phi N_{cb} = A_{Nc} / A_{Nco} * \psi_{ed,N} \psi_{cp,N} \psi_{bd} * N_b$   
 $N_b = k_c * h_{ef}^{1.5} \sqrt{f'_c}$   
 $k_c = 17$  (24 for cast in place, 17 for post installed)  
 $\psi_{cp,N} = 1.4$  (1.25 for cast in anchors, 1.4 for post installed, 1.0 if  $k_c$  taken from external document without further instructions)  
 $N_b = 15.80$  kips

$c_{ac} = 12$   
 $\psi_{cp,N} = 1$   
 $\psi_{ed,N} = 0.854167$   
 $A_{Nco} = 9 * h_{ef}^2 = 324$  in.<sup>2</sup>  
 $A_{Nc} = 147$  in.<sup>2</sup>  
 $A_{Nc} / A_{Nco} = 0.453704$

Note - Calculated based on influence area per anchor

$\phi N_{cb} = 10.48$  kips

Adhesive / Bond Failure:  $\phi N_a = A_{Na} / A_{Nao} * \psi_{ed,Na} \psi_{cp,Na} \psi_{bd} * N_{ba}$   
 $N_{ba} = \tau_{cr} \pi d_b h_{ef}$   
 $N_{ba} = 25.45$  kips

$A_{Nao} = (2 * c_{Na})^2$   
 $c_{Na} = 10 * d_b * \sqrt{(\tau_{cr} / 1100)}$   
 $c_{Na} = 9.59$  in.  
 $A_{Nao} = 368.18$  in.<sup>2</sup>  
 $A_{Na} = 154.1284$  in.<sup>2</sup>  
 $A_{Na} / A_{Nao} = 0.41862$

Note - Calculated based on influence area per anchor

$\psi_{cp,Na} = 1$  (should be the same as  $\psi_{cp,N}$ )  
 $\psi_{ed,Na} = 0.844621$

$\phi N_a = 8.68$  kips

Figure A-7. Tensile Adhesive Anchorage Calculations, Two-Bolt Offset Anchorage Concept

### SHEAR ANCHORS (BACK FACE)

Embedment Depth, $h_{ef}$ :	12 in.
Steel Bar Diameter, $d_b$ :	0.75 in.
Area of Steel, $A_s$ :	0.334 in. <sup>2</sup>
Anchor Spacing, $s$ :	6.5 in.
Anchor to Deck Edge Distance, $c_{ad}$ :	7.375 in.
Steel Ultimate Strength, $f_{uta}$ :	120 ksi
Concrete Strength, $f'_c$ :	4000 psi
Deck Thickness, $h_d$ :	26 in.
Deck Reinforced? (y/n):	y
Bond Strength, $\tau_{cr}$ :	1800 psi

### Shear Strengths

Failure Mode	Load (kips)
Steel Fracture:	18.44
Concrete Breakout:	14.56
Concrete Pryout:	16.47

Total Anchor Shear for Barrier

LCR:	20 ft
$\Phi V_{barrier}$ :	537.52 kips

### SHEAR CAPACITY

Steel Fracture:  $\Phi V_{sa} = 0.6 \cdot A_s \cdot f_{uta} \cdot \Psi_{sa}$   
 $\Phi V_{sa} = 18.44$  kips

Concrete Breakout:  $\Phi V_{cb} = A_{vc}/A_{vco} \cdot \Psi_{ed,v} \cdot \Psi_{c,v} \cdot \Psi_{h,v} \cdot \Psi_{ed} \cdot V_b$

$$V_{b1} = 7 \cdot \left( \frac{l_d}{d_b} \right)^{0.2} \cdot \sqrt{d_b} \cdot \sqrt{f'_c} \cdot C_{ad}^{1.5}$$

$$l_d = 6.00$$

$$V_{b1} = 11.64$$
 kips

$$V_{b2} = 9 \cdot C_{ad}^{1.5} \cdot \sqrt{f'_c}$$

$$11.40$$
 kips

$$V_b = \min(V_{b1}, V_{b2}) = 11.40$$
 kips

$$\Psi_{ed,v} = 1 \text{ (only reduced for anchor adjacent to deck discontinuity)}$$

$$\Psi_{c,v} = 1.4 \text{ (1.4 for uncracked deck, 1.2 for cracked reinforced, 1.0 for cracked unreinforced deck)}$$

$$\Psi_{h,v} = 1.00$$

$$A_{vco} = 4.5 \cdot (c_{ad})^2 = 244.7578$$
 in.<sup>2</sup>

$$A_{vc} = 158.332$$
 in.<sup>2</sup>

$$A_{vco}/A_{vc} = 0.646893$$

$$\Phi V_{cb} = 14.56$$
 kips

Concrete Pryout Strength:  $\Phi V_{cp} = k_{cp} \cdot N_p$

$$k_{cp} = 2$$

$$N_{cp} = \min(N_{cb}, N_a)$$

$$N_{cb} = A_{Nc}/A_{Nco} \cdot \Psi_{ed,N} \cdot \Psi_{c,N} \cdot \Psi_{cp,N} \cdot \Psi_{ed} \cdot N_b$$

$$N_b = k_c \cdot h_{ef}^{1.5} \cdot \sqrt{f'_c}$$

$$k_c = 17$$

$$\Psi_{c,N} = 1.4$$

$$N_b = 44.69$$
 kips

$$c_{ac} = 24$$

$$\Psi_{cp,N} = 1$$

$$\Psi_{ed,N} = 0.822917$$

$$A_{Nco} = 9 \cdot h_{ef}^2 = 1296$$
 in.<sup>2</sup>

$$A_{Nc} = 147$$
 in.<sup>2</sup>

$$A_{Nc}/A_{Nco} = 0.113426$$

$$N_{cb} = 10.98$$

$$N_{cp} = 10.98$$

$$\Phi V_{cp} = 16.47$$
 kips

$$N_a = A_{Na}/A_{Nao} \cdot \Psi_{ed,Na} \cdot \Psi_{c,Na} \cdot \Psi_{cp,Na} \cdot \Psi_{ed} \cdot N_a$$

$$N_{ba} = \tau_{cr} \cdot \pi \cdot d_b \cdot h_{ef}$$

$$N_{ba} = 50.89$$
 kips

$$A_{Nao} = (2 \cdot C_{Na})^2$$

$$C_{Na} = 10 \cdot d_b \cdot \sqrt{\tau_{cr}/1100}$$

$$C_{Na} = 9.59$$

$$A_{Nao} = 368.18$$
 in.<sup>2</sup>

$$A_{Na} = 154.1284$$
 in.<sup>2</sup>

$$A_{Na}/A_{Nao} = 0.41862$$

$$\Psi_{cp,Na} = 1 \text{ (should be the same as } \Psi_{cp,N})$$

$$\Psi_{ed,Na} = 0.930612$$

$$N_a = 29.42$$

Figure A-8. Shear Adhesive Anchorage Calculations, Two-Bolt Offset Anchorage Concept

## **Appendix B. Material Specifications**

The bill of materials and material specifications are all included in this appendix. This includes concrete cylinder test reports, chemical composition of concrete reports, and chemical composition of rebar reports.

Cast-in-Place (IBP-1)			
Item No.	Description	Material Spec	Reference
a1	Baseplate (3/4")	ASTM A36	R# 14-0486 various heat numbers
a2	5/8" [16] Dia. UNC, 12" [305] Long Threaded Rod	ASTM A193 Grade B7	R# 14-0481 Grainger COC "4FHF5"
a3	5/8" [16] Dia. Hex Nut	ASTM A563 DH	Item# DHHN063CG L# 124738C H# 1W259 Grainger# "1AY80"
a4	5/8" [16] Dia. SAE Flat Washer	ASTM F436	R# 14-0481 Grainger COC "6PU24"
a5	2"x7 3/8"x3/8" [51x187x10] Washer Plate	ASTM A36	R# 14-0486 H# 63134357/02
e5	HSS 4"x4"x3/16" [102x102x5] Steel Tube	ASTM A500 Grade B	R# 14-0486 H# NC4272
Four-Anchor Spread (IBP-2)			
Item No.	Description	Material Spec	Reference
b1	Baseplate (7/8")	ASTM A36	R# 14-0486 H# A3Q1399
b2	5/8" [16] Dia. UNC, 12" [305] Long Threaded Rod	ASTM A193 Grade B7	R# 14-0481 Grainger COC "4FHF5"
b3	5/8" [16] Dia. Hex Nut	ASTM A563 DH	Item# DHHN063CG L# 124738C H# 1W259 Grainger# "1AY80"
b4	5/8" [16] Dia. SAE Flat Washer	ASTM F436	R# 14-0481 Grainger COC "6PU24"
e5	HSS 4"x4"x3/16" [102x102x5] Steel Tube	ASTM A500 Grade B	R# 14-0486 H# NC4272
e6	Epoxy	Hilti RE-500 SD Epoxy	Same as SFH, See Tech Data Sheet

Figure B-1. Bill of Materials, Test Nos. IBP-1 through IBP-2

Two-Anchor Offset (IBP-3)			
Item No.	Description	Material Spec	Reference
c1	Baseplate (1")	ASTM A36	R# 14-0486 H# B4M5434
c2	3/4" [19] Dia. UNC, 14 1/2" [368] Long Threaded Rod	ASTM A193 Grade B7	R# 14-0481 Grainger COC "4FHF7"
c3	3/4" [19] Dia. Hex Nut	ASTM A563 DH	R# 12-0364(HTCT) L# 133507 Item# CHHNO75CP H# 330900831
c4	3/4" [19] Dia. SAE Flat Washer	ASTM F436	R# 14-0481 Grainger COC "6PU26"
e5	HSS 4"x4"x3/16" [102x102x5] Steel Tube	ASTM A500 Grade B	R# 14-0486 H# NC4272
e6	Epoxy	Hilti RE-500 SD Epoxy	Same as SFH, See Tech Data Sheet
US-20 River Bridge (IBP-4)			
Item No.	Description	Material Spec	Reference
d1	Baseplate (13/16" is shaved down from 3/4" plate)	ASTM A36	R# 14-0486 various heat numbers
d2	5/8" [16] Dia. UNC, 12" [305] Long Threaded Rod	ASTM A193 Grade B7	R# 14-0481 Grainger COC "4FHF5"
d3	5/8" [16] Dia. Hex Nut	ASTM A563 DH	Item# DHHN063CG L# 124738C H# 1W259 Grainger# "1AY80"
d4	5/8" [16] Dia. SAE Flat Washer	ASTM F436	R# 14-0481 Grainger COC "6PU24"
e5	HSS 4"x4"x3/16" [102x102x5] Steel Tube	ASTM A500 Grade B	R# 14-0486 H# NC4272
e6	Epoxy	Fastenal Pro-Poxy 300	L# 1305 EXP. 11/15 see (Tech Data Sheet)
Bill of Bars			
Item No.	Description	Material Spec	Reference
e1	1/2" [13] Dia., 79 1/2" [2019] Long Bent Rebar	ASTM A615 Grade 60	H# 112090 Red Paint R# 14-0497
e2	1/2" [13] Dia., 78 1/2" [1994] Long Bent Rebar	ASTM A615 Grade 60	H# 112090 Red Paint R# 14-0497
e3	1/2" [13] Dia., 73 1/2" [1867] Long Bent Rebar	ASTM A615 Grade 60	H# 112090 Red Paint R# 14-0497
e4	1/2" [13] Dia., 236" [5994] Long Rebar	ASTM A615 Grade 60	H# 57134866 Red Paint R# 14-0497

Figure B-2. Bill of Materials, Test Nos. IBP-3 through IBP-4

Concrete industries 6300 Cornhusker Highway P.O. Box 29529 Lincoln, NE 68529- Phone: (402)434-1800 FAX: (402)434-1899				JOB NUMBER 8000MISC.		RELEASE NUMBER DAVID-617		REQ. DELIVERY DATE		PAGE 1 of 1								
				JOB NAME JOB COMPLETE						CC 4HQ								
				CUSTOMER MIDWEST ROADSIDE SAFETY FACILITY						BY MEB								
MATERIAL TYPE Rebar, Grade 60, Black				REFERENCE		DRAWING ID		DESCRIPTION IOWA BRIDGE RAIL										
Item	Qty	Size	Length	Mark	Shape	Lbs	A	B	C	D	E	F/R	G	H	J	K	O	BC
1	14	4	7-05	E3	T1	69	0-042	2-02	1-02	2-02	1-02		0-042					107
2	15	4	7-00	E1		70		3-02	0-08	3-02								805
3	8	4	6-08	E2	S11	36		6-08						3-022				0-07
4	12	4	19-08	E4		158												0
49						333												
Total Weight: 333 Lbs																		
Longest Length: 19-08																		

## REBAR PLANT

WEIGHT SUMMARY												
TOTAL				STRAIGHT			LIGHT BENDING			HEAVY BENDING		
SIZE	ITEMS	PIECES	LBS	ITEMS	PIECES	LBS	ITEMS	PIECES	LBS	ITEMS	PIECES	LBS
Rebar, Grade 60, Black												
4	4	49	333	1	12	158	2	22	105	1	15	70
	4	49	333	1	12	158	2	22	105	1	15	70
Total Weight: 333 Lbs												
Longest Length: 19-08												

Heat # Please

Coil - Evraz 112090

# 4 - Garden 57134866

APR 30 2014

FOR CONSTRUCTION

Iowa Bridge Rail Rebar

R# 14-0497 May 2014 SMT

Iowa Bridge Rail Rebar & Concrete portfolio

September 9, 2014

v13.01.4015 (T) (LIN)
©2014 ASA UNAUTHORIZED REPRODUCTION PROHIBITED
Wednesday, April 30, 2014 12:19 PM

Figure B-3. Rebar Material Specification, Test Nos. IBP-1 through IBP-4



ROCKY MOUNTAIN STEEL  
A DIVISION OF EVRAZ INC. NA

P.O. Box 316  
Pueblo, CO 81002 USA

# MATERIAL TEST REPORT

Date Printed: 21-APR-14

Date Shipped: 21-APR-14      Product: DEF #4 (1/2")      Specification: ASTM A-706/A-615  
FWIP: 52815362      Customer: CONCRETE INDUSTRIES INC      Cust. PO: 106081

CHEMICAL ANALYSIS												
Heat Number	C	Mn	P	S	Si	Cu	Ni	Cr	Mo	Al	V	Ti

(Heat chemistry entered 03/24/14)

0.016 0.0060

Carbon Equivalent = 0.497

MECHANICAL PROPERTIES						
Heat Number	Sample No.	Yield (Psi)	Ultimate (Psi)	Elongation (%)	Reduction (%)	Bend

112090	01	0.2% offset	69715	16.9	ok	0.671
		(MPa)	480.7			
112090	02	0.0035 EUL	64851	15.2	ok	0.670
		(MPa)	447.1			


All melting and manufacturing processes of the material subject to this test certificate occurred in the United States of America.  
ERMIS also certifies this material to be free from Mercury contamination.

This material has been produced and tested in accordance with the requirements of the applicable specifications. We hereby certify that the above test results represent those contained in the records of the Company.

*Mark F. Espinosa*

Quality Assurance Department

Figure B-4. Rebar Material Test Report, Test Nos. IBP-1 through IBP-4



6S-ML-KNOXVILLE  
1919 TENNESSEE AVENUE N. W.  
KNOXVILLE, TN 37921  
USA

**CERTIFIED MATERIAL TEST REPORT**

Page 1/1

CUSTOMER SHIP TO NEBCO INC STEEL DIVISION HAVELOCK, NE 68529 USA		CUSTOMER BILL TO CONCRETE INDUSTRIES INC LINCOLN, NE 68529-0529 USA		GRADE 60 (420) TMX	SHAPE / SIZE Rebar / #4 (13MM)	WEIGHT 111.576 LB	HEAT / BATCH 57134866/02
SALES ORDER 507829/000010		CUSTOMER MATERIAL N°		SPECIFICATION / DATE OF REVISION 1-ASTM A615/A615M-09			
CUSTOMER PURCHASE ORDER NUMBER 101828		BILL OF LADING 1326-0000008527		DATE 08/22/2013			

CHEMICAL COMPOSITION																																																											
C	%	0.25	P	%	0.015	S	%	0.095	Si	%	0.20	Cu	%	0.30	Ni	%	0.16	Cr	%	0.18	Mo	%	0.025	Sn	%	0.003	V	%	0.004	CE <sub>eq</sub> A706	%	0.39																											
MECHANICAL PROPERTIES										UTS										G/L																																							
YS MPa										380										UTS MPa										98030										G/L mm										200.0									
MECHANICAL PROPERTIES										BendTest										OK																																							
GEOMETRIC CHARACTERISTICS										Def Hgt										Def Gap										Def Space																													
%Light										4.79										0.031										0.108										0.332																			
COMMENTS / NOTES																																																											

The above figures are certified chemical and physical test records as contained in the permanent records of company. This material, including the billets, was melted and manufactured in the USA. CMTR complies with EN 10204 3.1.

*Shackay* BIASKAR YALAMANCHILI  
QUALITY DIRECTOR

*Lisa Churnetski* LISA CHURNETSKI  
QUALITY ASSURANCE MGR.

Figure B-5. Rebar Material Test Report, Test Nos. IBP-1through IBP-4



# LINCOLN OFFICE COMPRESSION TEST OF CYLINDRICAL CONCRETE SPECIMENS - 6x12

825 "J" Street  
Lincoln, NE 68508  
Phone: (402) 479-2200  
Fax: (402) 479-2276



ASTM Designation: C 39

Date 04-Sep-14

Client Name: Midwest Roadside Safety Facility

Project Name: Iowa Bridge Rail Footing

Placement Location: Iowa Bridge Rail Head, 8/5/14

Mix Designation: 3600 Required Strength: 3600

## Laboratory Test Data

Laboratory Identification	Field Identification	Date Cast	Date Received	Date Tested	Days Cured in Field	Days Cured in Laboratory	Age of Test, Days	Length of Specimen, in.	Diameter of Specimen, in.	Cross-Sectional Area, sq. in.	Maximum Load, lbf	Compressive Strength, psi	Required Strength, psi	Type of Fracture	ASTM Practice for Capping Specimen
IBR- 8	E	8/5/2014	9/4/2014	9/4/2014	30	0	30	12	6.00	28.27	115,800	4,100	3,600	5	C 1231
IBR- 9	F	8/5/2014	9/4/2014	9/4/2014	30	0	30	12	6.00	28.27	117,260	4,150	3,600	5	C 1231

1 cc: Mr. Shaun Tighe  
Midwest Roadside Safety Facility

## Remarks:

Concrete test specimens along with documentation and test data were submitted by Midwest Roadside Safety Facility.

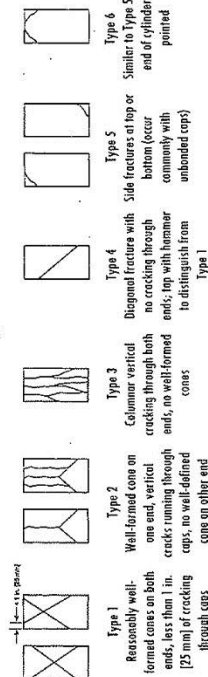
Test results presented relate only to the concrete specimens as received from Midwest Roadside Safety Facility.

This report shall not be reproduced except in full, without the written approval of Alfred Benesch & Company.

Report Number 2147366596

Page 1

## Sketches of Types of Fractures



ALFRED BENESCH & COMPANY  
CONSTRUCTION MATERIALS LABORATORY

By Brant Wells  
Brant Wells, Coordinator

Figure B-6. Concrete Material Test Report for Footing Pour

 <p><b>benesch</b> engineers · scientists · planners</p>	<p><b>LINCOLN OFFICE</b> 825 "J" Street Lincoln, NE 68508 Phone: (402) 479-2200 Fax: (402) 479-2276</p>	<p style="text-align: center;"><b>COMPRESSION TEST OF CYLINDRICAL CONCRETE SPECIMENS - 6x12</b></p> <p style="text-align: center;"><b>ASTM Designation: C 39</b></p>
<p><b>Client Name:</b> Midwest Roadside Safety Facility</p> <p><b>Project Name:</b> Iowa Bridge Rail Footing</p> <p><b>Placement Location:</b> UNL</p> <p><b>Mix Designation:</b> 3600</p>		<p><b>Date:</b> 24-Jul-14</p> <p><b>Required Strength:</b> 3600</p>

Laboratory Test Data															
Laboratory Identification	Field Identification	Date Cast	Date Received	Date Tested	Days Cured in Field	Days Cured in Laboratory	Age of Test, Days	Length of Specimen, in.	Diameter of Specimen, in.	Cross-Sectional Area, sq. in.	Maximum Load, lbf	Compressive Strength, psi	Required Strength, psi	Type of Fracture	ASTM Practice for Capping Specimen
IBR- 1	A	6/23/2014	7/21/2014	7/21/2014	28	0	28	12	5.99	28.18	121,010	4,290	3,600	5	C 1231
IBR- 2	B	6/23/2014	7/21/2014	7/21/2014	28	0	28	12	5.98	28.09	128,150	4,560	3,600	6	C 1231
IBR- 3	C	6/23/2014	7/21/2014	7/21/2014	28	0	28	12	6.03	28.56	123,600	4,330	3,600	6	C 1231
cc: Mr. Shaun Tighe Midwest Roadside Safety Facility															

1 cc Mr. Shaun Tighe  
Midwest Roadside Safety Facility

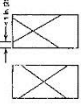
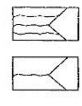

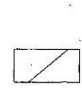
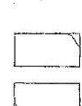

<p><b>Remarks:</b></p> <p>Concrete test specimens along with documentation and test data were submitted by Midwest Roadside Safety Facility.</p> <p>Test results presented relate only to the concrete specimens as received from Midwest Roadside Safety Facility.</p> <p>This report shall not be reproduced except in full, without the written approval of Alfred Benesch &amp; Company.</p> <p>Report Number 2147366387</p> <p>Page 1</p>	<p style="text-align: center;"><b>Sketches of Types of Fractures</b></p> <div style="display: flex; justify-content: space-around;">       </div> <p style="text-align: right;">ALFRED BENESCH &amp; COMPANY CONSTRUCTION MATERIALS LABORATORY</p> <p style="text-align: right;">By <i>Brant Wells</i> Brant Wells, Coordinator</p>
--	--

Figure B-7. Concrete Material Test Report for Footing Pour

# COMPRESSION TEST OF CYLINDRICAL CONCRETE SPECIMENS - 6x12

LINCOLN OFFICE  
825 "J" Street  
Lincoln, NE 68508  
Phone: (402) 479-2200  
Fax: (402) 479-2276



**Client Name:** Midwest Roadside Safety Facility  
**Project Name:** Iowa Bridge Rail Footing  
**Placement Location:** Iowa Bridge Rail Head

**Mix Designation:** 3600

**ASTM Designation:** C 39

**Date** 27-Aug-14

**Required Strength:** 3600

## Laboratory Test Data

Laboratory Identification	Field Identification	Date Cast	Date Received	Date Tested	Days Cured in Field	Days Cured in Laboratory	Age of Test, Days	Length of Specimen, in.	Diameter of Specimen, in.	Cross-Sectional Area, sq. in.	Maximum Load, lbf	Compressive Strength, psi	Required Strength, psi	Type of Fracture	ASTM Practice for Capping Specimen
IBR- 6	C	8/5/2014	8/26/2014	8/27/2014	21	1	22	12	6.01	28.37	108,740	3,830	3,600	6	C 1231
IBR- 7	D	8/5/2014	8/26/2014	8/27/2014	21	1	22	12	6.02	28.46	112,200	3,940	3,600	6	C 1231

1 cc: Mr. Shaun Tighe  
Midwest Roadside Safety Facility

## Remarks:

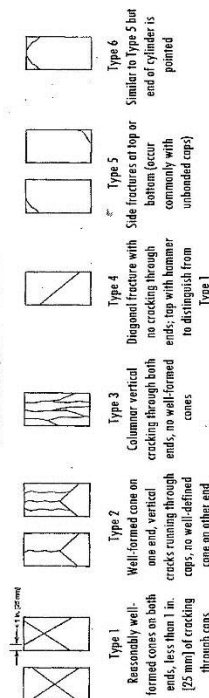
Concrete test specimens along with documentation and test data were submitted by Midwest Roadside Safety Facility.

Test results presented relate only to the concrete specimens as received from Midwest Roadside Safety

This report shall not be reproduced except in full, without the written approval of Alfred Benesch & Company.

Report Number 2147366574  
Page 1

## Sketches of Types of Fractures



ALFRED BENESCH & COMPANY  
CONSTRUCTION MATERIALS LABORATORY

By \_\_\_\_\_  
Brant Wells, Coordinator

Figure B-8. Concrete Material Test Report for Parapet Pour

**CAUTION**

**FRESH CONCRETE**

Body and or eye contact with fresh (moist) concrete should be avoided because it contains alkali and is caustic.

**Ready Mixed Concrete Company**  
6200 Cornhusker Highway, P.O. Box 29288  
Lincoln, Nebraska 68529  
Telephone 402-434-1844

PLANT <b>01</b>	MIX CODE <b>235131PF</b>	YARDS <b>3.50</b>	TRUCK <b>0106</b>	DRIVER	DESTINATION <b>NTE</b>	CLASS	TIME <b>09:30AM</b>	DATE <b>06/23/14</b>	TICKET <b>1178830</b>
CUSTOMER <b>00003</b>	JOB	CUSTOMER NAME <b>CIA---MWRS</b>			TAX CODE	PARTIAL	NIGHT R	LOADS <b>1</b>	
DELIVERY ADDRESS <b>4800 NW 35TH</b>				SPECIAL INSTRUCTIONS <b>NW 36TH &amp; W CUMINS NORTH OF OLD N/ GOODYEAR HANGER</b>			P.O. NUMBER <b>402-4506250 / J</b>		

LOAD QUANTITY	CUMULATIVE QUANTITY	ORDERED QUANTITY	PRODUCT CODE	PRODUCT DESCRIPTION	UNIT PRICE	AMOUNT
<b>3.50</b>	<b>3.50</b>	<b>3.50</b>	<b>235131PF</b>	<b>47B(1PF)</b> <b>MINIMUM HAUL</b>	<b>4.00</b>	<b>98.25</b> <b>343.88</b> <b>35.00</b>

WATER ADDED ON JOB AT CUSTOMER'S REQUEST 0 GAL

RECEIVED BY

SUBTOTAL **378.88**

TAX

TOTAL **378.88**  
**378.88**

**TRUCK**    **USER LOGIN**    **DISP**    **TICKET NUM**    **TICKET NUM**    **TICKET ID**    **TIME**    **DATE**

0106    USER    1178830    198703    49780    09:30    06/23/2014

**LOAD SIZE**    **MIX CODE**

3.50 yd    235131PF

**MATERIAL**    **SOURCE**    **DESIGN QTY**    **REQUIRED**    **BATCHED**    **VAR**    **% VAR**    **%MOISTURE**    **ACTUAL WAT**

G47B    47B GRAVEL    2070 lb    7375 lb    7360    -15    -20%    1.80 M    15.59 gl

L47B    47B ROCK    901 lb    3179 lb    3160    -19    -60%    0.80 M    3.01 gl

CEM1PF    CEM1PF    564 lb    1974 lb    1965    -9    -46%            

LRWR    POZZ 322N    17.00 oz    59.50 oz    59.00    -.50    -84%            

AIR    MB-AE 90 A    5.50 oz    19.25 oz    19.00    -.25    -1.30%            

WATER    WATER    29.0 GL    86.3 GL    86.3    0.0    0.00%            

WATER2    WATER2    0.0 gl #    0.0 gl    0.0    0.0    0.00%            

NON-SIMULATED    NUM BATCHES: 1

LOAD TOTAL: 13210 lb    DESIGN W/C: 0.429    WATER/CEMENT: 0.445A    DESIGN WATER: 101.5 gl    ACTUAL WATER: 104.9 gl    TO ADD: 0.0 gl

SLUMP: 4.00 " # WATER IN TRUCK: 0.0 gl    ADJUST WATER: 0.0 gl /load    TRIM WATER: 0.0 gl /yd

Iowa Bridge Rail Concrete Footing

ORIGINAL

Figure B-9. Concrete Material Specification, Footing Pour



**CAUTION  
FRESH CONCRETE**

Body and or eye contact with fresh (moist) concrete should be avoided because it contains alkali and is caustic.

**Ready Mixed  
Concrete Company**  
6200 Cornhusker Highway, P.O. Box 29288  
Lincoln, Nebraska 68529  
Telephone 402-434-1844

PLANT 04	MIX CODE 235131PF	YARDS 2.00	TRUCK 0203	DRIVER 010	DESTINATION	CLASS	TIME 09:55AM	DATE 08/05/14	TICKET 4162072
CUSTOMER 00003	JOB	CUSTOMER NAME CIA---MIDWEST ROADSIDE SAFETY			TAX CODE	PARTIAL	NIGHT R	LOADS 1	
DELIVERY ADDRESS 4800 NW 35TH STREET			SPECIAL INSTRUCTIONS NORTHEAST OF THE NORTH GOODYEAR HANGER				P.O. NUMBER 7709121 KEN		

LOAD QUANTITY	CUMULATIVE QUANTITY	ORDERED QUANTITY	PRODUCT CODE	PRODUCT DESCRIPTION	UNIT PRICE	AMOUNT
2.00	2.00	2.00	235131PF	47B (1PF) MINIMUM HAUL	98.25	196.50
						50.00

WATER ADDED ON JOB  
AT CUSTOMER'S REQUEST

RECEIVED BY

SUBTOTAL 246.50

TAX

TOTAL 246.50

TRUCK	USER LOGIN	DISP	TICKET NUM	TICKET NUM	TICKET ID	TIME	DATE	
0203	USER		4162072	4162324	197331	09:55	08/05/2014	
LOAD SIZE	MIX CODE	SEQ	LOAD ID					
2.00 yd	235131PF	W	199449					
MATERIAL	SOURCE	DESIGN QTY	REQUIRED	BATCHED	VAR	% VAR	%MOISTURE	ACTUAL WAT
647B	47B GRAVEL	2070.0 lb	4255.9 lb	4280.0	24.1	0.57%	2.80 M	13.97 gl
L47B	47B ROCK	901.0 lb	1811.0 lb	1800.0	-11.0	-.61%	0.50 M	1.07 gl
CEM1PF	INTERGRDUN	564.0 lb	1128.0 lb	1125.0	-3.0	-.27%		
LRWR	POZZ 322N	17.0 oz	34.0 oz	34.0	0.0	0.00%		
AIR	MB-AE 90 A	4.8 oz	9.6 oz	10.0	0.4	4.17%		
WATER	WATER	27.0 gl	41.0 gl	42.4	1.4	3.41%		42.42 gl
WATER2	RECYCLE WA	0.0 gl	0.0 gl	0.0	0.0	0.00%		
NON-SIMULATED NUM BATCHES: 1								
LOAD TOTAL: 7562 lb DESIGN W/C: 0.400 WATER/CEMENT: 0.426A DESIGN WATER: 54.0 gl ACTUAL WATER: 57.5 gl								
SLUMP: 4.00 # WATER IN TRUCK: 0.0 gl								

IOWA  
BRIDGE  
(HEA)  
15-0084

ORIGINAL

Figure B-10. Concrete Material Specification, Parapet Pour



# Central Plains Cement Company

## Type IP (25) Mill Test Report

Month of Issue: Jun-14

Plant: Omaha Terminal  
Product: Type IP (25)  
Manufactured: May-14

The current version of ASTM C 595 and AASHTO M 240 Standard Requirements

CHEMICAL ANALYSIS			PHYSICAL ANALYSIS		
Item	Spec limit	Test Result	Item	Spec limit	Test Result
Rapid Method, X-Ray (C 114)			Air content of mortar (%) (C 185)	12 max	9
SiO <sub>2</sub> (%)	---	27.3	Blaine Fineness (m <sup>2</sup> /kg) (C 204)	---	340
Al <sub>2</sub> O <sub>3</sub> (%)	---	9.0	Fineness, Residue retained on a 45 um sieve (%) sieve (%)	---	8.0
Fe <sub>2</sub> O <sub>3</sub> (%)	---	8.3	Autoclave expansion (%) (C 151)	0.80 max -0.20 min	-0.01
CaO (%)	---	48.2	Compressive strength (PSI) (C 109)		
MgO (%)	6.0 max	1.1	1 days		1710
Sulphate as SO <sub>3</sub> (%)	4.0 max	2.4	28 days (Reflects previous month's data)	3620 min	5900
Loss on ignition (%)	5.0 max	1.9	Time of setting (minutes)		
Total Alkalis	---	0.96	Vicat Initial (C 191)	45 - 420	125
			Specific Gravity (C188)	---	2.98

We certify that the above described cement meets the chemical and physical requirements of the current version of ASTM C 595 and AASHTO M 240.

Sugar Creek Plant  
2200 N Courtney Rd.  
Sugar Creek, MO 64050  
816-257-3604

Certified By:

  
Adam Doppenberg - Quality Coordinator

6/13/2014

Figure B-11. Concrete Material Specification, Footing Pour

# ASH GROVE CEMENT COMPANY

Quantity (tons):  
Trailer/Car:  
Shipped:



16215 Highway 50  
Louisville, NE 68037  
Phone: 402-234-2415  
FAX: 402-234-4825

Type IP (25)  
Duracem® F

Production Period: June 1 thru 30, 2014

Date: 7/9/2014

The following information is based on average test data during the production period. The data is typical of cement shipped from the Louisville, Nebraska plant.  
Individual shipments may vary.

STANDARD REQUIREMENTS							
ASTM C595-13							
CHEMICAL				PHYSICAL			
Item	A.S.T.M. Test Method	Spec. Limit	Test Result	Item	A.S.T.M. Test Method	Spec. Limit	Test Result
SiO <sub>2</sub> (%)	C114	A	30.6	Air content of mortar (volume %)	C185	12 max	5
Al <sub>2</sub> O <sub>3</sub> (%)	C114	A	8.7	Fineness			
Fe <sub>2</sub> O <sub>3</sub> (%)	C114	A	3.5	Air permeability (m <sup>2</sup> /kg)	C204	A	496
CaO (%)	C114	A	48.0	325 mesh (%)	C151	A	94.6
MgO (%)	C114	6.0 max	2.8	Autoclave expansion (%)	C151	0.80 max	0.00
SO <sub>3</sub> (%)	C114	4.0 max	3.2	Compressive strength (psi)			
Loss on ignition (%)	C114	5.0 max	1.4	1 Day	C109	A	2550
Na <sub>2</sub> O (%)	C114	A	0.26	3 Days	C109	1890 min	3700
K <sub>2</sub> O (%)	C114	A	0.71	7 Days	C109	2900 min	4470
Equivalent alkalies (%)	C114	A	0.73	28 Days	C109	3620 min	C
				Time of setting (minutes)			
				(Vicat)			
				Initial: Not less than	C191	45	85
				Not more than		420	
				Sulfate resistance <sup>1</sup>	C1012	0.10	0.04
				Specific Gravity	C188		2.95
				Heat of hydration (kJ/kg)	C186		
				7 Days		B	73

<sup>1</sup> Optional requirement

A = Not applicable.

B = Test result represents most recent value and is provided for information only.

C = Test results for this period not available.

We certify that the above described cement, at the time of shipment, meets the chemical and physical requirement of the ASTM C595/C595M-13 or (other) \_\_\_\_\_ specification.

Signature:

Douglas R. Jaquier  
Title: Chief Chemist

Figure B-12. Concrete Material Specification, Parapet Pour



# GENERAL TESTING LABORATORIES

TELEPHONE (402)434-1891

August 4, 2014

P.O. BOX 28529

FAX (402)434-2161

LINCOLN, NEBRASKA 68529

Mix Design Number 235131PF

NDOR 3500 - 1PF

Mix proportions (per cubic yard)

PROJECT INFORMATION			
PROJECT NAME	Iowa DOT Test Mix		
CITY, ST	Lincoln, NE		
CONTRACTOR INFORMATION			
CONTRACTOR NAME	University of Nebraska - Lincoln		
CONTACT PERSON			
CONTACT NUMBER	CONTACT EMAIL		
CONCRETE INFORMATION			
Supplier Mix Design Number	235131PF	NDOR 3500 - 1PF Mix Type	
Design Strength (f' c)	3500 - 1PF	psi	
Design Water / Cementitious Ratio	0.43	=	29 Gallons
Specification Water / Cementitious Allowed	0.48	=	32.5 Gallons
Total Air Content	7.25	+ 1.5%	
Mix Developed From		Density (Estimated)	
Trial Mix Test Data		Fresh	140.2 pcf
Field Experience		Cured	139.5 pcf
Slump (Spread if SCC)			
3" (+ 1.5") WITHOUT WR Admixture			
(+ 1.5") WITH Type A, B, D Water Reducer Admixture			
(+ 2.5") WITH TYPE F, G Admixture			
Specification Maximum			
ADMIXTURE INFORMATION			
ASTM Admix Type	ASTM Designation	Product (Manufacturer/Brand)	Dosage (ounces) See RATE
Air Entraining	ASTM C-260	Master Builders / MasterAir AE 90	No Limit 8.5 1.5
Air Entraining	ASTM C-260	Master Builders / MasterAir AE 400	
Water Reducing *	A, B, D ASTM C-494	Master Builders / MasterPozzolith 322	3 - 5 17 3.0
Set Retarding *	B, D ASTM C-494	Master Builders / MasterSet R 300	
Set Retarding * (Note 1)	B, D ASTM C-494	Master Builders / MasterSet DELVO	
Mid Range Water Reducing (Note 2)	A ASTM C-494	Master Builders / MasterPolyheed 900	
Full Range Water Reducing (Note 2)	F ASTM C-494	Master Builders / MasterGlenium 3030 NS	
Full Range Water Reducing (Note 2)	F ASTM C-494	Master Builders / MasterGlenium 7700	
Accelerating Chloride Base *	C, E ASTM C-494	Master Builders / MasterSet AC 122	
Accelerating Non Chlor Base	C ASTM C-494	Master Builders / MasterSet AC 534	
Corrosion Inhibiting	C ASTM C-494	Master Life CI 30	
Rheological	S ASTM C-494-08a	Master Builders / MasterMatrix VMA 362	
Rheological **	S ASTM C-494-10	ActiveMinerals/Acti-Gel 208	
Consistency Control	S ASTM C-494	Master Builders / MasterSure Z-60	
Water Repellence	S ASTM C-494	Master Builders / MasterPel 240	
Durability Enhancing	C ASTM C-494	Master Builders / MasterLife CI 30	
Drying Enhancing	S ASTM C-494	Specialty Products Group - Vapor Lock 20/20	
Fibermesh	ASTM C-116-03	Proper Concrete Systems - Fibermesh 300	
Fibermesh	ASTM C-116-03	Proper Concrete Systems - Novomesh 500	
Type A - Water Reducing	Type D - Water Reducing & Retarding	Type G - Water Reducing High Range & Retarding	
Type B - Retarding	Type E - Water Reducing & Accelerating	Type S - Specific Performance (Rheology)	
Type C - Accelerating	Type F - Water Reducing High Range		
RATE: Admixture quantities will vary due to external forces including ambient temperatures, humidity, wind, etc.			
* Meets multiple ASTM specifications according to dosage volume.			
** Acti-Gel addition calculated on total weight of all dry materials included in the mix design.		*** As required at contractor request	
Note 1: May be required for set control and slump retention with environmental conditions.		to adjust mix physical properties.	
Note 2: Jobsite conditions and contractor requests may require use of this admixture.			
Bayer Color System			
Color	No Color Added	Color Originator	Color 1100 Color 9200 Color 1300 Color 3000
Product Code			Lt. Red Yellow Dark Red Black
Total Load Rate			

	Identification (Type,size,source,etc.)	Weight (lb.)	Density SSD	Volume (cubic feet)	% Aggregate Absorption				
Cement	Ⅶ								
Cement	Ⅲ								
Cement	Max Cem								
Cement	1PF	Ash Grove, Central Plains	564	2.95	3.06				
Cement	White								
Fly Ash	Class C								
Slag	Size 120								
Komponent									
Interplast N									
Silica Fume									
Coarse Agg. No. 1	47B, Size 57 Limestone	901	2.66	5.43	1.2%				
Coarse Agg. No. 2									
Coarse Agg. No. 3									
Fine Agg. No. 1	47B Sand/Gravel	2071	2.62	12.67	0.6%				
Fine Agg. No. 2									
Fine Agg. No. 3									
		Gal	Lbs						
Water	Lincoln Water System	29	242	1	3.88				
Air Content	Master Builders	7.25%	0	1.96					
Other									
	TOTALS	3778	Lbs.	27.00	Cubic Feet				
Coarse & Fine Aggregate Gradation Information									
	% Passing Each Sieve (All Sieves Sizes must be entered)						Combined % Retained		
Sieve	Coarse # 1 Limestone	Coarse # 2 Limestone	Coarse # 3	Fine # 1 Sand/Gravel	Fine # 2 Sand	Fine # 3 Sand	Combined % Passing	Cumulative	Individual
Size	3. Size 57 Limestone	Size 47 Limestone		7B Sand/Gravel	C.33 Sand	Masonry Sand			
1-1/2"	100			100			100%	0%	0%
1"	94.6			100			98%	2%	2%
3/4"	74.9			100			92%	8%	6%
1/2"	43.0			100			83%	17%	10%
3/8"	26.1			98			76%	24%	6%
No. 4	6.7			88			64%	36%	13%
No. 8	4.6			68			49%	51%	15%
No. 16	4.0			47			34%	66%	15%
No. 30	3.6			26			19%	81%	15%
No. 50	3.3			7			6%	94%	14%
No. 100	3.2			0.5			1%	99%	4%
No. 200	3.0			0.1			1.0%	99.0%	0.3%
% of Vol	30%	0%		70%	0%	0%			
	Fineness Modulus:			3.34					
Aggregate Ratios									
Combined % cumulative retained 3/8" sieve									
Coarseness Factor =		Combined % cumulative retained # 8 sieve					=	46	
Workability Factor =		Combined % passing # 8 sieve					=	49	
Adj-Workability Factor =		WF + [(Cementitious Material - 564) / 37.6]					=	49	
Allowable Adj-WF =		[(11.25 - .15 CF) + 36] + 2.5					= Low	38	High 43
Mortar Fraction								65.7%	

Figure B-13. Concrete Gradation Specification, Test Nos. IBP-1 through IBP-4



# GENERAL TESTING LABORATORIES

Typical Aggregate Quality Analysis (Supplied by Nebraska Department of Roads)

Western Sand & Gravel		Kereford Limestone	
Typical Sand/Gravel Qualities all Sizes		Typical Limestone Qualities all Sizes	
Bulk Specific Gravity (SSD):	2.62	Bulk Specific Gravity (SSD):	2.66
24 Hour Absorption:	0.6%	24 Hour Absorption:	1.1%
LA Abrasion Loss:	26%	LA Abrasion Loss:	30%
Sulfate Soundness Loss:	2.0%	Sulfate Soundness Loss:	3.1%
Deleterious Materials:	< 0.5%	Deleterious Materials:	< 0.5%
Soluble Chloride Ion Content:	< 0.001%	Soluble Chloride Ion Content:	< 0.001%
Organic Impurities:	None		

Figure B-14. Aggregate Quality Analysis, Test Nos. IBP-1 through IBP-4

### **Appendix C. Bogie Test Results**

The results of the recorded data from each accelerometer for every dynamic bogie test are provided in the summary sheets found in this appendix. Summary sheets include acceleration, velocity, and deflection versus time plots as well as force versus deflection and energy versus deflection plots.

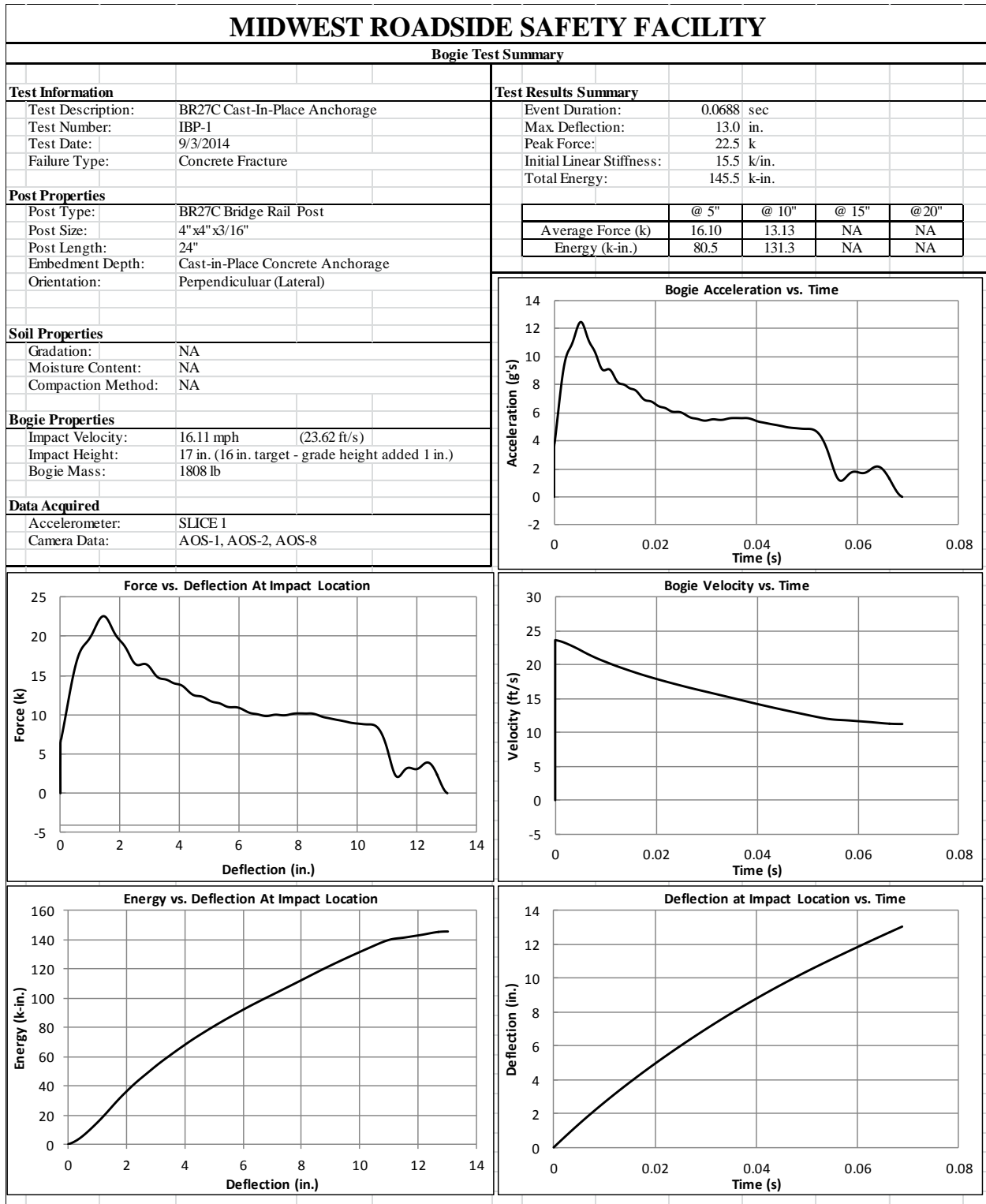


Figure C-1. Test No. IBP-1 Results (SLICE-1)

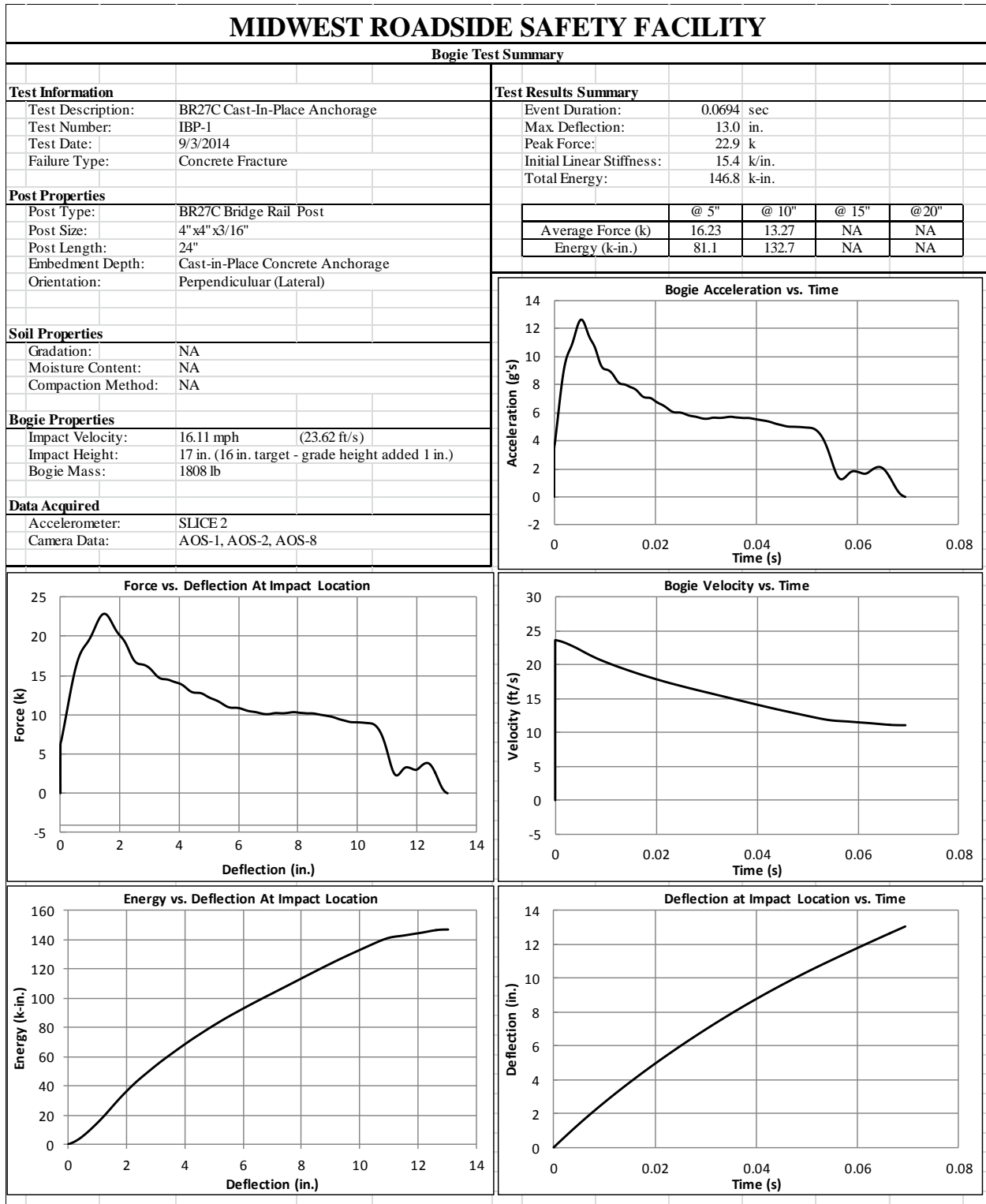


Figure C-2. Test No. IBP-1 Results (SLICE-2)

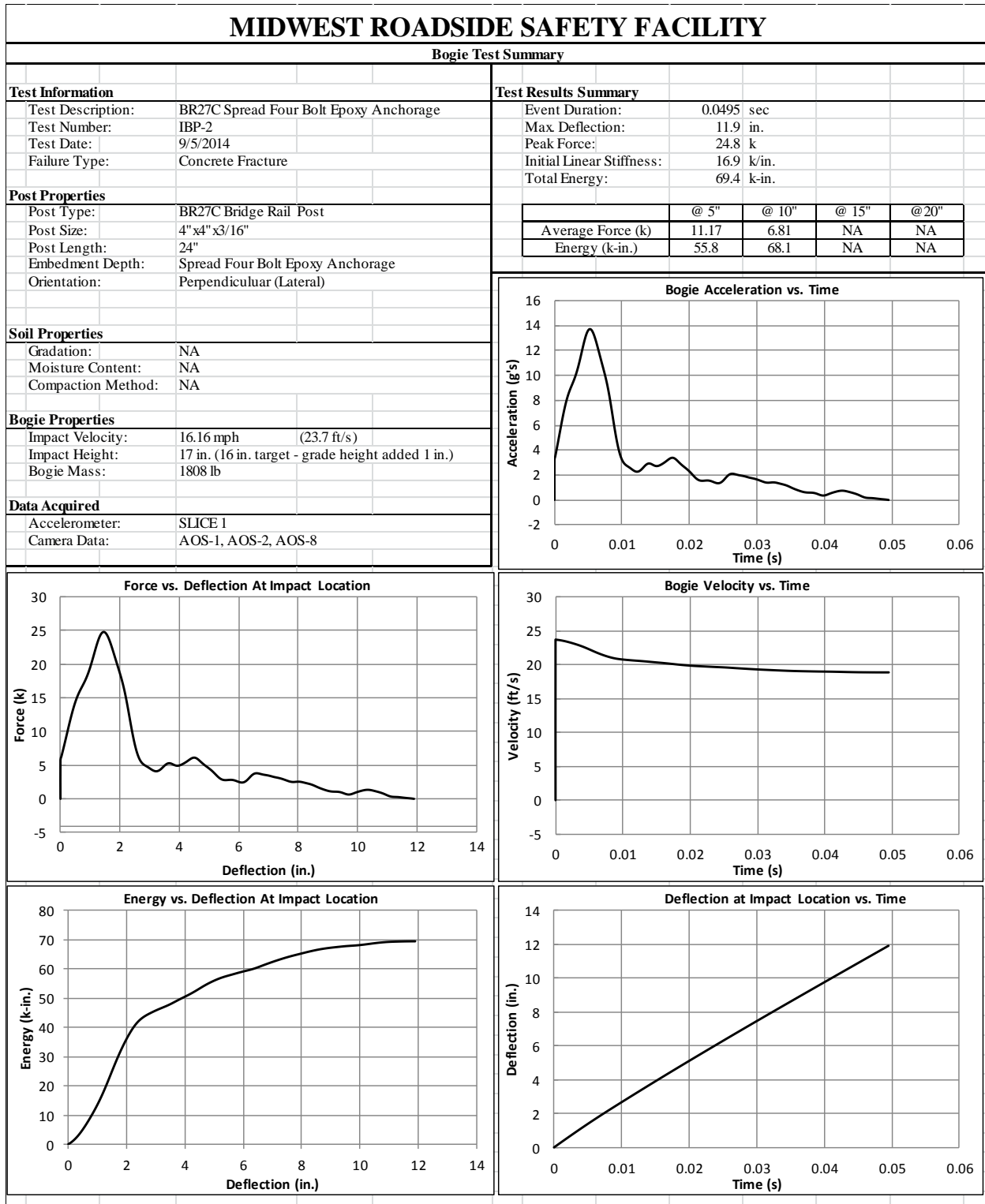


Figure C-3. Test No. IBP-2 Results (SLICE-1)

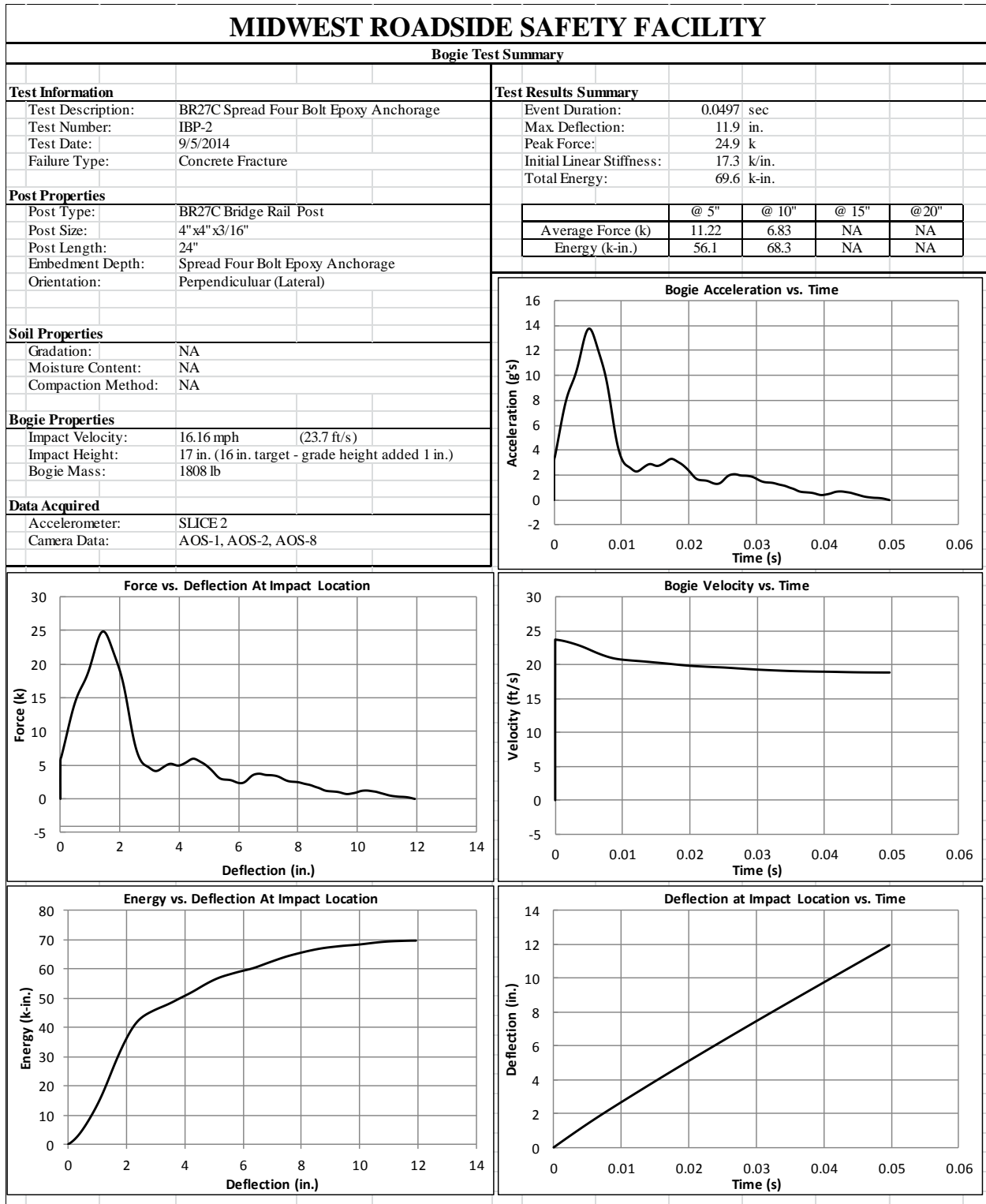


Figure C-4. Test No. IBP-2 Results (SLICE-2)

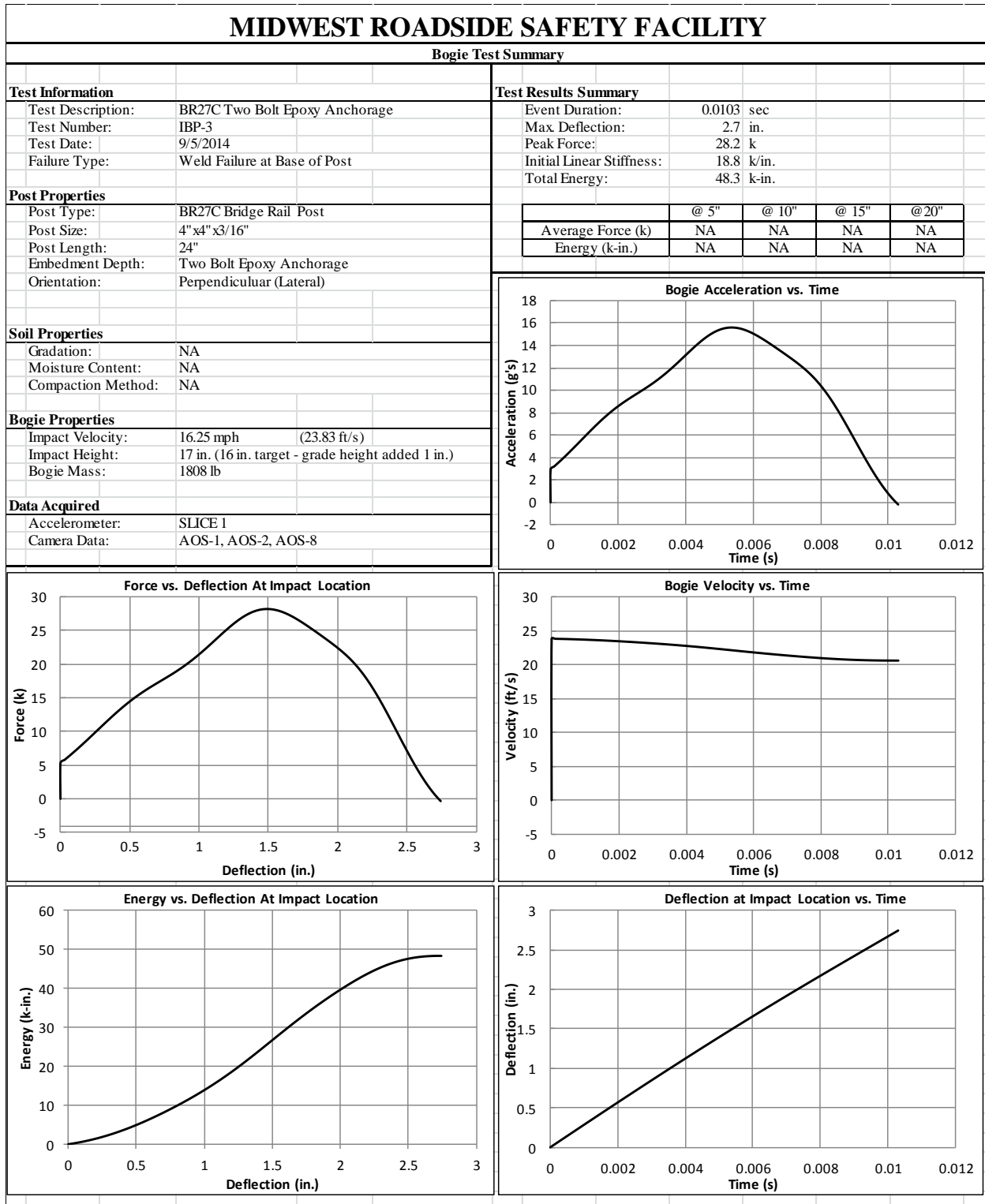


Figure C-5. Test No. IBP-3 Results (SLICE-1)

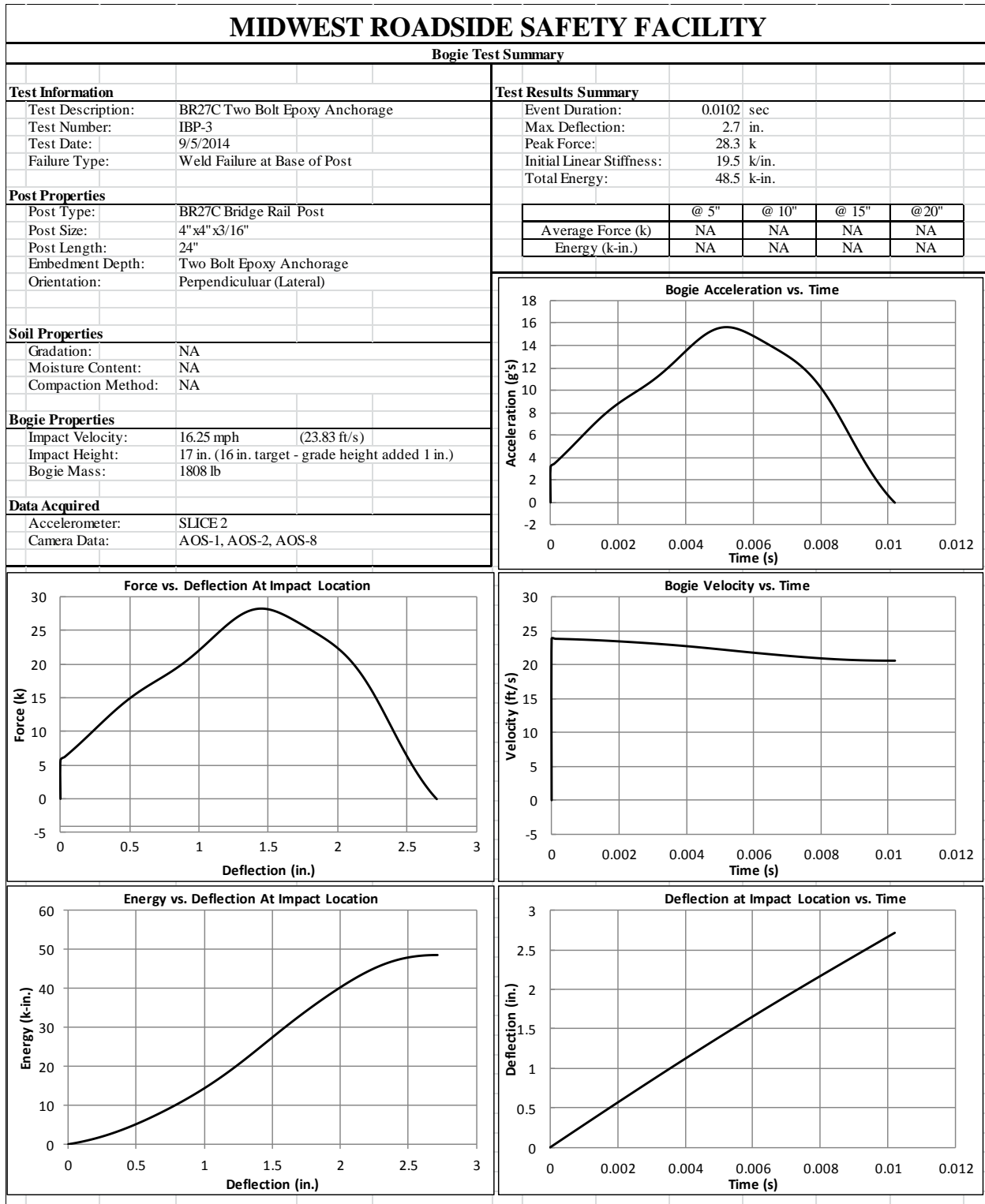


Figure C-6. Test No. IBP-3 Results (SLICE-2)



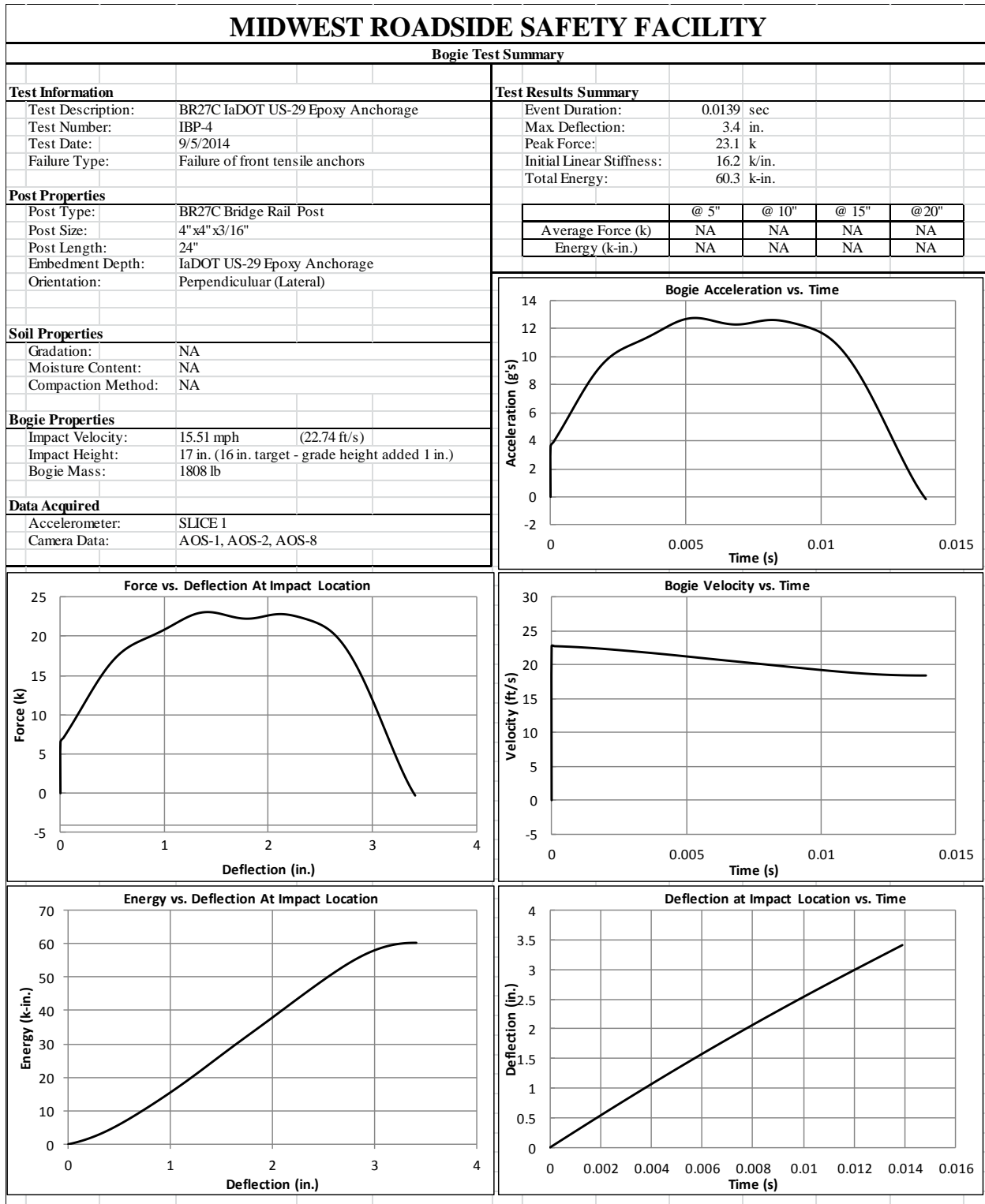


Figure C-7. Test No. IBP-4 Results (SLICE-1)

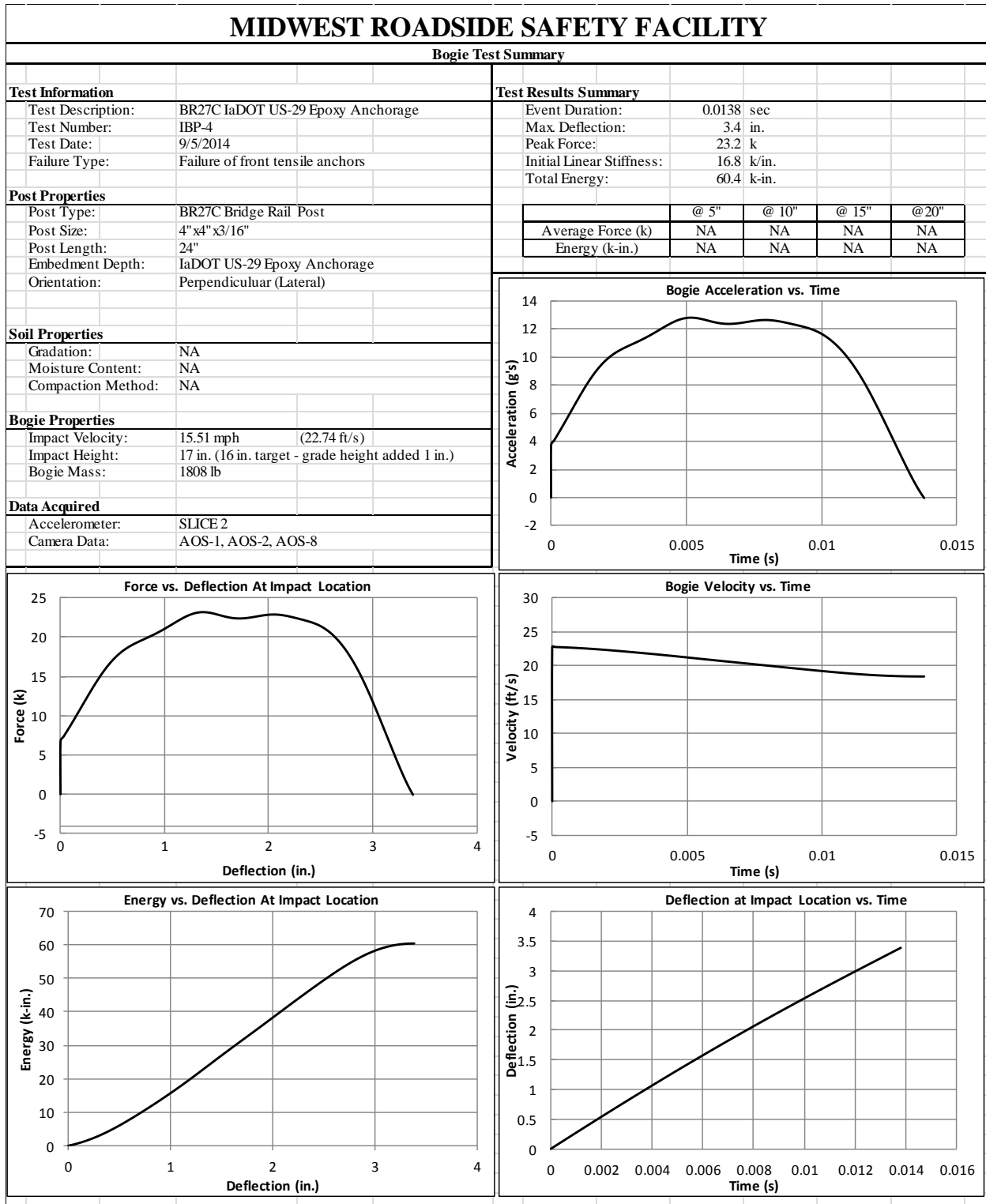


Figure C-8. Test No. IBP-4 Results (SLICE-2)

**END OF DOCUMENT**